

<https://www.mdc-berlin.de/de/veroeffentlichungstypen/clinical-journal-club>

The weekly Clinical Journal Club by Dr. Friedrich C. Luft

Usually every Wednesday 17:00 - 18:00



Klinische Forschung

Experimental and Clinical Research Center (ECRC) von MDC und Charité

Als gemeinsame Einrichtung von MDC und Charité fördert das Experimental and Clinical Research Center die Zusammenarbeit zwischen Grundlagenwissenschaftlern und klinischen Forschern. Hier werden neue Ansätze für Diagnose, Prävention und Therapie von Herz-Kreislauf- und Stoffwechselerkrankungen, Krebs sowie neurologischen Erkrankungen entwickelt und zeitnah am Patienten eingesetzt. Sie sind eingeladen, uns beizutreten. [Bewerben Sie sich!](#)



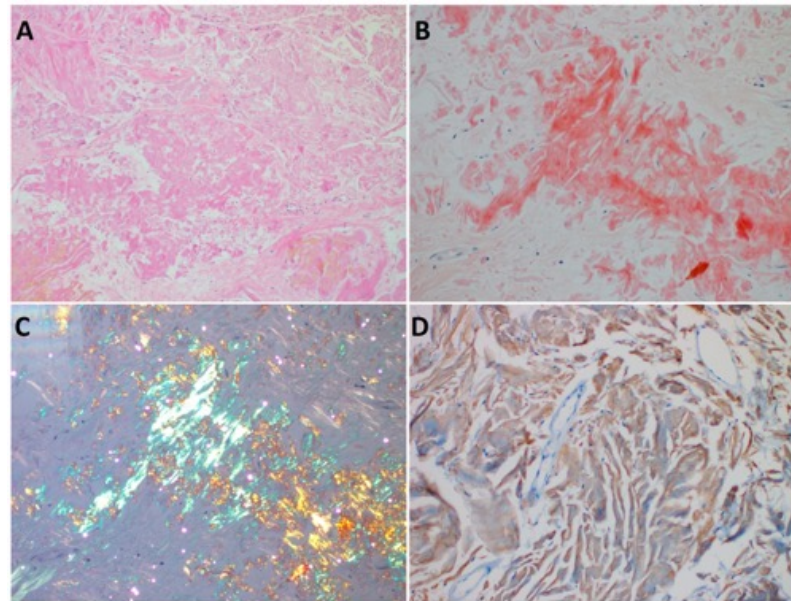
A 47-year-old man with type 2 diabetes presented to the endocrinology clinic owing to several years of progressive growth of skin lesions on his lower abdominal wall where he had repeatedly injected insulin. He also reported unpredictable episodes of hypoglycemia. A physical examination was notable for two pendulous skin masses on the lower abdominal wall. The glycated hemoglobin level was 9.2% (reference value, <7.1). What is the most likely diagnosis?

- Inguinal hernias
- Injection site granulomas
- Insulin-derived amyloidosis
- Lipoatrophy
- Lipomas



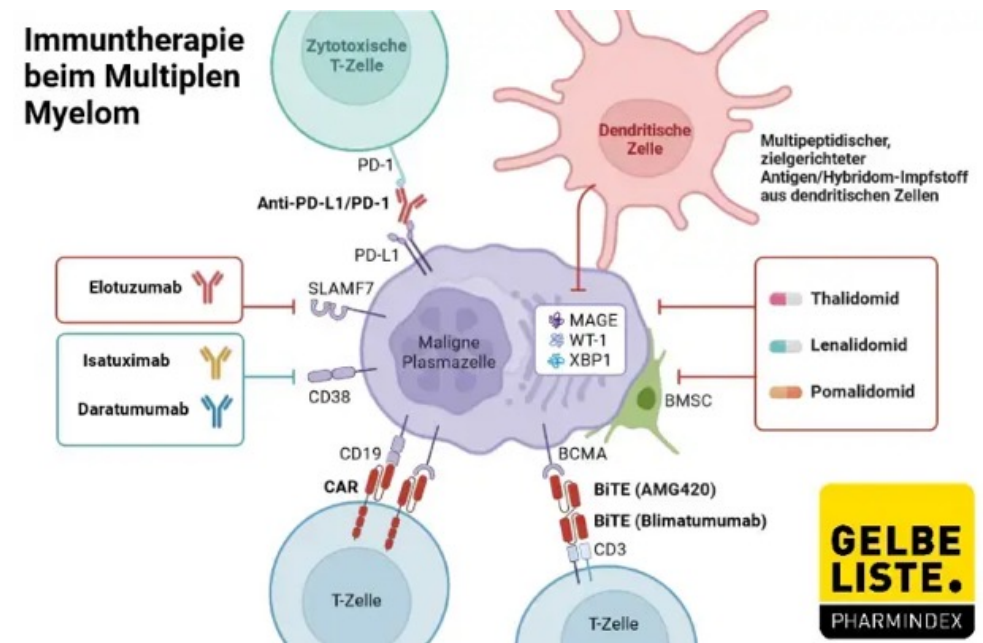
Insulin-derived amyloidosis is the accumulation of subcutaneous amyloid deposits at sites of repeated insulin injection. Insulin-derived amyloidosis is challenging to differentiate from lipohypertrophy — another cutaneous complication of repeated insulin injections — without histopathological assessment. Both conditions are prevented by frequent rotation of insulin-injection sites. In this case, surgical resection was performed for cosmesis. Histopathological assessment showed amorphous eosinophilic deposits, positive Congo red staining, and apple-green birefringence under polarized light. The specimen also stained positive for thioflavin T under fluorescence.

Insulin-derived amyloidosis, also known as insulin ball or amyloidoma, is a rare complication of insulin therapy where insulin accumulates in subcutaneous tissue at injection sites, forming hard masses called amyloid deposits. These deposits can affect glycemic control, potentially leading to poor blood sugar management.



CD38 ist ein Glykoprotein und ein Enzym, das auf der Oberfläche vieler Immunzellen, insbesondere Plasmazellen, vorkommt. Es spielt eine wichtige Rolle bei der Aktivierung und Proliferation von Immunzellen und wird als Marker für Zellaktivierung und als Ziel für immuntherapeutische Maßnahmen verwendet.

Daratumumab ist ein humaner monoklonaler Antikörper (IgG1κ) der zur Behandlung von multipler Myelom, einer malignen Erkrankung des Knochenmarks, eingesetzt wird. Er bindet an das Glykoprotein CD38, welches auf Myelomzellen stark exprimiert wird, und löst dadurch verschiedene Mechanismen aus, die zum Zelltod der Myelomzellen führen. Daratumumab ist unter dem Handelsnamen Darzalex erhältlich.

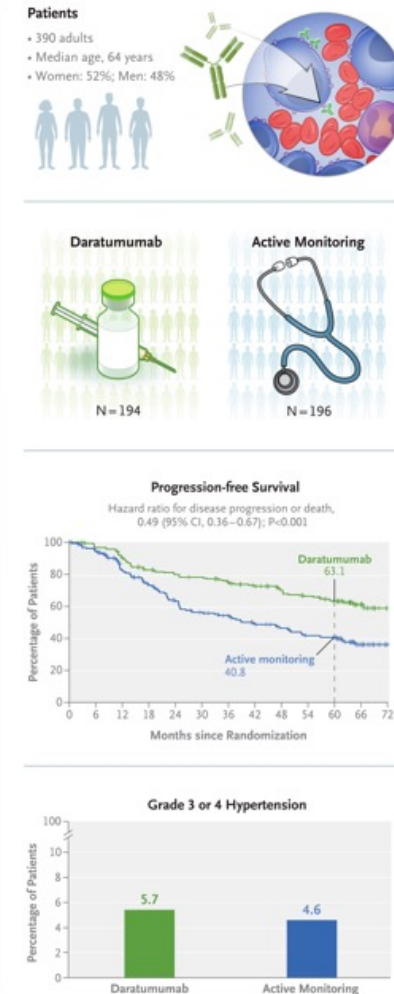


Daratumumab or Active Monitoring for High-Risk Smoldering Multiple Myeloma

(schwelend; glimmen)

Daratumumab, an anti-CD38 monoclonal antibody, has been approved for the treatment of multiple myeloma. Data are needed regarding the use of daratumumab for high-risk smoldering multiple myeloma, a precursor disease of active multiple myeloma for which no treatments have been approved.

In this phase 3 trial, we randomly assigned patients with high-risk smoldering multiple myeloma to receive either subcutaneous daratumumab monotherapy or active monitoring. Treatment was continued for 39 cycles, for 36 months, or until confirmation of disease progression, whichever occurred first. The primary end point was progression-free survival; progression to active multiple myeloma was assessed by an independent review committee in accordance with International Myeloma Working Group diagnostic criteria.



Smoldering multiple myeloma is an asymptomatic precursor disease of active multiple myeloma, and the current standard care is observation. However, patients with smoldering multiple myeloma who are at high risk for progression to active multiple myeloma may benefit from early treatment, although no treatments have been approved for this indication.

Daratumumab, a human IgGκ monoclonal antibody targeting CD38, has been approved for use as monotherapy or in combination with standard regimens for multiple myeloma. The phase 2 CENTAURUS study showed that daratumumab had single-agent activity in patients with intermediate-risk or high-risk smoldering multiple myeloma.

Patients

Patients were required to be at high risk for progression to active multiple myeloma, with a percentage of clonal plasma cells in bone marrow of at least 10% and the presence of at least one of the following risk factors (which were based on data available at the time of trial development): a serum M-protein level of at least 30 g per liter, IgA smoldering multiple myeloma, immunoparesis with reduced levels of two uninvolved immunoglobulin isotypes, a ratio of involved free light chains to uninvolved free light chains (FLC ratio) in serum of 8 to less than 100, or a percentage of clonal plasma cells in bone marrow of more than 50% to less than 60%.

End Points and Assessments

The primary end point was progression-free survival, which was evaluated in an analysis of the time from randomization to the initial documentation of progression to active multiple myeloma or death from any cause, whichever occurred first.

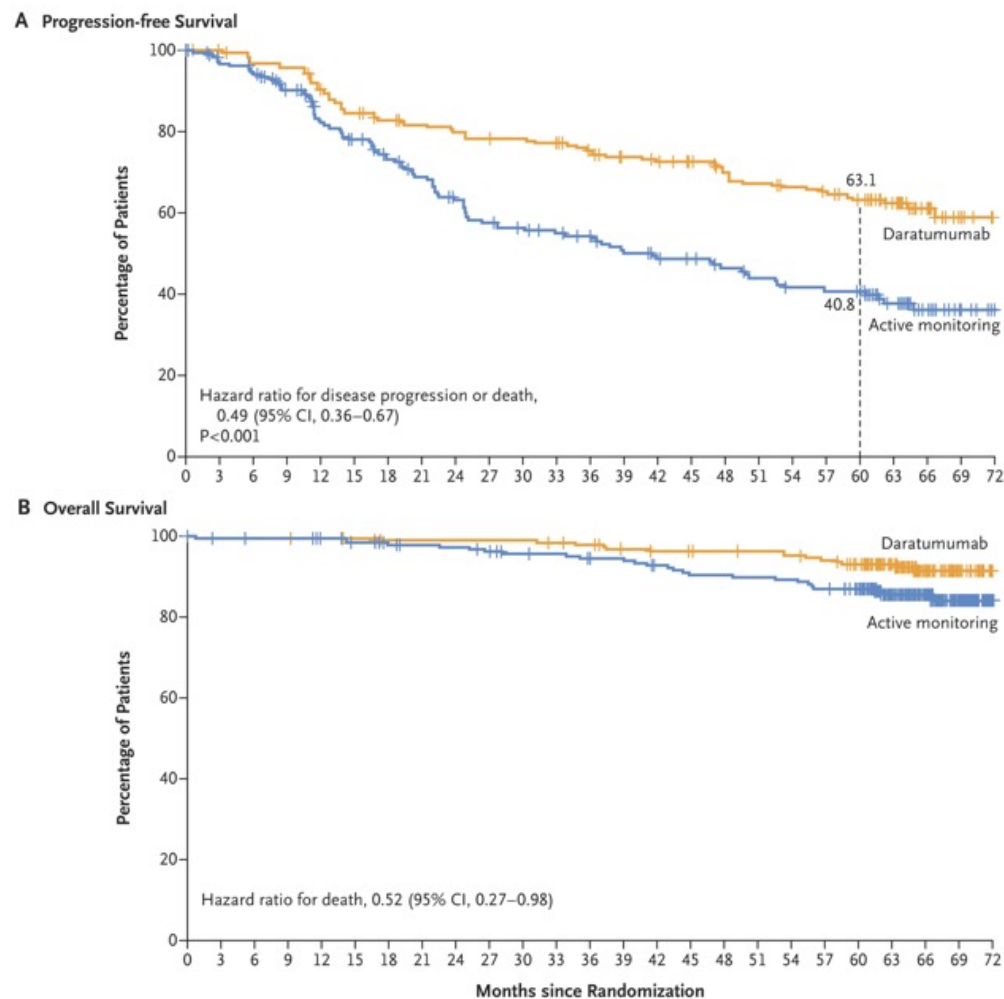
| Characteristic | Daratumumab (N = 194) | Active Monitoring (N = 196) |
|---|--------------------------|--------------------------------|
| Age | | |
| Median (range) — yr | 63.0 (31–86) | 64.5 (36–83) |
| Distribution — no. (%) | | |
| 18 to <65 yr | 106 (54.6) | 98 (50.0) |
| 65 to <75 yr | 67 (34.5) | 74 (37.8) |
| ≥75 yr | 21 (10.8) | 24 (12.2) |
| Male sex — no. (%) | 95 (49.0) | 93 (47.4) |
| Race or ethnic group — no. (%) [†] | | |
| White | 161 (83.0) | 162 (82.7) |
| Asian | 18 (9.3) | 13 (6.6) |
| Black | 4 (2.1) | 7 (3.6) |
| American Indian or Alaska Native | 0 | 3 (1.5) |
| Native Hawaiian or other Pacific Islander | 0 | 2 (1.0) |
| Multiple | 1 (0.5) | 0 |
| Not reported | 10 (5.2) | 9 (4.6) |
| ECOG performance-status score — no. (%) [‡] | | |
| 0 | 165 (85.1) | 160 (81.6) |
| 1 | 29 (14.9) | 36 (18.4) |
| Type of myeloma — no. (%) | | |
| IgG | 127 (65.5) | 138 (70.4) |
| IgA | 55 (28.4) | 42 (21.4) |
| Other | 12 (6.2) | 16 (8.2) |
| Clonal plasma cells in bone marrow — no. (%) | | |
| <10% | 1 (0.5) | 0 |
| 10% to ≤20% | 124 (63.9) | 102 (52.0) |
| >20% to <40% | 50 (25.8) | 66 (33.7) |
| ≥40% | 19 (9.8) | 28 (14.3) |
| Risk factors for progression to multiple myeloma — no. (%) [§] | | |
| <3 | 154 (79.4) | 156 (79.6) |
| ≥3 | 40 (20.6) | 40 (20.4) |
| Cytogenetic risk profile — no./total no. (%) [¶] | | |
| ≥1 High-risk cytogenetic abnormality | 29/167 (17.4) | 22/170 (12.9) |
| del(17p) | 3/166 (1.8) | 8/166 (4.8) |
| t(4;14) | 19/151 (12.6) | 11/157 (7.0) |
| t(14;16) | 7/146 (4.8) | 3/145 (2.1) |
| Risk of progression according to Mayo 2018 risk criteria | | |
| Low | 45 (23.2) | 34 (17.3) |
| Intermediate | 77 (39.7) | 76 (38.8) |
| High | 72 (37.1) | 86 (43.9) |
| Median time from diagnosis of smoldering multiple myeloma to randomization (range) — yr | 0.80 (0–4.7) | 0.67 (0–5.0) |

Summary of Progression Events (Intention-to-Treat Population).

| Event | Daratumumab (N = 194) | Active Monitoring (N = 196) |
|---|--------------------------|--------------------------------|
| Disease progression or death — no. (%) | 67 (34.5) | 99 (50.5) |
| Disease progression — no./total no. (%) [*] | 62/67 (92.5) | 94/99 (94.9) |
| CRAB criteria | | |
| Calcium level elevation | 0/62 | 2/94 (2.1) |
| Renal insufficiency | 0/62 | 0/94 |
| Anemia | 2/62 (3.2) | 14/94 (14.9) |
| Bone disease | 10/62 (16.1) | 18/94 (19.1) |
| SLiM criteria | | |
| ≥60% Clonal plasma cells in bone marrow | 5/62 (8.1) | 16/94 (17.0) |
| Serum FLC ratio ≥100 | 33/62 (53.2) | 33/94 (35.1) |
| >1 Focal lesion on magnetic resonance imaging | 12/62 (19.4) | 16/94 (17.0) |
| Death without disease progression — no./total no. (%) | 5/67 (7.5) | 5/99 (5.1) |

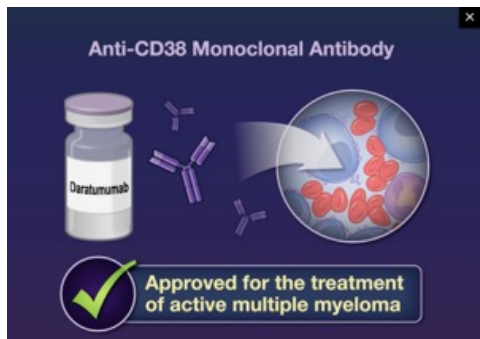
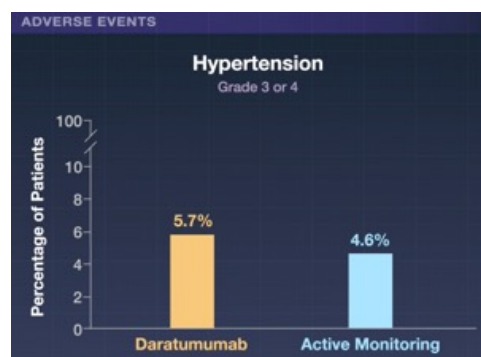
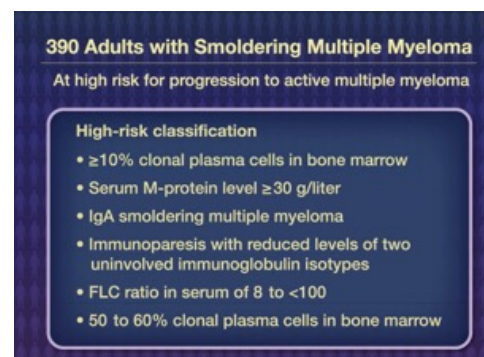
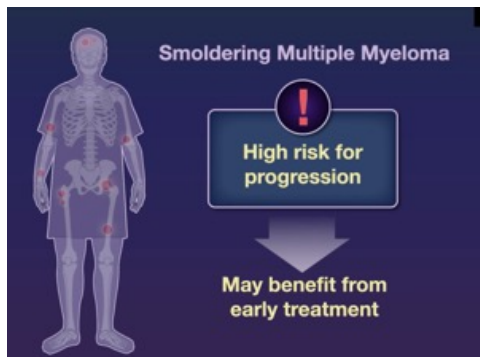
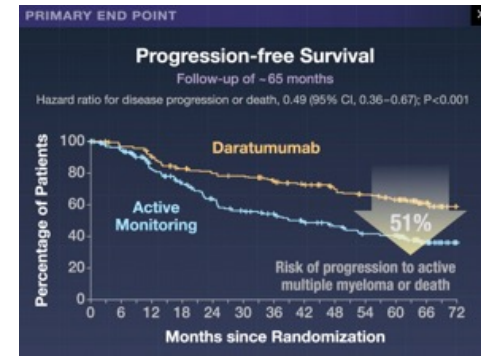
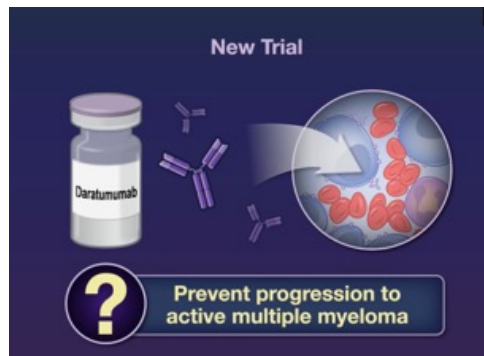
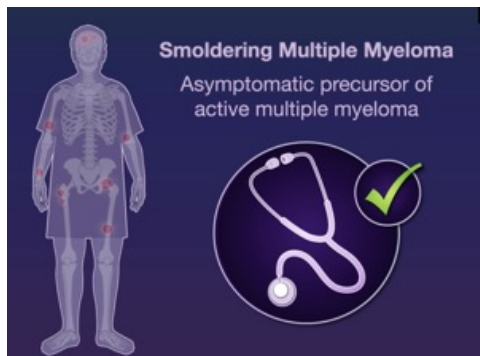
Adverse events

| Event | Daratumumab (N=193) | Active Monitoring (N=196) |
|--|-------------------------------------|------------------------------|
| | <i>number of patients (percent)</i> | |
| Any adverse event | 187 (96.9) | 162 (82.7) |
| Most common adverse events* | | |
| Fatigue | 66 (34.2) | 26 (13.3) |
| Upper respiratory tract infection | 58 (30.1) | 15 (7.7) |
| Diarrhea | 53 (27.5) | 10 (5.1) |
| Arthralgia | 52 (26.9) | 35 (17.9) |
| Nasopharyngitis | 49 (25.4) | 23 (11.7) |
| Back pain | 46 (23.8) | 38 (19.4) |
| Insomnia | 43 (22.3) | 5 (2.6) |
| Grade 3 or 4 adverse event | 78 (40.4) | 59 (30.1) |
| Most common grade 3 or 4 adverse event: hypertension | 11 (5.7) | 9 (4.6) |
| Serious adverse event | 56 (29.0) | 38 (19.4) |
| Most common serious adverse event: pneumonia | 7 (3.6) | 1 (0.5) |
| Adverse event that led to death† | 2 (1.0) | 4 (2.0) |
| Second primary cancer | 18 (9.3) | 20 (10.2) |



Progression-free Survival and Overall Survival.

Panel A shows Kaplan–Meier estimates of progression-free survival in the intention-to-treat population. Progression-free survival was evaluated in an analysis of the time from randomization to the initial documentation of progression to active multiple myeloma or death from any cause, whichever occurred first. Disease progression was assessed by an independent review committee in accordance with the International Myeloma Working Group SLiM–CRAB diagnostic criteria for multiple myeloma.⁶ The primary analysis of progression-free survival was performed after 166 events had occurred. Tick marks indicate censored data. The dashed line indicates the 5-year estimate. Panel B shows Kaplan–Meier estimates of overall survival in the intention-to-treat population.



The BCG vaccine, which stands for Bacillus Calmette-Guérin, is a live attenuated vaccine used to prevent tuberculosis (TB) and other mycobacterial infections. It is currently the only vaccine available against TB and is primarily given to infants in countries where TB is prevalent.

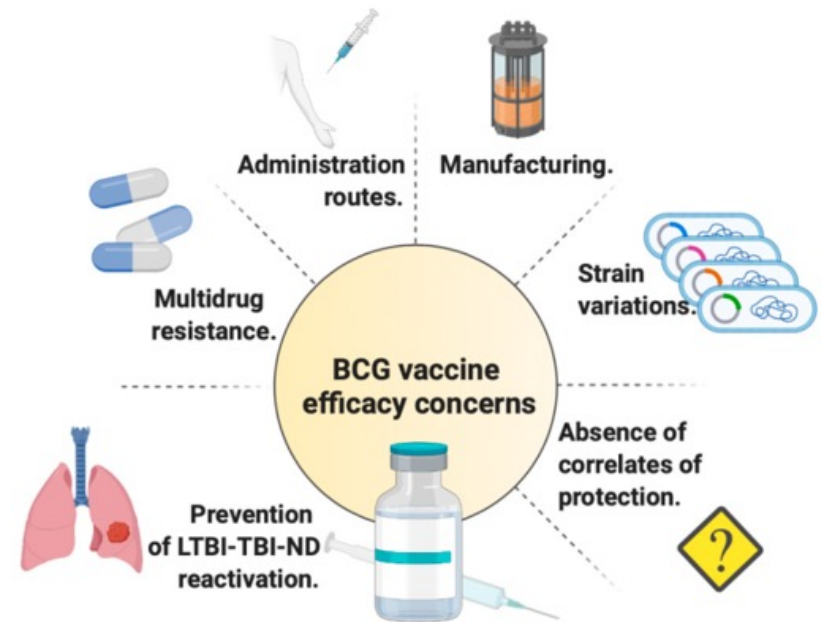
Purpose:

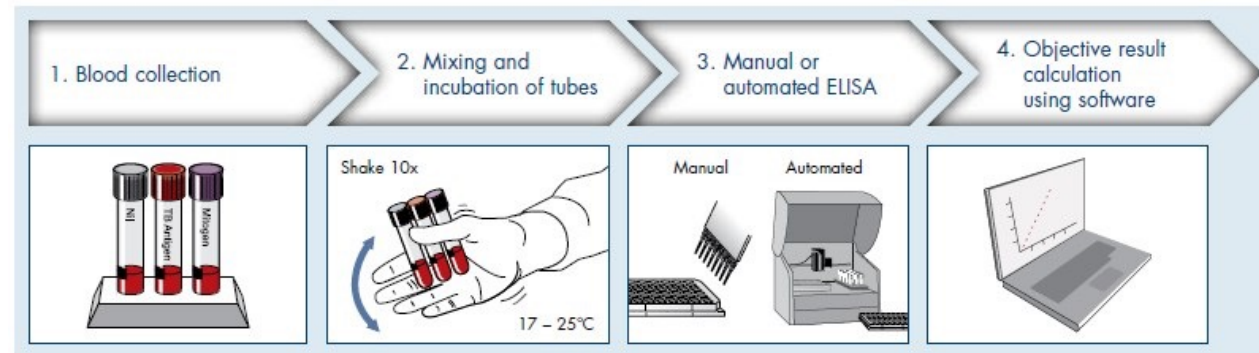
TB Prevention:

The BCG vaccine is primarily used to prevent severe forms of TB, particularly in children, such as TB meningitis (inflammation of the lining of the brain) and miliary TB (spread of TB infection to multiple organs).

Limited Protection:

While effective in preventing severe forms of TB in children, the BCG vaccine provides less protection against pulmonary TB in adults, according to the Centers for Disease Control and Prevention (CDC).





Der QFT (QuantiFERON®-TB Gold Test) ist ein in-vitro Test zur Diagnose einer Tuberkuloseinfektion. Er misst die zellvermittelte Immunantwort des Körpers auf Antigene von *Mycobacterium tuberculosis*. Ein positives Ergebnis deutet auf eine latente oder aktive Tuberkuloseinfektion hin.

Mehr Details:

Funktionsweise:

Der QFT verwendet eine Blutprobe und misst die Freisetzung von Interferon-Gamma (IFN- γ) durch T-Zellen, die durch die Antigene von *M. tuberculosis* stimuliert werden.

Anwendung:

Der QFT wird häufig als Alternative zum Tuberkulin-Hauttest eingesetzt, insbesondere bei Verdacht auf eine Tuberkuloseinfektion oder bei Kontakt zu erkrankten Personen.

Interpretation:

Ein positives Ergebnis weist auf eine latente oder aktive Tuberkuloseinfektion hin.

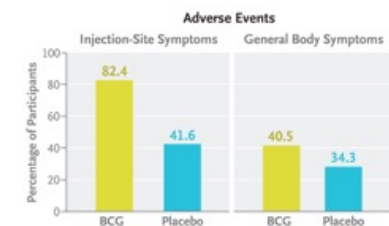
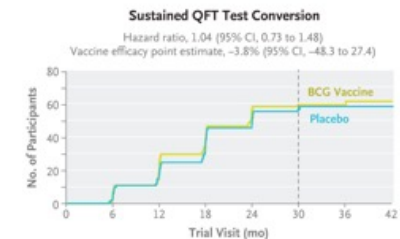
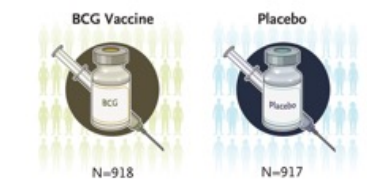
Vorteile:

Im Gegensatz zum Tuberkulin-Hauttest ist der QFT nicht durch die BCG-Impfung beeinflusst.

BCG Revaccination for the Prevention of *Mycobacterium tuberculosis* Infection

In a previous phase 2 trial, bacille Calmette–Guérin (BCG) revaccination was not shown to provide protection from primary *Mycobacterium tuberculosis* infection but prevented sustained *M. tuberculosis* infection, defined by an initial conversion on a QuantiFERON-TB (QFT) test (an interferon- γ release assay) from negative to positive, followed by two additional positive QFT tests at 3 and 6 months after the initial conversion (a secondary end point). A vaccine efficacy of 45% (95% confidence interval [CI], 6 to 68) was observed.


We performed a phase 2b, double-blind, randomized, placebo-controlled trial to evaluate the efficacy of BCG revaccination, as compared with placebo, for the prevention of sustained QFT test conversion (primary end point) in QFT test–negative, human immunodeficiency virus (HIV)–negative adolescents. Adverse events were assessed in a secondary analysis, and immunogenicity was assessed in an exploratory analysis. Vaccine efficacy was evaluated in the modified intention-to-treat population, which included all the participants who had undergone randomization, received the BCG vaccine or placebo, and had a negative QFT test 10 weeks after receipt of BCG vaccine or placebo; the last criterion was added to exclude participants with *M. tuberculosis* infection around the time that the vaccine or placebo was administered. Hazard ratios and 95% confidence intervals were estimated from a stratified Cox proportional-hazards model.



Approximately 1.7 billion people are estimated to be infected with *Mycobacterium tuberculosis* worldwide, of whom approximately 56 million are newly infected and at high risk for progression to tuberculosis disease. In 2022, an estimated 10.6 million new cases of tuberculosis disease were reported worldwide, which included 1.3 million cases in children younger than 15 years of age. Tuberculosis disease was responsible for 1.3 million deaths worldwide in 2022, which included 167,000 deaths in persons living with human immunodeficiency virus (HIV) infection. The incidence of tuberculosis disease in South Africa is among the highest in the world, with an estimated 468 cases per 100,000 persons in 2022. Cohort studies in the Western Cape province showed that the prevalence of *M. tuberculosis* infection, as assessed by means of an *M. tuberculosis*–specific interferon- γ release assay (IGRA) such as QuantiFERON-TB (QFT) tests, increases quickly among adolescents, with an incidence of QFT test conversion (from negative to positive) as high as 10% per year. In the absence of a licensed vaccine for the prevention of tuberculosis disease in adolescents and adults, we aimed to confirm that BCG revaccination confers protection against sustained *M. tuberculosis* infection in a larger population with an expanded age range and geographic area and to identify candidate correlates of protection for this trial end point. We assumed that a confirmatory trial could potentially support a policy change for BCG revaccination in South Africa or motivate funders to invest in a large phase 3 trial of BCG revaccination for the prevention of disease in support of the global effort to accelerate the end of the tuberculosis disease epidemic. Here we report the results of a phase 2b trial to assess the efficacy of BCG revaccination for the prevention of sustained *M. tuberculosis* infection in South Africa.

Participant eligibility criteria

Participants were included in the trial if they met all the following criteria:

1. ≥ 10 years and ≤ 18 years on trial Day 1
2. General good health, confirmed by medical history and physical examination
-  3. Vaccinated with BCG at least 5 years ago, documented through medical history or by presence of healed BCG scar
4. Tested QFT negative at screening
5. For female participants: not pregnant and agreed to avoid pregnancy throughout the first 12 months of the trial. Women physically capable of pregnancy must agree to use an acceptable method of avoiding pregnancy during this period. Acceptable methods of avoiding pregnancy included sexual abstinence (not engaging in sexual intercourse), a confirmed sterile partner, or at least 2 contraception methods from the following list: male or female condom, diaphragm, intrauterine devices (IUDs), hormonal contraceptive (oral, injection, transdermal patch, or implant)
6. Agreed to stay in contact with the trial site for the duration of the trial, provided updated contact information as necessary, and had no current plans to move from the trial area for the duration of the trial
7. Capable of giving signed informed consent/assent and completed the written informed consent/assent process

Participants were excluded if they had one of the following:

1. Acute illness or body temperature $\geq 37.5^{\circ}\text{C}$ on trial Day 1. This was a temporary exclusion for which the subject may be re-evaluated.

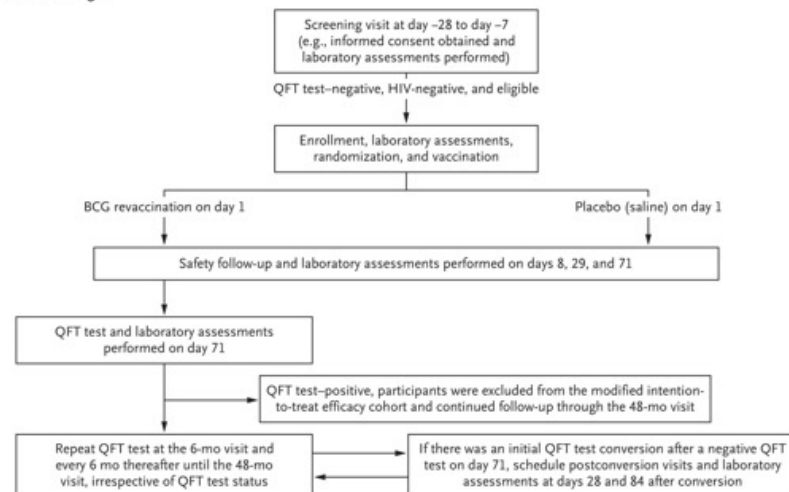
2. History or evidence of any clinically significant disease, including severe eczema and severe asthma, or any acute or chronic illness that might affect the safety, immunogenicity, or efficacy of trial vaccine in the opinion of the investigator
3. Any current medical, psychiatric, occupational, or substance abuse problems that, in the opinion of the investigator, will make it unlikely that the participant will comply with the protocol
4. History of autoimmune disease or allergic disease that is likely to be exacerbated by any component of the trial vaccine, or latent *Mtb* infection
5. History or evidence of active TB disease, or of any past or present possible immunodeficiency state including, but not limited to, any laboratory indication of HIV-1 infection
6. History of treatment for active TB disease or received investigational TB vaccine at any time prior to trial Day 1
7. Received a tuberculin skin test within 6 months prior to Day 1
8. Received immunosuppressive treatment, e.g., chemotherapy, biologics or radiation therapy, or used immunosuppressive medication (daily steroid equivalent of $\geq 5\text{mg}$ prednisone) within 42 days before trial Day 1.
9. Received immunoglobulin or blood products within 42 days before trial Day 1
10. Planned administration/administration of a licensed vaccine in the period starting 28 days before and ending 28 days after trial Day 1
11. Received any investigational drug therapy or investigational vaccine within 180 days before Day 1, or planned participation in any other clinical trial using investigational product during the trial period
12. Laboratory values from the most recent blood collected prior to randomization outside the normal range that are suggestive of a disease state

Methods

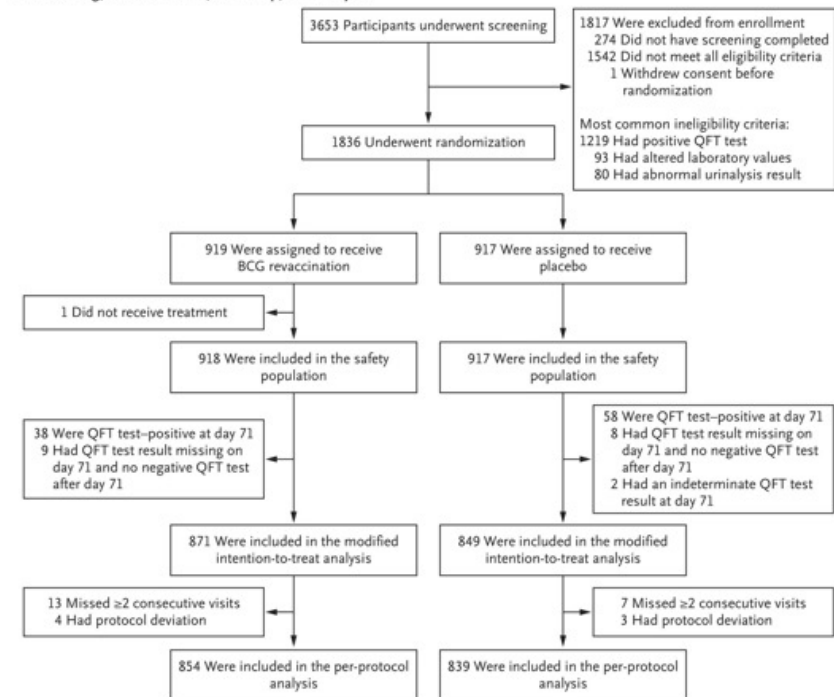
Trial Design and Objectives

In this double-blind, phase 2b, randomized, placebo-controlled trial, participants were enrolled at five sites in South Africa: Worcester, Cape Town, and Mbekweni in Western Cape province; Durban in KwaZulu-Natal province; and Johannesburg in Gauteng province. The primary objective was to show the efficacy of BCG revaccination, as compared with placebo, against sustained *M. tuberculosis* infection in QFT test-negative, healthy adolescents. The QFT Gold-Plus test was used for the assessment of *M. tuberculosis* infection.

A Trial Design



B Screening, Randomization, Follow-up, and Analysis



Sustained and Initial QFT Test Conversions.

| Variable | BCG Vaccine (N=871) | Placebo (N=849) |
|--|------------------------------|------------------------------|
| Initial QFT test conversion on or after day 71 — no. (%)† | 135 (15.5) | 125 (14.7) |
| Not evaluable for QFT test reversion because of missing or indeterminate QFT results — no. | 24 | 24 |
| QFT test reversion at day 84 or 6 mo after conversion — no. | 49 | 42 |
| Sustained QFT test conversion‡ | | |
| No. with event | 62 | 59 |
| Proportion (95% CI)§ | 0.0712 (0.0541 to 0.0883) | 0.0695 (0.0524 to 0.0866) |
| Person-time accrued — mo¶ | 19,719 | 19,383 |
| Overall incidence — no. of events per person-mo (95% CI)‖ | 0.0031 (0.0024 to 0.0040) | 0.0030 (0.0023 to 0.0039) |
| Hazard ratio (95% CI)** | 1.04 (0.73 to 1.48)†† | — |
| Vaccine efficacy — % (95% CI)‡‡ | –3.8 (–48.3 to 27.4) | — |
| Initial QFT test conversion — proportion (95% CI)§ | 0.16 (0.13 to 0.18) | 0.15 (0.12 to 0.17) |
| Person-time accrued — mo¶ | 19,695 | 19,371 |
| Overall incidence — no. of events per person-mo (95% CI)‖ | 0.0069 (0.0057 to 0.0081) | 0.0065 (0.0054 to 0.0077) |

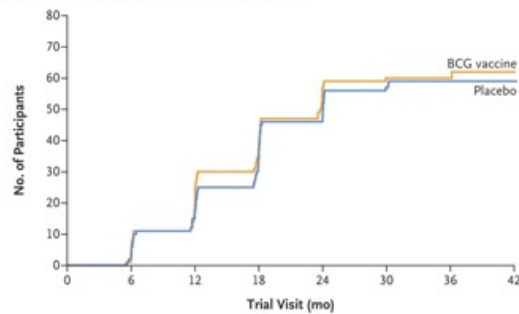
Incidence of Adverse Events and Medication Use.

| Adverse Event or Medication Use | BCG Vaccine (N=918) | Placebo (N=917) |
|---|------------------------|---------------------|
| Solicited adverse events and medication use | | |
| Any injection-site symptom | | |
| No. with event/total no. | 754/915 | 381/915 |
| Percent (95% CI) | 82.4 (79.8 to 84.8) | 41.6 (38.5 to 44.9) |
| Any general body symptom | | |
| No. with event/total no. | 371/916 | 314/915 |
| Percent (95% CI) | 40.5 (37.4 to 43.7) | 34.3 (31.3 to 37.4) |
| Use of medication 1 to 7 days after vaccination | | |
| No. with event/total no. | 30/903 | 27/899 |
| Percent (95% CI) | 3.3 (2.3 to 4.6) | 3.0 (2.0 to 4.3) |
| Injection-site symptoms according to severity† | | |
| Swelling — no./total no. (%) | | |
| Any severity | 657/912 (72.0) | 248/910 (27.3) |
| Severe or life-threatening | 2/912 (0.2) | 1/910 (0.1) |
| Pain — no./total no. (%) | | |
| Any severity | 381/914 (41.7) | 148/915 (16.2) |
| Severe or life-threatening | 17/914 (1.9) | 6/915 (0.7) |
| Redness — no./total no. (%) | | |
| Any severity | 349/912 (38.3) | 111/911 (12.2) |
| Severe or life-threatening | 0 | 0 |
| Solicited systemic adverse events according to severity† | | |
| Tiredness — no./total no. (%) | | |
| Any severity | 229/913 (25.1) | 184/913 (20.2) |
| Severe or life-threatening | 8/913 (0.9) | 6/913 (0.7) |
| Headache — no./total no. (%) | | |
| Any severity | 195/913 (21.4) | 164/913 (18.0) |
| Severe or life-threatening | 7/913 (0.8) | 9/913 (1.0) |
| Stomach problems — no./total no. (%) | | |
| Any severity | 136/913 (14.9) | 140/913 (15.3) |
| Severe or life-threatening | 8/913 (0.9) | 8/913 (0.9) |
| Fever — no./total no. (%)‡ | | |
| Any severity | 24/911 (2.6) | 27/907 (3.0) |
| Severe or life-threatening | 5/911 (0.5) | 5/907 (0.6) |

| Adverse-event categories‡ | | |
|---|---------------------|---------------------|
| Mild adverse events | | |
| Any mild event — no. | 315 | 90 |
| Percent (95% CI) | 34.3 (31.3 to 37.4) | 9.8 (8.0 to 11.9) |
| Moderate adverse events | | |
| Any moderate event — no. | 47 | 28 |
| Percent (95% CI) | 5.1 (3.8 to 6.7) | 3.1 (2.1 to 4.3) |
| Severe adverse events | | |
| Any severe event — no. | 5 | 3 |
| Percent (95% CI) | 0.5 (0.2 to 1.2) | 0.3 (0.1 to 0.9) |
| Related adverse events¶ | | |
| Any related event — no. | 273 | 9 |
| Percent (95% CI) | 29.7 (26.8 to 32.8) | 1.0 (0.5 to 1.8) |
| Related severe adverse events¶ | | |
| Any related severe event — no. | 1 | 0 |
| Percent (95% CI) | 0.1 (0 to 0.5) | — |
| Unsolicited nonserious adverse events | | |
| Any unsolicited nonserious event — no. | 185 | 117 |
| Percent (95% CI) | 20.2 (17.7 to 22.8) | 12.8 (10.7 to 15.0) |
| Serious adverse events | | |
| Any serious event — no. | 3 | 3 |
| Percent (95% CI) | 0.3 (0.1 to 0.9) | 0.3 (0.1 to 0.9) |
| Serious adverse event with outcome of death — no. | 0 | 0 |
| Serious adverse drug reaction — no. | 0 | 0 |
| Adverse events leading to premature trial discontinuation — no. | 0 | 0 |
| Adverse events of special interest | | |
| Any event of special interest — no. | 5 | 0 |
| Percent (95% CI) | 0.5 (0.2 to 1.2) | — |
| Most common nonserious adverse events** | | |
| Headache — no. (%) | 36 (3.9) | 27 (2.9) |
| Injection-site pain — no. (%) | 21 (2.3) | 0 |
| Injection-site ulceration — no. (%) | 20 (2.2) | 0 |
| Pyrexia — no. (%) | 12 (1.3) | 3 (0.3) |
| Oropharyngeal pain — no. (%) | 9 (1.0) | 4 (0.4) |
| Upper respiratory tract infection — no. (%) | 8 (0.9) | 15 (1.6) |

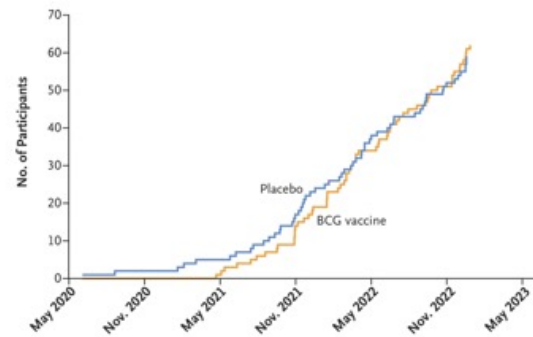
Of about 900 in each group

A Sustained QFT Test Conversion According to Trial Visit

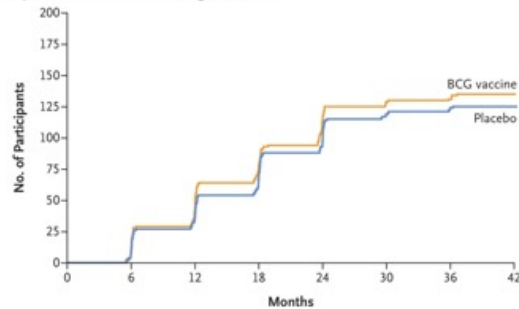


| | | | | | | | | |
|-------------|-----|-----|-----|-----|-----|-----|----|---|
| No. at Risk | | | | | | | | |
| BCG vaccine | 871 | 853 | 808 | 758 | 529 | 201 | 76 | 4 |
| Placebo | 849 | 834 | 790 | 749 | 505 | 197 | 84 | 6 |

B Sustained QFT Test Conversion According to Calendar Month

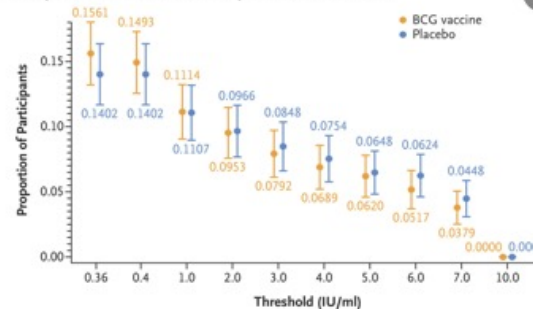


C Initial QFT Test Conversion According to Trial Visit



| | | | | | | | | |
|-------------|-----|-----|-----|-----|-----|-----|----|---|
| No. at Risk | | | | | | | | |
| BCG vaccine | 871 | 853 | 807 | 756 | 527 | 201 | 76 | 4 |
| Placebo | 849 | 834 | 790 | 749 | 503 | 197 | 84 | 6 |

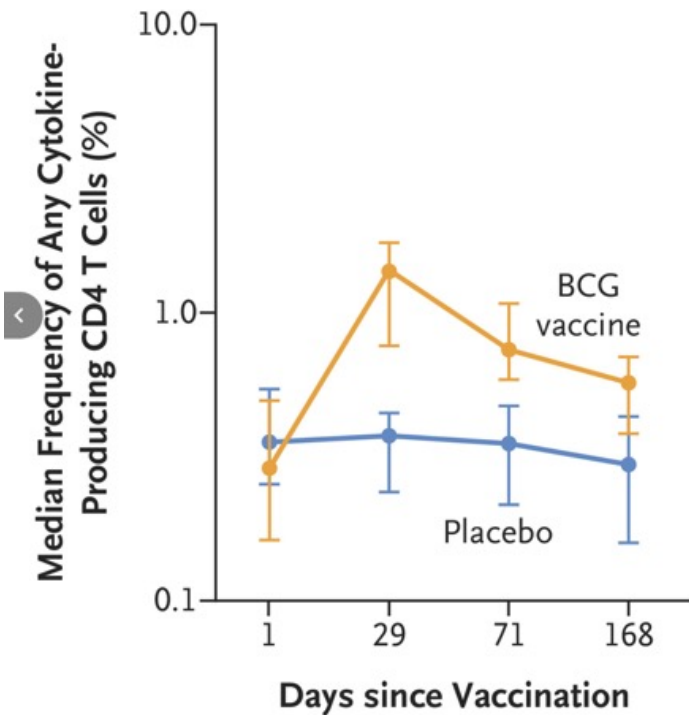
D Initial QFT Test Conversions based on QFT Conversion Thresholds



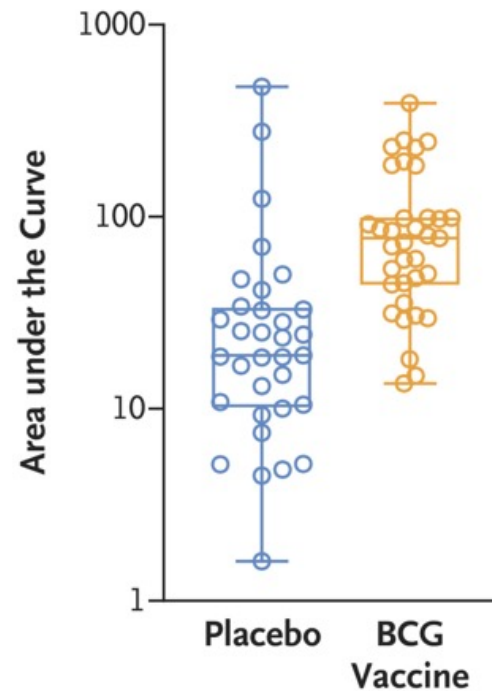
Vaccine Efficacy in the Modified Intention-to-Treat Population.

Panel A shows the cumulative event curves for a sustained QFT test conversion (primary efficacy end point) according to trial visit. Panel B shows the cumulative event curves for a sustained QFT test conversion according to calendar month. Panel C shows the cumulative event curves for an initial QFT test conversion according to trial visit. Panel D shows the proportion of participants with an initial QFT test conversion based on a range of increasingly stringent QFT test conversion thresholds higher than 0.35 IU per milliliter. I bars represent 95% confidence intervals.

A Longitudinal Response after Vaccination

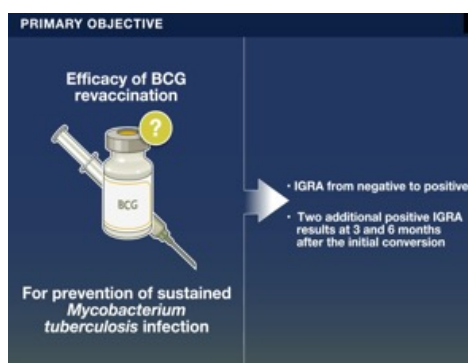
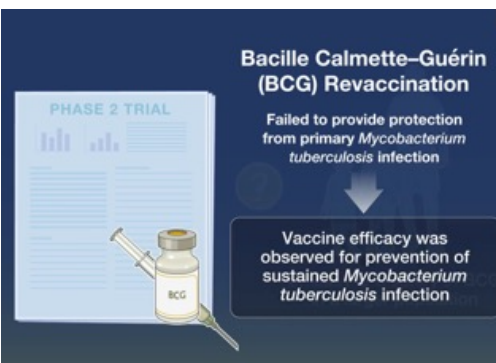
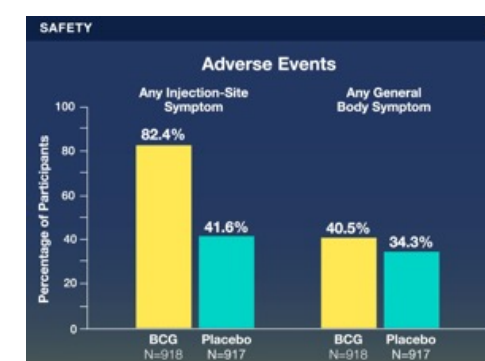
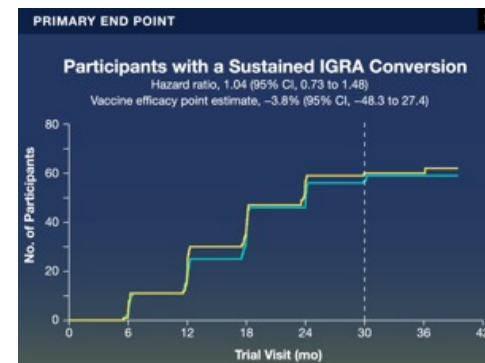
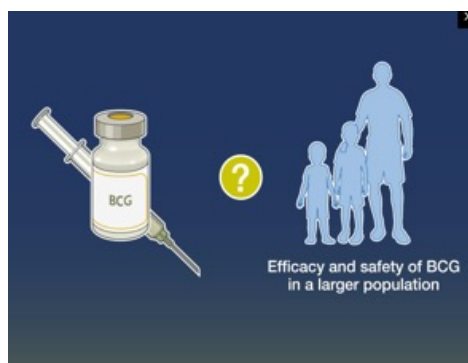
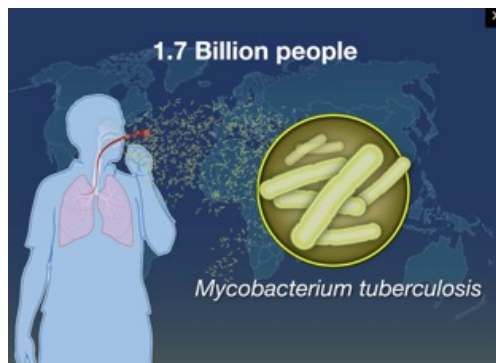


B Antigen-Specific CD4 T-Cell Response after Vaccination



Immunogenicity of BCG Revaccination.

Shown are the frequencies of antigen-specific CD4 T cells expressing any combination of interferon- γ , tumor necrosis factor, interleukin-2, interleukin-17, or interleukin-22 after stimulation with BCG vaccine, as measured with the use of whole-blood intracellular cytokine staining assay in participants who received BCG revaccination (orange) or placebo (blue). Panel A shows longitudinal responses (plotted on a logarithmic scale) during the first 168 days after vaccination. I bars indicated 95% confidence intervals. Panel B shows the area under the curve (plotted on a logarithmic scale) for BCG-specific CD4 T-cell frequencies per participant during the first 168 days after vaccination. Each circle represents an individual participant. The horizontal line within each box indicates the median, the box indicates the interquartile range (quartile 1 to quartile 3), and the whiskers indicate the minimum and maximum values.



Tenofovirafenamid, kurz TAF, ist ein Medikament zur Behandlung einer Hepatitis-B- oder HIV-Infektion. Es ist ein Prodrug von Tenofovir und gehört zur Gruppe der nukleotidischen Reverse-Transkriptase-Inhibitoren (NtRTI).

Emtricitabin ist ein Arzneimittel, das zur Behandlung von HIV-Infektionen und zur Prävention von HIV-Infektionen eingesetzt wird. Es gehört zur Wirkstoffklasse der nukleosidischen Reverse-Transkriptase-Inhibitoren (NRTI).

Dolutegravir ist ein antiretroviraler Wirkstoff aus der Gruppe der Integrase-Strangtransfer-Inhibitoren (INSTI), der in der HIV-Therapie eingesetzt wird. Er hemmt ein Enzym, das für die Vermehrung des HI-Virus notwendig ist, indem er an das aktive Zentrum der viralen Integrase bindet.

What is the HIV regimen for children?

Preferred regimens are as follows: Infants, birth to < 14 days: 2 NRTIs plus nevirapine. Aged ≥ 14 days to < 3 years: 2 NRTIs plus lopinavir/ritonavir. Aged ≥ 2 years to < 3 years: 2 NRTIs plus lopinavir/ritonavir or 2 NRTIs plus raltegravir.

Children with HIV infection face unique challenges due to the severity of the disease and the complexities of managing it in children. Early diagnosis and treatment are crucial for improving outcomes and preventing long-term complications. Approximately 1.4 million children under 15 were living with HIV in 2023, and 120,000 new cases were reported, highlighting the ongoing impact of HIV on children worldwide.

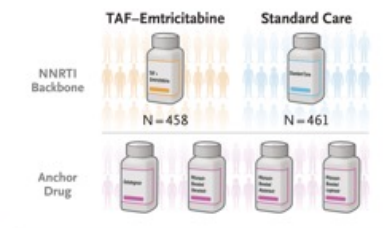


Second-Line Antiretroviral Therapy for Children Living with HIV in Africa

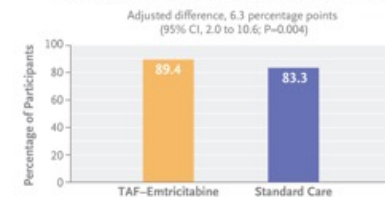
Children living with human immunodeficiency virus (HIV) have limited options for second-line antiretroviral therapy (ART). In this open-label trial with a 2-by-4 factorial design, we randomly assigned children with HIV who had first-line treatment failure to receive **second-line therapy with tenofovir alafenamide fumarate (TAF)–emtricitabine** or **standard care (abacavir or zidovudine, plus lamivudine)** as the backbone and dolutegravir or ritonavir-boosted darunavir, atazanavir, or lopinavir as the anchor drug. The primary outcome was a viral load of less than 400 copies per milliliter at 96 weeks. We hypothesized that TAF–emtricitabine would be noninferior to standard care, that dolutegravir and ritonavir-boosted darunavir would each be superior to ritonavir-boosted lopinavir analyzed in combination, and that ritonavir-boosted atazanavir would be noninferior to ritonavir-boosted lopinavir. Safety was also assessed.

Participants

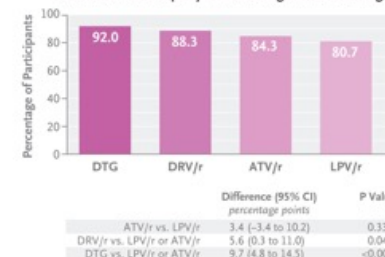
- 919 children
- Median age, 10 years
- Male: 54%; Female: 46%



Viral Load <400 copies/ml According to NNRTI Backbone



Viral Load <400 copies/ml According to Anchor Drug



Globally, the number of children living with human immunodeficiency virus (HIV) who are receiving first-line antiretroviral therapy (ART) is increasing. This increase in access to ART, coupled with increased monitoring of HIV viral load, is in turn increasing the number of children in need of second- or subsequent-line ART after virologic failure. Most children with HIV live in Africa, where until recently first-line nonnucleoside reverse-transcriptase inhibitor (NNRTI)–based regimens were widely used. After the failure of first-line NNRTI-based ART, guidelines recommend an anchor drug from a new class (a ritonavir-boosted protease inhibitor or integrase inhibitor), plus a backbone of two nucleoside (or nucleotide) reverse-transcriptase inhibitors (NRTIs). Maximizing effectiveness and acceptability to patients while minimizing side effects is particularly important for children in need of lifelong ART. Which backbone and anchor drugs are safest and most effective for pediatric second-line ART remains unclear.

Participants

Participants were children with HIV who were 3 to 15 years of age, weighed at least 14 kg, were receiving first-line NNRTI-based ART, had treatment failure according to World Health Organization (WHO) criteria (a confirmed viral load of >1000 copies per milliliter after receiving counseling about adherence to the treatment regimen, or immunologic or clinical criteria for failure), and had a viral load above 400 copies per milliliter at the screening visit. Postmenarchal girls were required to have a pregnancy test with negative results.

Randomization and Procedures

Participants were randomly assigned to receive one of two backbone drug combinations — TAF–emtricitabine or standard care (abacavir–lamivudine or zidovudine–lamivudine, whichever was not used in first-line ART) — and were simultaneously randomly assigned to receive one of four anchor drugs (dolutegravir, ritonavir-boosted darunavir, ritonavir-boosted atazanavir, or ritonavir-boosted lopinavir).

Outcomes

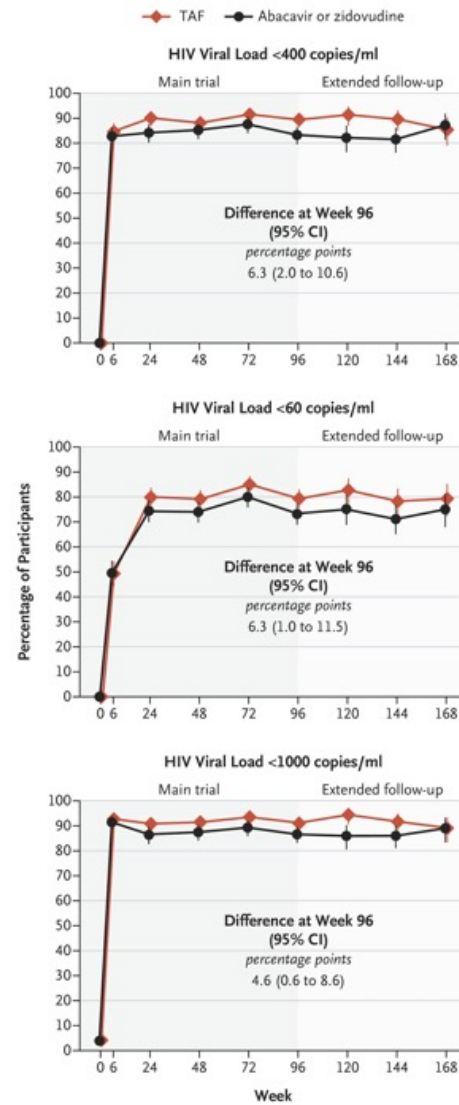
The primary outcome was a viral load of less than 400 copies per milliliter at 96 weeks; death before week 96 was considered to be treatment failure.

Grade 3 and 4 Adverse Events

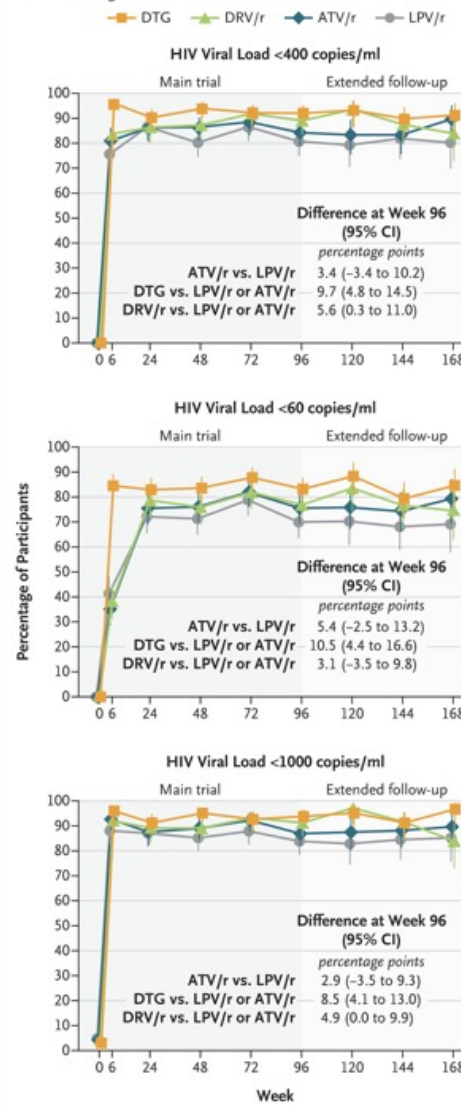
| Characteristic | NRTI Backbone Randomization | | Anchor Drug Randomization | | | | All (N=919) |
|--|-----------------------------|-----------------------------|---|--|---|-----------------------------|-----------------------------|
| | Standard Care (N=461) | TAF (N=458) | Ritonavir-Boosted Lopinavir (N=227) | Ritonavir-Boosted Atazanavir (N=231) | Ritonavir-Boosted Darunavir (N=232) | Dolutegravir (N=229) | |
| Male sex — no. (%) | 256 (55.5) | 241 (52.6) | 120 (52.9) | 129 (55.8) | 121 (52.2) | 127 (55.5) | 497 (54.1) |
| Age | | | | | | | |
| Median (IQR) — yr | 10 (7–13) | 10 (8–13) | 10 (7–12) | 10 (8–13) | 10 (8–12) | 11 (8–13) | 10 (8–13) |
| Distribution — no. (%) | | | | | | | |
| 3–4 yr | 21 (4.6) | 18 (3.9) | 12 (5.3) | 14 (6.1) | 7 (3.0) | 6 (2.6) | 39 (4.2) |
| 5–9 yr | 178 (38.6) | 180 (39.3) | 95 (41.9) | 83 (35.9) | 96 (41.4) | 84 (36.7) | 358 (39.0) |
| 10–15 yr | 262 (56.8) | 260 (56.8) | 120 (52.9) | 134 (58.0) | 129 (55.6) | 139 (60.7) | 522 (56.8) |
| WHO clinical stage — no. (%)† | | | | | | | |
| 1 | 244 (52.9) | 239 (52.2) | 114 (50.2) | 121 (52.4) | 130 (56.0) | 118 (51.5) | 483 (52.6) |
| 2 | 140 (30.4) | 154 (33.6) | 79 (34.8) | 74 (32.0) | 65 (28.0) | 76 (33.2) | 294 (32.0) |
| 3 | 63 (13.7) | 50 (10.9) | 30 (13.2) | 29 (12.6) | 27 (11.6) | 27 (11.8) | 113 (12.3) |
| 4 | 14 (3.0) | 15 (3.3) | 4 (1.8) | 7 (3.0) | 10 (4.3) | 8 (3.5) | 29 (3.2) |
| Median CD4 cell count (IQR) — cells/mm ³ ‡ | 667 (405 to 963) | 673 (434 to 982) | 692 (432 to 1035) | 685 (446 to 943) | 685 (416 to 1000) | 670 (349 to 891) | 669 (413 to 971) |
| Median CD4 cell percentage (IQR)§ | 27.5 (19.0 to 35.4) | 28.3 (20.3 to 37.0) | 28.3 (19.2 to 36.0) | 28.0 (20.5 to 35.2) | 28.0 (19.4 to 37.1) | 27.0 (18.0 to 36.0) | 28.0 (19.2 to 36.0) |
| Median viral load (IQR) — copies/ml | 17,909 (5,417 to 58,359) | 17,265 (5,764 to 50,655) | 16,885 (6,333 to 59,994) | 16,784 (5,070 to 56,600) | 18,675 (6,673 to 49,668) | 19,409 (4,992 to 57,076) | 17,573 (5,549 to 55,700) |
| Median weight (IQR) — kg | 26.1 (20.2 to 33.5) | 25.8 (21.0 to 32.8) | 25.1 (20.0 to 33.4) | 25.2 (20.3 to 32.1) | 26.0 (21.0 to 32.3) | 27.0 (21.3 to 34.0) | 25.9 (20.5 to 33.1) |
| Median weight-for-age z score (IQR)¶ | −1.6 (−2.4 to −0.9) | −1.6 (−2.4 to −0.9) | −1.5 (−2.3 to −0.8) | −1.6 (−2.5 to −0.9) | −1.7 (−2.4 to −0.9) | −1.6 (−2.5 to −0.9) | −1.6 (−2.4 to −0.9) |
| Median height (IQR) — cm | 130.9 (118.0 to 142.5) | 130.1 (120.7 to 141.6) | 130.0 (118.2 to 142.0) | 129.5 (119.0 to 140.8) | 131.6 (118.7 to 142.3) | 133.0 (120.6 to 143.5) | 130.5 (118.4 to 142.0) |
| Median height-for-age z score (IQR)¶ | −1.5 (−2.3 to −0.9) | −1.6 (−2.4 to −0.8) | −1.5 (−2.3 to −0.6) | −1.7 (−2.4 to −1.0) | −1.6 (−2.3 to −0.8) | −1.5 (−2.5 to −0.9) | −1.6 (−2.3 to −0.8) |
| Median BMI (IQR)‖ | 15.4 (14.4 to 16.5) | 15.5 (14.3 to 16.8) | 15.5 (14.4 to 16.8) | 15.5 (14.3 to 16.7) | 15.4 (14.1 to 16.5) | 15.5 (14.5 to 16.8) | 15.5 (14.3 to 16.7) |
| Median BMI-for-age z score (IQR)¶ | −1.0 (−1.6 to −0.4) | −0.9 (−1.8 to −0.3) | −0.8 (−1.6 to −0.3) | −1.0 (−1.8 to −0.3) | −1.0 (−1.7 to −0.5) | −1.0 (−1.7 to −0.3) | −1.0 (−1.7 to −0.4) |
| Median duration of first-line ART (IQR) — yr | 5.6 (3.2 to 7.8) | 5.5 (3.3 to 7.7) | 5.2 (3.2 to 7.5) | 5.4 (3.0 to 7.6) | 6.0 (3.3 to 7.8) | 5.7 (3.5 to 8.1) | 5.6 (3.3 to 7.8) |
| First-line NRTI — no. (%) | | | | | | | |
| Abacavir | 244 (52.9) | 246 (53.7) | 121 (53.3) | 124 (53.7) | 123 (53.0) | 122 (53.3) | 490 (53.3) |
| Zidovudine | 217 (47.1) | 212 (46.3) | 106 (46.7) | 107 (46.3) | 109 (47.0) | 107 (46.7) | 429 (46.7) |
| First-line NNRTI — no. (%) | | | | | | | |
| Efavirenz | 247 (53.6) | 267 (58.3) | 131 (57.7) | 128 (55.4) | 124 (53.4) | 131 (57.2) | 514 (55.9) |
| Nevirapine | 214 (46.4) | 191 (41.7) | 96 (42.3) | 103 (44.6) | 108 (46.6) | 98 (42.8) | 405 (44.1) |
| Assigned NRTI backbone therapy — no. (%) | | | | | | | |
| Standard care | 461 (100) | 0 | 115 (50.7) | 115 (49.8) | 114 (49.1) | 117 (51.1) | 461 (50.2) |
| TAF | 0 | 458 (100) | 112 (49.3) | 116 (50.2) | 118 (50.9) | 112 (48.9) | 458 (49.8) |
| Assigned anchor drug — no. (%) | | | | | | | |
| Ritonavir-boosted lopinavir | 115 (24.9) | 112 (24.5) | 227 (100) | 0 | 0 | 0 | 227 (24.7) |
| Ritonavir-boosted atazanavir | 115 (24.9) | 116 (25.3) | 0 | 231 (100) | 0 | 0 | 231 (25.1) |
| Ritonavir-boosted darunavir | 114 (24.7) | 118 (25.8) | 0 | 0 | 232 (100) | 0 | 232 (25.2) |
| Dolutegravir | 117 (25.4) | 112 (24.5) | 0 | 0 | 0 | 229 (100) | 229 (24.9) |

| Adverse Events | NRTI Backbone Randomization | | Anchor Drug Randomization | | | | All (N=919) |
|--|-----------------------------|-------------|-------------------------------------|--------------------------------------|-------------------------------------|----------------------|-------------|
| | Standard Care (N=461) | TAF (N=458) | Ritonavir-Boosted Lopinavir (N=227) | Ritonavir-Boosted Atazanavir (N=231) | Ritonavir-Boosted Darunavir (N=232) | Dolutegravir (N=229) | |
| Grade 3 or 4 adverse events | | | | | | | |
| Any grade 3 or 4 adverse event | | | | | | | |
| No. of participants (%) | 64 (13.9) | 63 (13.8) | 26 (11.5) | 69 (29.9) | 20 (8.6) | 12 (5.2) | 127 (13.8) |
| No. of events | 93 | 83 | 36 | 92 | 28 | 20 | 176 |
| Elevated bilirubin | | | | | | | |
| No. of participants (%) | 25 (5.4) | 34 (7.4) | 1 (0.4) | 57 (24.7) | 1 (0.4) | 0 | 59 (6.4) |
| No. of events | 32 | 36 | 1 | 66 | 1 | 0 | 68 |
| Serious adverse events | | | | | | | |
| Any serious adverse event | | | | | | | |
| No. of participants (%) | 14 (3.0) | 15 (3.3) | 10 (4.4) | 5 (2.2) | 8 (3.4) | 6 (2.6) | 29 (3.2) |
| No. of events | 14 | 17 | 10 | 6 | 9 | 6 | 31 |
| Death† | | | | | | | |
| No. of participants (%) | 0 | 1 (0.2) | 0 | 0 | 0 | 1 (0.4) | 1 (0.1) |
| No. of events | 0 | 1 | 0 | 0 | 0 | 1 | 1 |
| Any life-threatening event | | | | | | | |
| No. of participants (%) | 1 (0.2) | 1 (0.2) | 1 (0.4) | 1 (0.4) | 0 | 0 | 2 (0.2) |
| No. of events | 1 | 2 | 1 | 2 | 0 | 0 | 3 |
| Any event leading to or prolonging hospitalization | | | | | | | |
| No. of participants (%) | 13 (2.8) | 14 (3.1) | 9 (4.0) | 5 (2.2) | 8 (3.4) | 5 (2.2) | 27 (2.9) |
| No. of events | 13 | 16 | 9 | 6 | 9 | 5 | 29 |
| Any important medical condition emerging during the trial‡ | | | | | | | |
| No. of participants (%) | 1 (0.2) | 1 (0.2) | 2 (0.9) | 0 | 0 | 0 | 2 (0.2) |
| No. of events | 1 | 1 | 2 | 0 | 0 | 0 | 2 |
| Events leading to ART modification | | | | | | | |
| Any event leading to ART modification | | | | | | | |
| No. of participants (%) | 13 (2.8) | 11 (2.4) | 7 (3.1) | 5 (2.2) | 5 (2.2) | 7 (3.1) | 24 (2.6) |
| No. of events | 22 | 19 | 11 | 11 | 9 | 10 | 41 |
| Psychiatric disorder | | | | | | | |
| No. of participants (%) | 0 | 1 (0.2) | 0 | 0 | 0 | 1 (0.4) | 1 (0.1) |
| No. of events | 0 | 1 | 0 | 0 | 0 | 1 | 1 |
| Acute hepatitis | | | | | | | |
| No. of participants (%) | 1 (0.2) | 0 | 1 (0.4) | 0 | 0 | 0 | 1 (0.1) |
| No. of events | 1 | 0 | 1 | 0 | 0 | 0 | 1 |
| Hypersensitivity reaction | | | | | | | |
| No. of participants (%) | 2 (0.4) | 0 | 2 (0.9) | 0 | 0 | 0 | 2 (0.2) |
| No. of events | 4 | 0 | 4 | 0 | 0 | 0 | 4 |
| Tuberculosis | | | | | | | |
| No. of participants (%) | 9 (2.0) | 9 (2.0) | 4 (1.8) | 5 (2.2) | 4 (1.7) | 5 (2.2) | 18 (2.0) |
| No. of events | 16 | 17 | 6 | 11 | 8 | 8 | 33 |
| Pregnancy | | | | | | | |
| No. of participants (%) | 0 | 1 (0.2) | 0 | 0 | 0 | 1 (0.4) | 1 (0.1) |
| No. of events | 0 | 1 | 0 | 0 | 0 | 1 | 1 |
| Anemia | | | | | | | |
| No. of participants (%) | 1 (0.2) | 0 | 0 | 0 | 1 (0.4) | 0 | 1 (0.1) |
| No. of events | 1 | 0 | 0 | 0 | 1 | 0 | 1 |

A Backbone



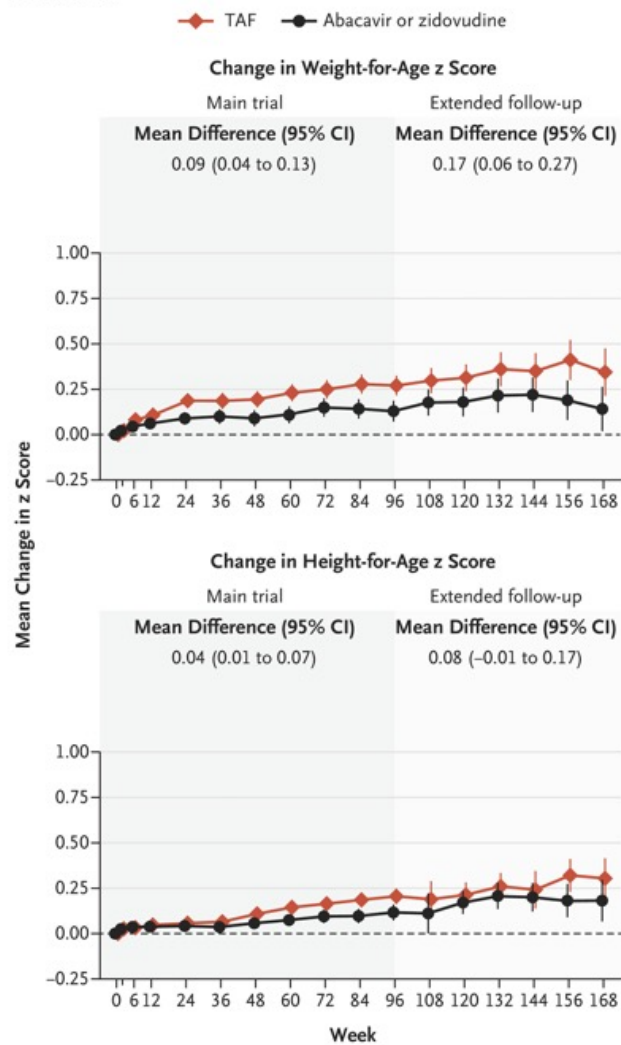
B Anchor Drug



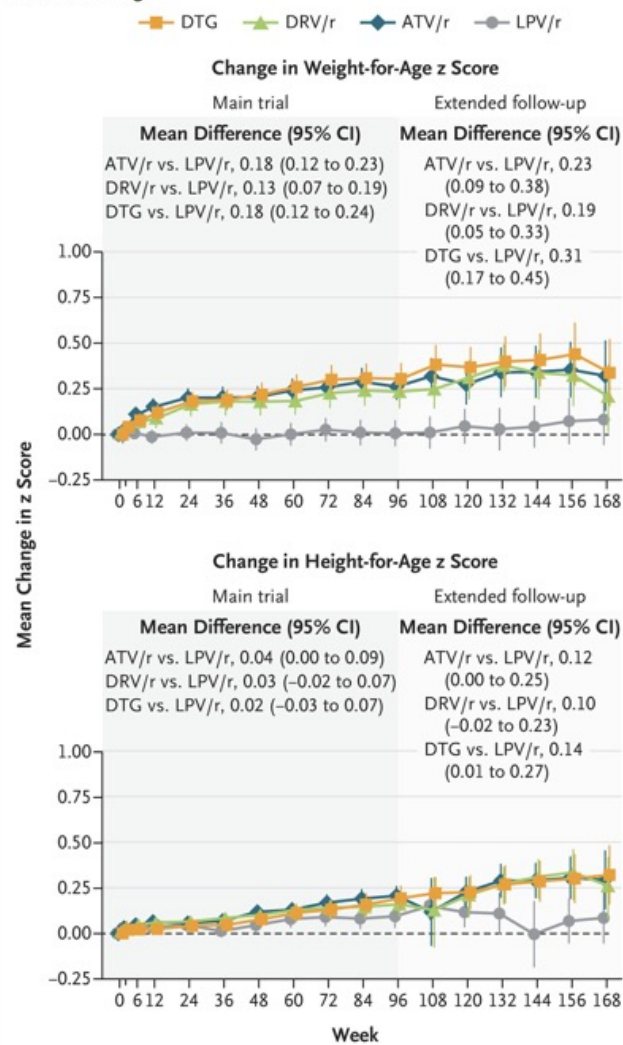
HIV Viral Load According to Assigned Treatment.

Shown are percentages of participants with a human immunodeficiency virus (HIV) viral load of less than 400 copies per milliliter, less than 60 copies per milliliter, and less than 1000 copies per milliliter over time during the main trial and during the extended follow-up period according to the assigned backbone (Panel A) or anchor drug (Panel B).

A Backbone

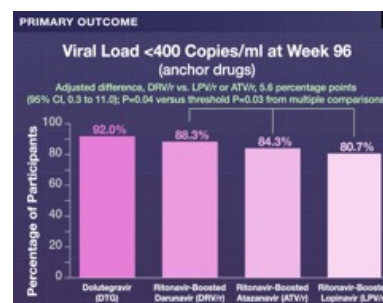
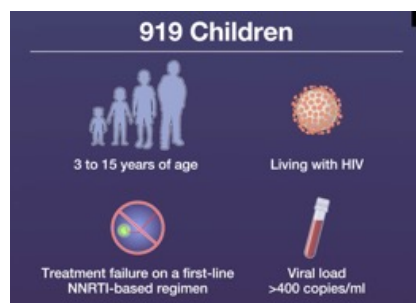
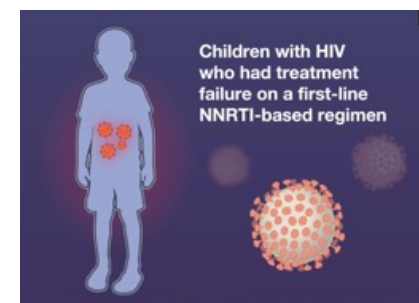
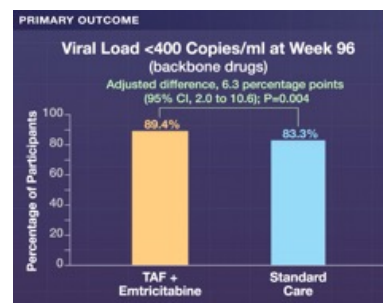
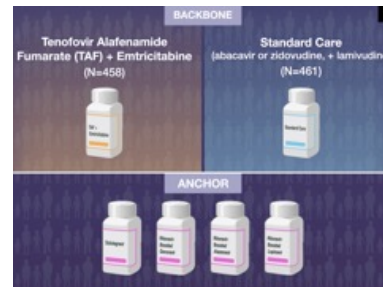
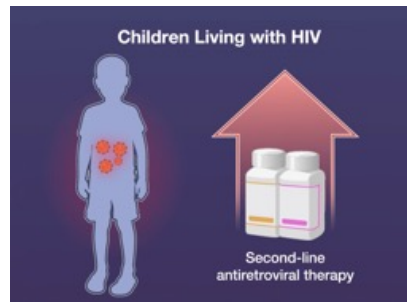


B Anchor Drug

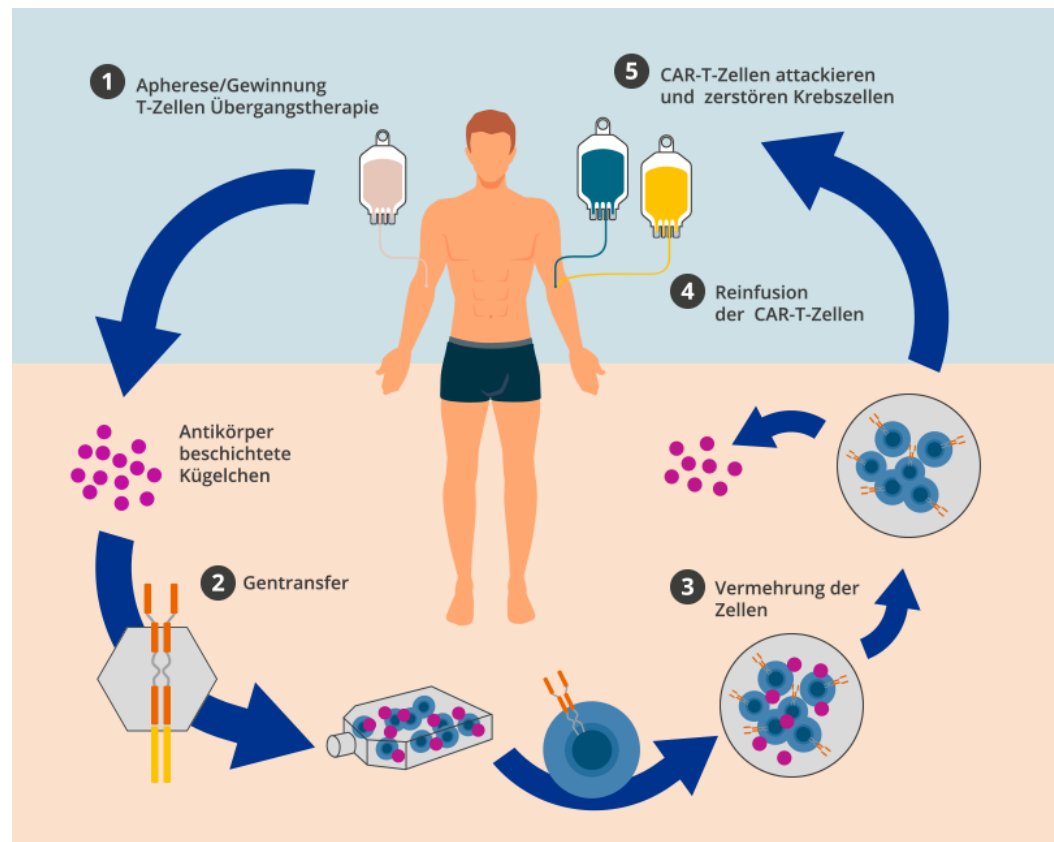


Changes in Weight-for-Age and Height-for-Age z Scores.

Changes are shown according to the assigned backbone (Panel A) or anchor drug (Panel B).



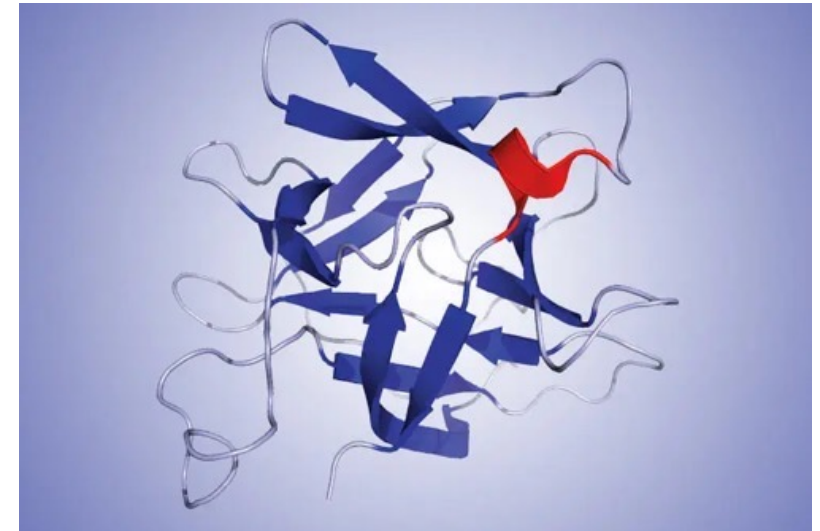
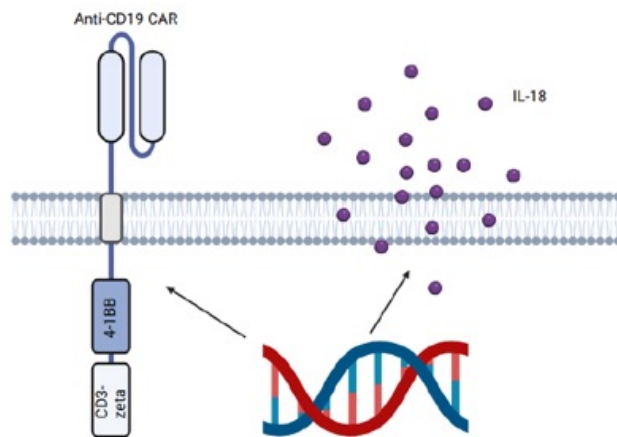
Die CAR-T-Zelltherapie ist eine innovative Krebsbehandlung, bei der T-Zellen aus dem Blut des Patienten entnommen und im Labor gentechnisch so verändert werden, dass sie Krebszellen gezielt erkennen und zerstören können. Diese modifizierten T-Zellen, die CAR-T-Zellen genannt werden, werden dann wieder in den Körper des Patienten gegeben, wo sie die Krebszellen angreifen.



DIE VIERTE GENERATION MACHT'S BESSER

IL-18 boostet CAR-T-Zell-Funktion

HuCART19-IL-18, ein CAR-T-Zell-Konstrukt der vierten Generation, erzielte bei 88 Prozent von nach einer CAR-T-Zell-Therapie rezidierten oder refraktären Patienten mit Non-Hodgkin-Lymphomen zumindest ein partielles Ansprechen. Die zusätzliche Expression von Interleukin 18 zu CD19 CAR scheint die Wirksamkeit eines CAR-T-Zell-Produktes also zu unterstützen.



Ein zusätzliches Interleukin-18-Transkript ist das Schlüsselrezept des neuen huCART19-IL18-Konstruktes.

Interleukin-18, kurz IL-18, ist ein proinflammatorisches Zytokin, das zur IL-1-Superfamilie gehört. Es wird von Makrophagen und anderen Zelltypen (u.a. dendritische Zellen, Kupffer-Zellen, Keratinozyten, Osteoblasten, Mikroglia und Fibroblasten) produziert. Interleukin-18 entsteht aus einem Vorläuferpeptid (Pro-IL-18) mit 24 kDa, das durch die Caspase 1 in seine bioaktive 18-kDa-Form aufgespalten wird. In dieser Form bindet es an den Interleukin-18-Rezeptor (IL-18R). Zusammen mit Interleukin-12 induziert es nach einer Konfrontation mit mikrobiellen Lipopolysacchariden (LPS) die zellvermittelte Immunabwehr. Wenn sie mit IL-18 stimuliert werden, sezernieren natürliche Killerzellen und bestimmte T-Zellen Interferon- γ (IFN- γ) oder Typ-II-Interferon, das eine wichtige Rolle bei der Stimulation von Makrophagen spielt.

Enhanced CAR T-Cell Therapy for Lymphoma after Previous Failure

BACKGROUND

Chimeric antigen receptor (CAR) T cells targeting CD19 have transformed the treatment of B-cell cancers, but many patients do not have long-term remission. We designed an anti-CD19 enhanced (armored) CAR T-cell product (huCART19-IL18) that secretes interleukin-18 to enhance antitumor activity.

METHODS

In this study, we assessed the safety, feasibility, and preliminary efficacy of huCART19-IL18 in patients with relapsed or refractory lymphoma after previous anti-CD19 CAR T-cell therapy. Using a 3-day manufacturing process, we administered huCART19-IL18–positive cells in doses ranging from 3×10^6 to 3×10^8 .

RESULTS

A total of 21 patients received huCART19-IL18. Cytokine release syndrome occurred in 62% of the patients (47% with grade 1 or 2), and immune effector-cell–associated neurotoxicity syndrome occurred in 14% (all grade 1 or 2). No unexpected adverse events were observed. Robust CAR T-cell expansion was detected across all dose levels. At 3 months after infusion, a complete or partial response was seen in 81% of the patients (90% confidence interval [CI], 62 to 93) and a complete response in 52% (90% CI, 33 to 71). With a median follow-up of 17.5 months (range, 3 to 34), the median duration of response was 9.6 months (90% CI, 5.5 to not reached).

CONCLUSIONS

In this small study, huCART19-IL18 had a safety profile consistent with other CAR T-cell treatments and showed promising efficacy at low cell doses in patients with lymphoma after the failure of previous anti-CD19 CAR T-cell therapy. (ClinicalTrials.gov number, [NCT04684563](#).)

A promising strategy to improve CAR T-cell efficacy involves developing fourth-generation armored CAR T cells that secrete proinflammatory cytokines to bolster antitumor activity. This approach is currently being explored in solid tumors according to the hypothesis that cytokine secretion enhances the cytotoxicity of CAR and tumor-infiltrating T cells while modifying the immunosuppressive tumor microenvironment. One such cytokine, interleukin-18, is a proinflammatory molecule that is primarily produced by macrophages and dendritic cells. Interleukin-18 enhances the activation of T cells and natural killer cells, promotes the production of interferon- γ , and has potential therapeutic applications. Preclinical studies conducted by our group and others have shown that interleukin-18–armored CAR T cells have superior antitumor efficacy and result in prolonged survival in mouse models. Building on this concept, we developed huCART19-IL18, an autologous anti-CD19 CAR T-cell product that constitutively secretes interleukin-18. In addition, huCART19-IL18 is manufactured in a rapid, 3-day process that is designed to preserve stem-cell–like characteristics and reduce exhaustion in T cells. To mitigate immunogenicity and improve CAR T-cell persistence, we incorporated a humanized anti-CD19 single-chain variable fragment.

Treatment

Autologous T cells were obtained from the patients by means of leukapheresis. Bridging therapy was optional. Manufacturing and cryopreservation of huCART19-IL18 was performed by the Clinical Cell and Vaccine Production Facility at the University of Pennsylvania. Dose levels of huCART19-IL18 between 3×10^6 and 3×10^8 cells were administered as a single intravenous infusion 2 to 5 days after lymphodepleting chemotherapy. Lymphodeletion was performed with either bendamustine (at a dose of 90 mg per square meter of body-surface area) for 2 days or a combination of cyclophosphamide (at a dose of 250 mg per square meter) and fludarabine (at a dose of 25 mg per square meter) for 3 days at the discretion of the investigator. Patients who had a clinical benefit after the huCART19-IL18 infusion but who had residual or relapsing disease could receive retreatment with huCART19-IL18.

Efficacy and Safety Measures

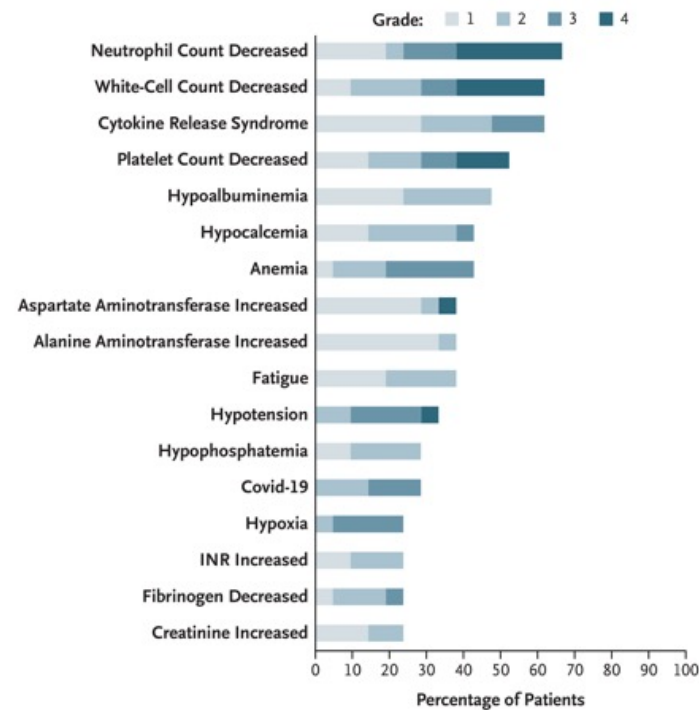
The initial response assessment was performed 3 months after the huCART19-IL18 infusion according to the Lugano 2014 response criteria. Patients were then transitioned to long-term follow-up. The grading of cytokine release syndrome and immune effector cell–associated neurotoxicity syndrome (ICANS) was performed according to consensus criteria.

Correlative Studies

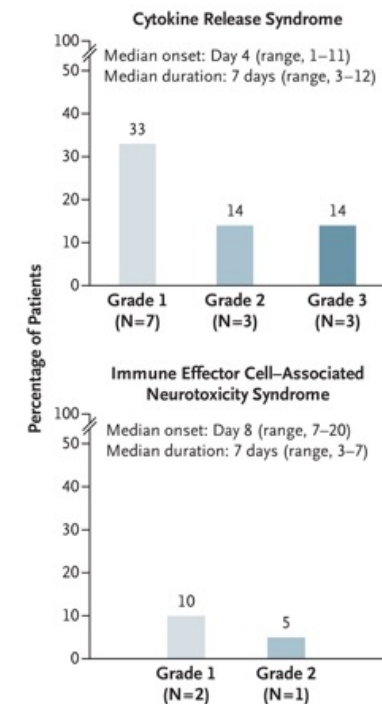
We determined the degree of huCART19-IL18 expansion and persistence by measuring the number of copies of huCART19 transgene per microgram of genomic DNA using real-time quantitative polymerase-chain-reaction (qPCR) assays.

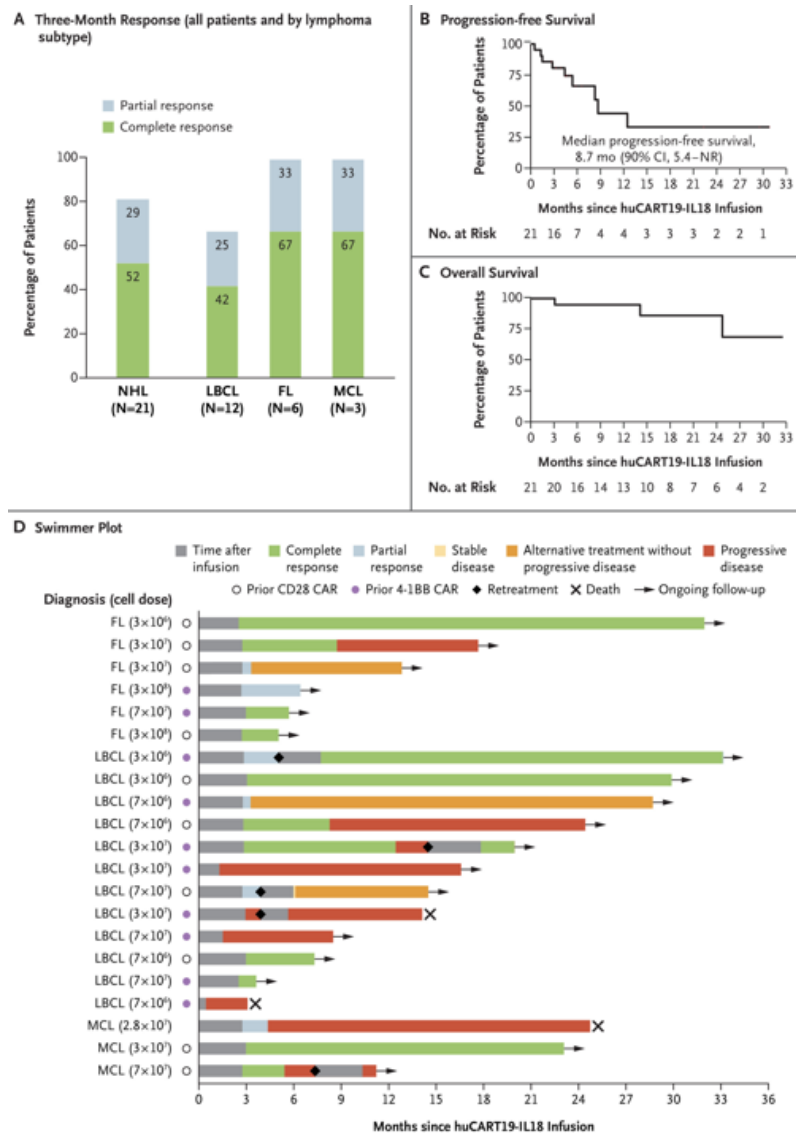
| Characteristic | Patients (N=21) |
|---|--------------------|
| Median age (range) — yr | 64 (47–74) |
| Male sex — no. (%) | 16 (76) |
| ECOG performance-status score — no. (%)† | |
| 0 | 2 (10) |
| 1 | 19 (90) |
| Lymphoma subtype — no. (%) | |
| Large B-cell lymphoma | 12 (57) |
| Diffuse large B-cell lymphoma, not other- wise specified | 8 (38) |
| Transformed follicular lymphoma | 2 (10) |
| High-grade B-cell lymphoma | 1 (5) |
| T-cell histiocyte-rich large B-cell lym- phoma | 1 (5) |
| Follicular lymphoma | 6 (29) |
| Mantle-cell lymphoma | 3 (14) |
| Median no. of previous medications (range) | 7 (4–14) |
| Previous therapy or procedure — no. (%) | |
| Autologous stem-cell transplantation | 7 (33) |
| Allogeneic stem-cell transplantation | 1 (5) |
| Bispecific antibody therapy | 7 (33) |
| Previous CAR therapy — no./total no. (%) | |
| CD28-based product | 10/20 (50) |
| Axicabtagene ciloleucel | 8/20 (40) |
| Brexucabtagene autoleucel | 2/20 (10) |
| 4-1BB-based product | 10/20 (50) |
| Tisagenlecleucel | 8/20 (40) |
| Lisocabtagene maraleucel | 2/20 (10) |
| Response to previous therapy | |
| Progressive disease — no./total no. (%) | 7/20 (35) |
| Median progression-free survival — mo (90% CI) | 6.7 (3.1–10.2) |

A Most Common Adverse Events



B Events of Special Interest

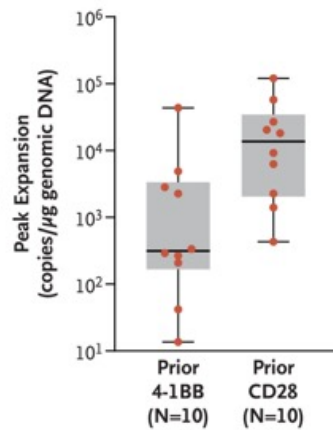




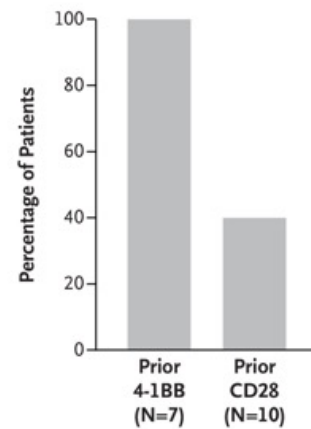
Clinical Response and Survival.

Shown are the responses at 3 months in all patients (left) and according to lymphoma subtype (right) (Panel A), Kaplan–Meier estimates of progression-free survival (Panel B) and overall survival (Panel C), and a swimmer plot indicating the response to treatment according to lymphoma subtype, huCART19-IL18 cell dose, previous second-generation CD19-directed chimeric antigen receptor (CAR) T-cell therapy, response to initial huCART19-IL18 therapy and retreatment (when applicable), and any alternative therapy that was used in patients without disease progression (Panel D). FL denotes follicular lymphoma, LBCL large B-cell lymphoma, MCL mantle-cell lymphoma, NHL non-Hodgkin’s lymphoma, and NR not reached.

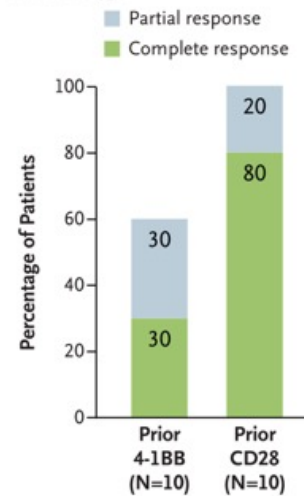
A Peak Mean Expansion of huCART19-IL18 by Prior Product Subtype



B Any Residual Second-Generation CAR in huCART19-IL18 by Prior Product Subtype



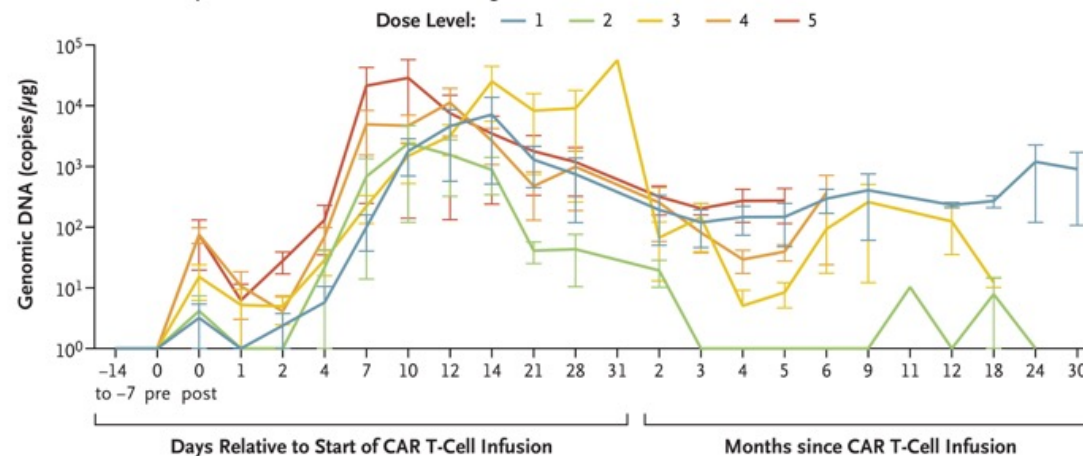
C Response Rate at 3 Months by Prior Product Subtype



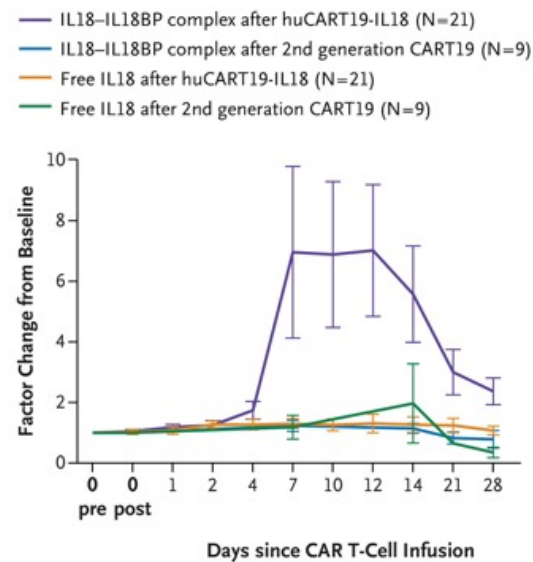
Effect of Previous CD19-Directed CAR T-Cell Therapy on Expansion and Efficacy of huCART19-IL18.

Panel A shows a comparison of values for the peak mean expansion of huCART19-IL18 according to the product subtype that the patient had previously received. The ratio of geometric means for peak expansion of huCART19-IL18 with prior CD28, as compared with prior 4-1BB product, was 16.3 (90% confidence interval [CI], 3.2 to 81.9). The huCART19-IL18 levels were assessed by means of quantitative real-time polymerase chain reaction (qPCR) and reported in copies per microgram of genomic DNA. Panel B shows the assessment of huCART19-IL18 products for the presence of previous second-generation CD19-directed CAR T cells in 17 patients. The assessment was performed with the use of Applied Biosystems TaqMan PCR to detect the sequences of integrated commercial CD19 CAR transgenes. Only 40% of the patients who had received previous treatment with a CD28-based product had detection of residual CAR, as compared with 100% of the patients who had previous treatment with a 4-1BB-based product. The odds ratio for residual CAR detection with prior CD28, as compared with prior 4-1BB product, was 0.1 (90% CI, 0 to 0.42). Panel C shows the differences in response distribution at 3 months according to previous CD19-directed CAR T-cell therapy. The odds ratio for a complete response with prior CD28, as compared with prior 4-1BB product, was 9.3 (90% CI, 1.2 to 84.0).

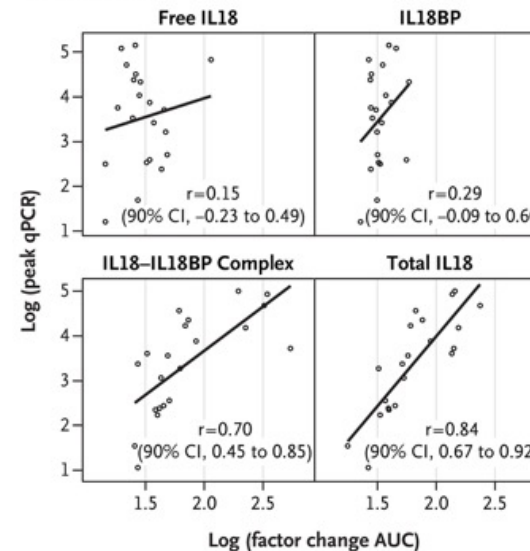
A huCART19-IL18 Expansion and Persistence According to Dose Level



B IL18–IL18BP Complex Levels after huCART19-IL18



C Correlation of IL18 Factor Change and huCART19-IL18 Cell Expansion



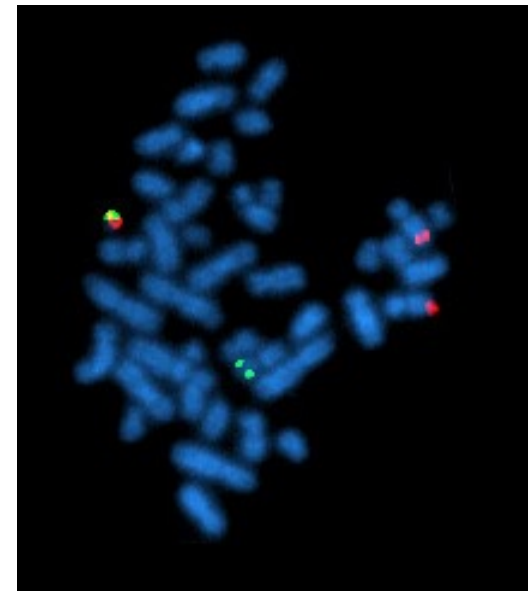
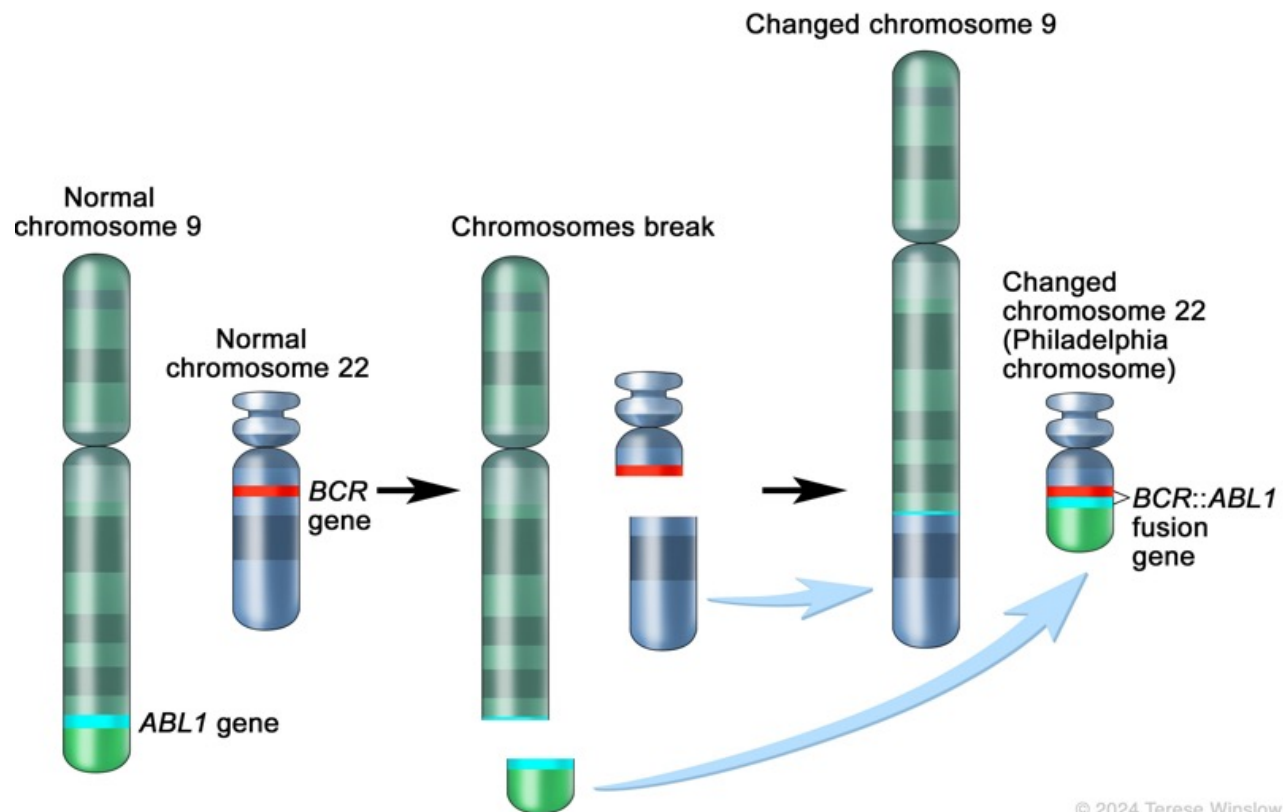
Correlative Studies.

Panel A shows the expansion of huCART19-IL18 T cells in peripheral blood as assessed by qPCR assay and measured as copies per microgram of genomic DNA, separated according to dose level 1 (DL1) through dose level 5 (DL5). Panel B shows the levels of free interleukin-18 (IL18) and interleukin-18 binding protein (IL18BP) complex, as measured by enzyme-linked immunosorbent assay. The amount of free interleukin-18 and interleukin-18 bound to IL18BP is plotted. Although serum levels of free interleukin-18 remained low (probably owing to rapid binding by IL18BP), the substantial increases in total levels of interleukin-18–IL18BP complex may serve as surrogate markers for interleukin-18 production by huCART19-IL18. The elevations in interleukin-18–IL18BP were not seen in historical blood samples after the infusion of second-generation anti-CD19 CAR T cells from the same patients. Panel C shows a scatter plot that illustrates the relationship between the log factor change in interleukin-18 forms (on the x axis) and huCART19-IL18 expansion in blood (on the y axis). Calculations of the Pearson correlation coefficient (r) and corresponding 90% confidence intervals are indicated for each plot. The increases in levels of total interleukin-18 and interleukin-18–IL18BP complex correlate with the expansion of huCART19-IL18 T cells, but no correlation is seen with levels of either free interleukin-18 or free IL18BP. AUC denotes area under the curve.

Discussion

In our trial, we found that autologous interleukin-18–armed CAR T cells had promising clinical activity in patients with relapsed or refractory CD19+ lymphomas after the failure of previous anti-CD19 CAR T-cell therapy. The treatment was associated mainly with toxic effects of grade 1 or 2, with no unexpected or delayed effects observed. Our findings indicate that 3-day manufacturing of huCART19-IL18 from autologous T cells is feasible, with 21 of 22 eligible patients receiving the product.

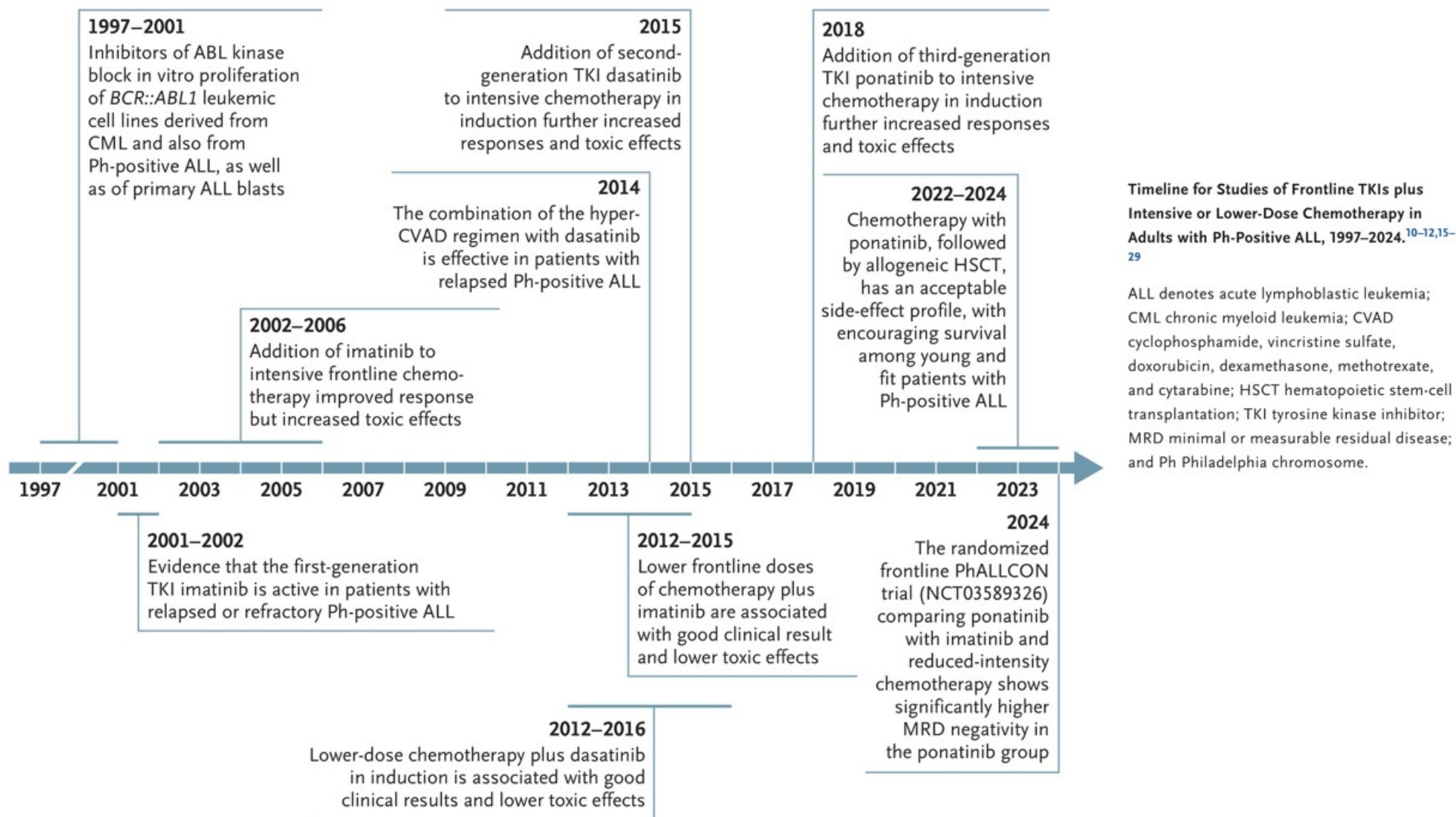
Our goal of using an expedited 3-day manufacturing process was to enrich the product with less differentiated naive-like CAR T cells, which could enhance in vivo expansion and activity. We observed the expansion of huCART19-IL18 with persistence for more than 2 years in some patients. Such persistence occurred even in patients who had received the lowest dose of huCART19-IL18 (3×10^6), which is lower than the dose used for treatment of lymphomas with currently available second-generation CAR T products by a factor of approximately 20 to 100. Although the median vein-to-vein time was more than 2 months in this trial because of the protocol-mandated safety stagger design, a shorter manufacturing process may have the additional benefit of reducing the time required to produce and administer the CAR T-cell therapy.



Ph-Positive Acute Lymphoblastic Leukemia — 25 Years of Progress

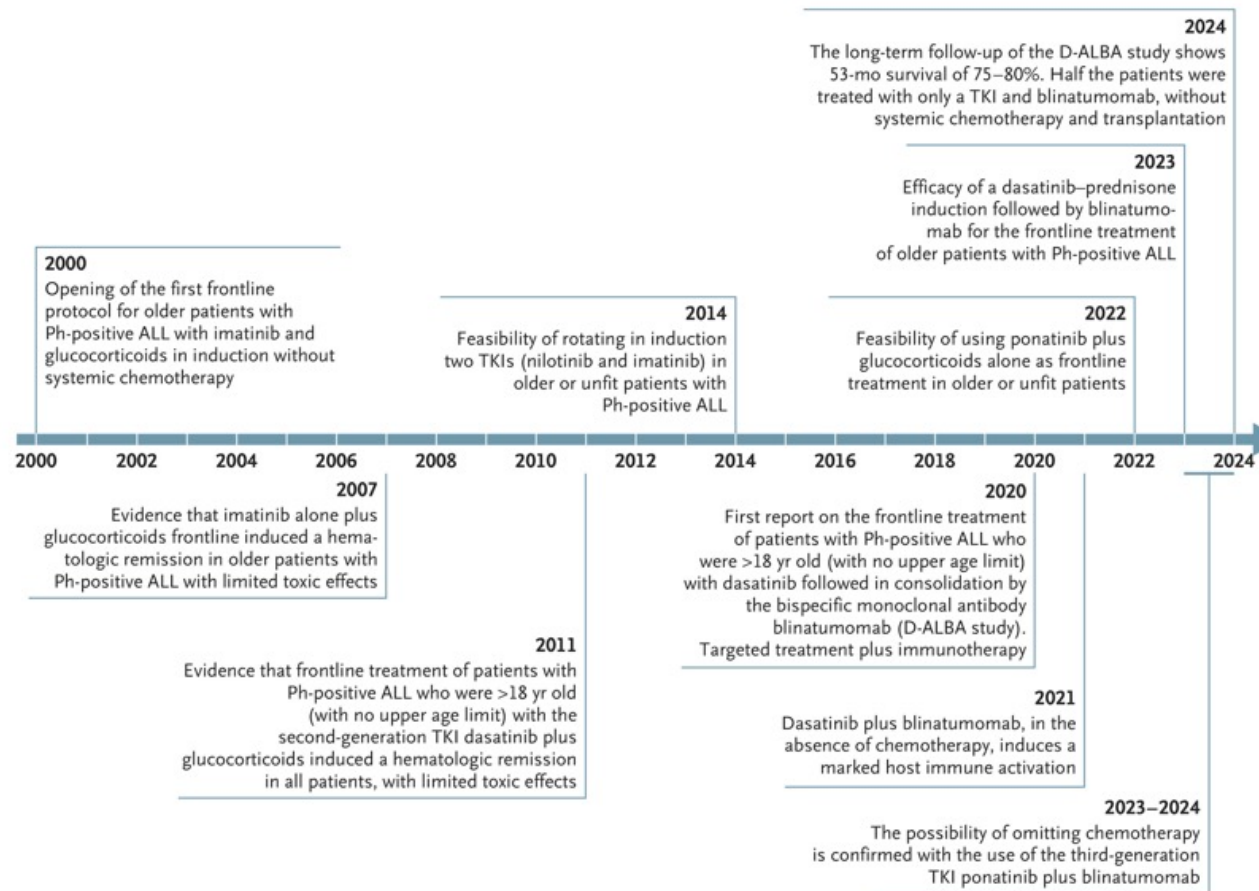
Ph-Positive Acute Lymphoblastic Leukemia

- Philadelphia chromosome–positive acute lymphoblastic leukemia (Ph-positive ALL) is the most common genetic ALL subgroup in adulthood, with a prevalence that increases with age. In patients over the age of 50 years, Ph-positive disease accounts for about 50% of cases of B-lineage ALL.
- Before the advent of tyrosine kinase inhibitors (TKIs), Ph-positive ALL was the hematologic cancer with the worst outcome. Only the few patients who could undergo allogeneic stem-cell transplantation had a chance of long-term survival.
- Initially, TKIs were added to conventional intensive chemotherapy. Since this approach had notable toxic effects, reduced-intensity chemotherapy programs, plus TKIs, were used, an approach resulting in improved responses and outcomes, with fewer toxic effects.
- In the year 2000, the GIMEMA cooperative study group started using a TKI plus glucocorticoids for induction without systemic chemotherapy. First-, second-, and third-generation TKIs have been used over the years. These studies have shown the feasibility of this approach, with hematologic complete responses in 94 to 100% of adults, irrespective of age, and with limited toxic effects.
- The addition of the bispecific monoclonal antibody blinatumomab (an anti-CD19 and anti-CD3 antibody) in consolidation therapy has further improved molecular response and survival.
- As for all forms of ALL, a sustained molecular MRD negativity in the bone marrow should be the primary goal of frontline treatment.
- The combination of TKI (targeted treatment) and blinatumomab (immunotherapy) is associated with long-term survival of 75 to 80%, with many patients never receiving systemic chemotherapy or undergoing transplantation.



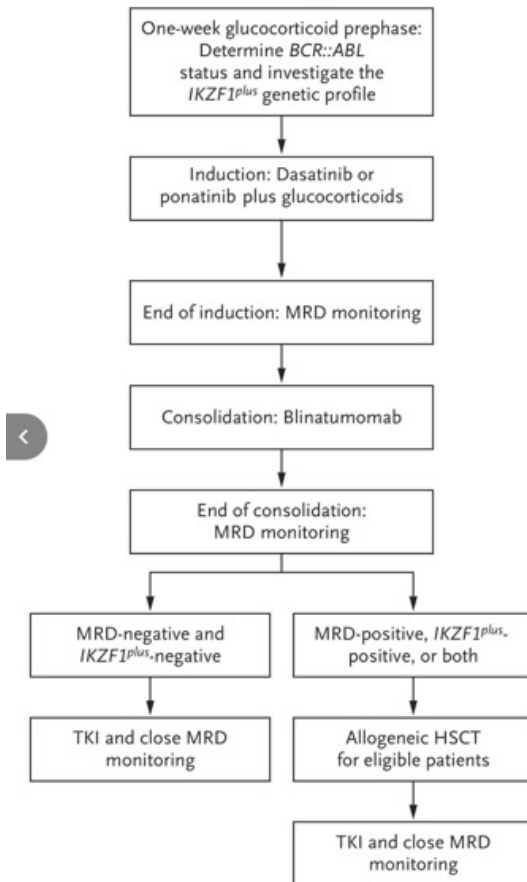
The GIMEMA Frontline Strategy without Chemotherapy from 2000 to 2025 in Patients with Ph-Positive ALL.

| Study Protocol | Age | Induction Therapy | Complete Remission |
|--------------------------------------|--------------|--|--------------------|
| | yr | | % of patients |
| LAL0201-B ³⁰ | >60 | Imatinib | 100 |
| LAL1205 ³¹ | >18 | Dasatinib | 100 |
| LAL0904, 3rd amendment ²⁰ | 16–60 | Imatinib followed by chemotherapy (with or without HSCT) | 96 |
| LAL1408 ³² | >60 or unfit | Nilotinib and imatinib | 94 |
| LAL1509 ³³ | 18–60 | Dasatinib and total therapy† | 97 |
| LAL1811 ³⁴ | >60 or unfit | Ponatinib | 95 |
| LAL2116 ^{35,36} | >18 | Dasatinib plus blinatumomab | 98 |
| ALL2820 ^{37,38} | >18 | Ponatinib plus blinatumomab | 95 |

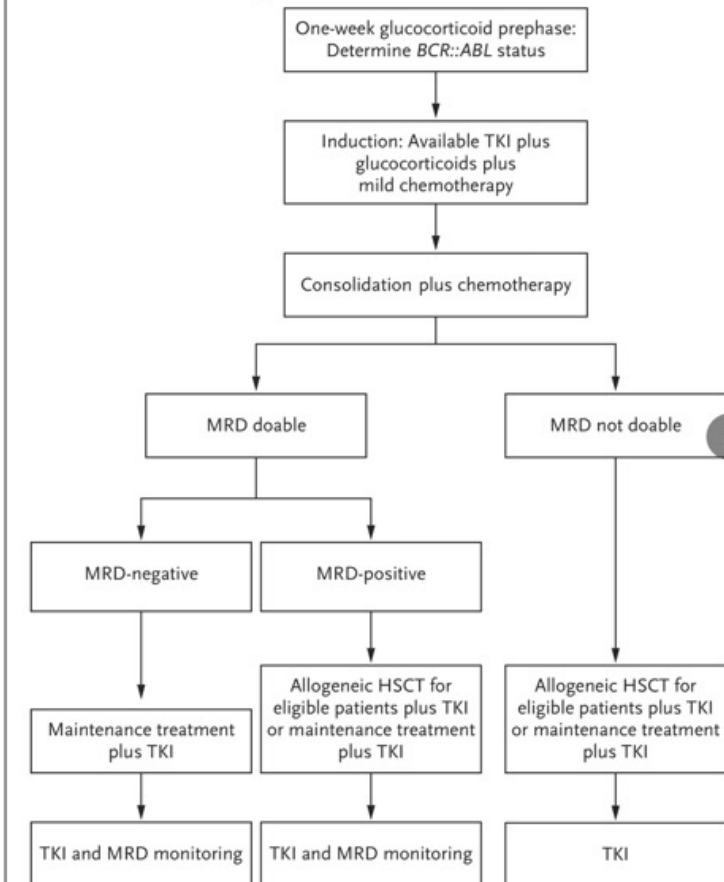


Timeline for Studies of Induction and Consolidation Treatment without Systemic Chemotherapy in Adults with Ph-Positive ALL, 2000–2024. [30–38,60,62,63](#)

A Recommended Frontline Strategy



B Real-Life Frontline Strategy



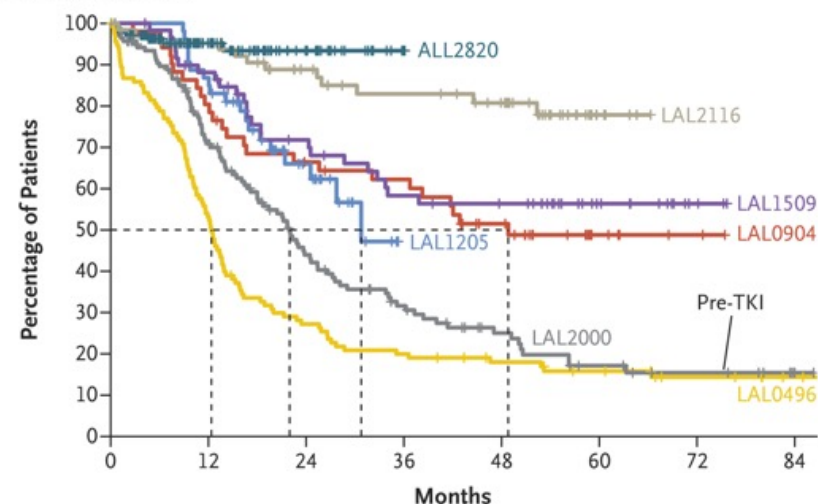
Recommended and Real-Life Strategies for Frontline Treatment in Adults of All Ages with Ph-Positive ALL.

Panel A shows the frontline strategy that is recommended when all the required components of frontline treatment are available. Panel B shows the strategy in real-life scenarios when one or more of the components of the recommended strategy are not available.

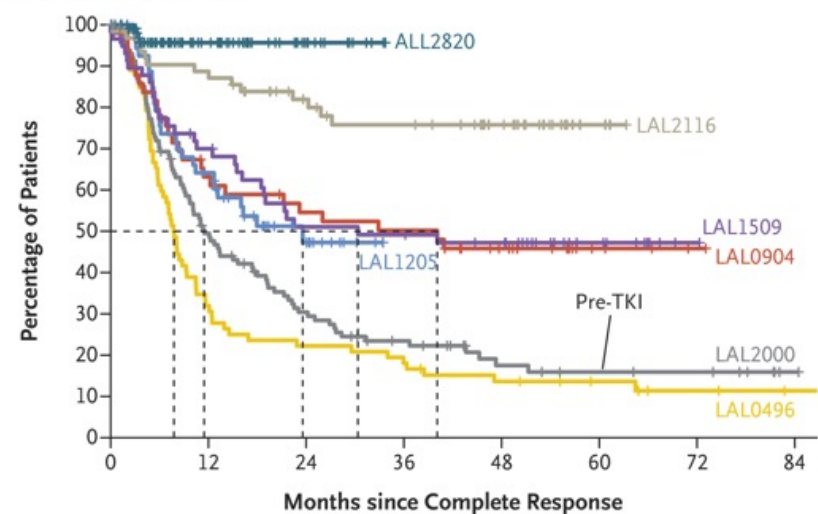
Conclusions

In the year 2000, a TKI without chemotherapy was introduced for the frontline treatment of older adults with Ph-positive ALL, which gave rise to a new era in the management of this disease. If every piece of the puzzle is in place — early diagnosis, TKI and blinatumomab availability, and MRD monitoring — today, 25 years later, we can expect to cure most adults with Ph-positive ALL, irrespective of age. Efforts to do so should ensure that all these components are widely available, including availability in middle- and low-income countries. A subcutaneous formulation of blinatumomab is under active investigation, with very encouraging early results. We can thus expect that soon most patients with Ph-positive ALL will be treated with an oral TKI plus subcutaneous blinatumomab. These past 25 years have witnessed a true revolution in the management and outcome of what used to be the most lethal hematologic cancer, as illustrated by the increases in overall and disease-free survival shown.

A Overall Survival



B Disease-free Survival

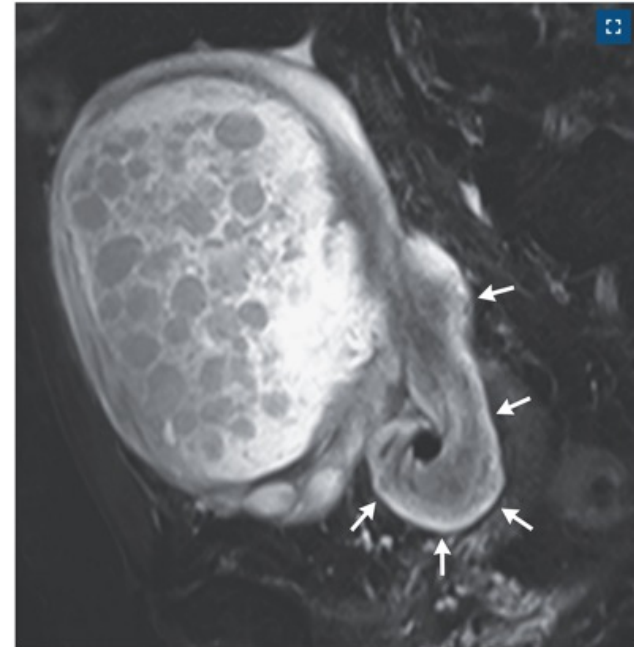


Paget's Disease of Bone



An 80-year-old woman presented to the endocrinology clinic with a several-year history of gradual forehead enlargement and progressive hearing loss. She reported no headache or bone pain. Sixteen years earlier, mild thickening of the skull had been noted on imaging studies that had been conducted to evaluate early-stage breast cancer, which was successfully treated. However, the patient had not followed up on the incidental radiographic finding as recommended. At the current presentation, physical examination was notable for frontal bossing (Panel A). The alkaline phosphatase level was 592 IU per liter (reference range, 38 to 113). A radiograph of the skull showed marked thickening of the calvarium with irregular patches of sclerosis and lucency, resulting in a cotton-wool appearance (Panel B). Whole-body computed tomography showed no evidence of cancer but did reveal severe cortical thickening, sclerosis, and focal osteolysis of the skull (Panel C). Audiometry confirmed sensorineural hearing loss. A radionuclide bone scan revealed increased uptake in the skull and the left side of the pelvis (Panel D). A diagnosis of Paget's disease of bone was made. Treatment with a bisphosphonate was initiated. At a 3-month follow-up visit, the alkaline phosphatase level had decreased, but the hearing loss and frontal bossing remained unchanged.

Torsion of a Mature Cystic Ovarian Teratoma



A 59-year-old woman presented with a 1-day history of sudden-onset, sharp pain in her left lower abdomen. Physical examination was notable for tenderness to palpation and a firm, nonmobile mass in the left lower quadrant. On pelvic examination, there was cervical motion tenderness. Although ultrasonography is the ideal imaging method for assessment of adnexal masses, magnetic resonance imaging of the abdomen and pelvis was performed in this case. A cystic mass measuring 11.9 cm by 9.0 cm by 12.5 cm was seen in the left adnexa (T2-weighted, fat-saturated sequence; sagittal view). Multiple free-floating, hypointense nodules were seen within the mass. This finding — known as the sack-of-marbles sign — represents globules of sebum or fat within a cystic lesion. There was also twisting of the ovarian pedicle — a finding known as the whirlpool sign — indicating ovarian torsion (arrows). A diagnosis of torsion of a mature cystic ovarian teratoma was confirmed during a laparotomy in which the cyst, left ovary, and left fallopian tube were removed. Sebaceous material, fat, and hair were found when the resected cyst was incised. Histopathological findings were consistent with a mature cystic teratoma with extensive hemorrhagic necrosis. The patient recovered well and had no recurrence over 10 years of follow-up.

Case 14-2025: A 29-Year-Old Woman with Peritonsillar Swelling and Bleeding

A 29-year-old woman was admitted to this hospital because of sore throat and peritonsillar swelling and bleeding. The patient had been well until 7 weeks before the current admission, when sore throat developed. When the soreness did not abate after 1 week, she sought evaluation at a primary care clinic of another hospital. Screening tests of a nasopharyngeal swab for severe acute respiratory syndrome coronavirus 2 RNA and streptococcal antigen were negative. The patient was instructed to rest and drink fluids.

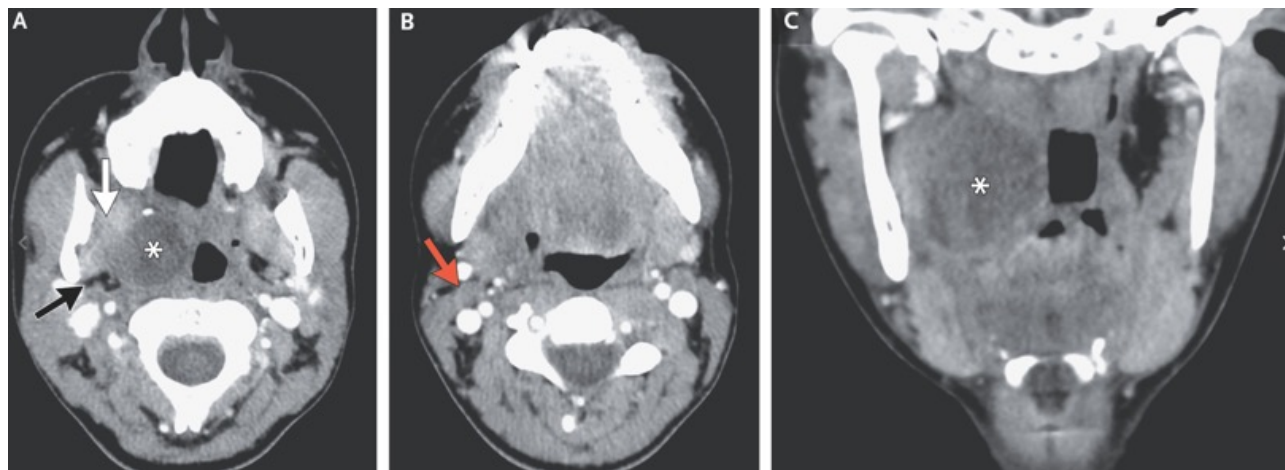
During the next 4 days, the throat soreness increased in severity to the point that the patient was unable to sleep through the night. She returned to the primary care clinic, and azithromycin was prescribed. During the subsequent 5 days, she took the prescribed antibiotic, but the throat soreness did not abate. She called the primary care clinic and was instructed to go to the emergency department of the other hospital.

On evaluation in the emergency department, 31 days before the current admission, the patient described pain and swelling on the right side of the throat and noted that when she swallowed food, it felt as though the food became “stuck.” She reported fatigue but no fever, headache, shortness of breath, cough, nausea, vomiting, abdominal pain, diarrhea, or rash.

On examination, the temporal temperature was 36.9°C, the blood pressure 105/77 mm Hg, the heart rate 74 beats per minute, and the oxygen saturation 99% while the patient was breathing ambient air. She appeared well and had a normal voice without hoarseness or stridor. The mucous membranes were moist. Edema and fluctuance were seen in the right peritonsillar area of the soft palate. The right tonsil had no erythema, swelling, or exudate. The uvula deviated to the left. No trismus was noted. The lungs were clear on auscultation. There was no palpable lymphadenopathy and no rash. The white-cell count was 6700 per microliter (reference range, 4000 to 11,000). Other laboratory test results are shown.

| Variable | Reference Range, Other Hospital | On Initial Presentation, Other Hospital | Reference Range, Adults, This Hospital* | On Admission, This Hospital |
|--|------------------------------------|---|---|--------------------------------|
| White-cell count (per μ l) | 4000–11,000 | 6700 | 4500–11,000 | 13,470 |
| Differential count (per μ l) | | | | |
| Neutrophils | 1600–8300 | 4400 | 1800–7700 | 8970 |
| Lymphocytes | 600–5900 | 1800 | 1000–4800 | 2750 |
| Monocytes | 200–1400 | 500 | 200–1200 | 1420 |
| Eosinophils | 0–800 | 0 | 0–900 | 200 |
| Basophils | 0–100 | 0 | 0–300 | 70 |
| Hemoglobin (g/dl) | 11.2–15.7 | 13.9 | 12.0–16.0 | 15.1 |
| Hematocrit (%) | 34.1–44.9 | 41.5 | 36.0–46.0 | 44.9 |
| Platelet count (per μ l) | 150,000–400,000 | 261,000 | 150,000–400,000 | 339,000 |
| Prothrombin time (sec) | — | — | 11.5–14.5 | 12.5 |
| Prothrombin-time international normalized ratio | — | — | 0.9–1.1 | 0.9 |
| Activated partial-thromboplastin time (sec) | — | — | 22.0–36.0 | 28.5 |

Computed tomography (CT) of the neck, performed after the intravenous administration of contrast material, revealed a hypodense lesion in the right peritonsillar region of the oropharynx that measured 2.6 cm by 2.1 cm by 3.8 cm. There was minimal peripheral enhancement. The presence of the lesion resulted in mild effacement of the oropharynx. Minimal fat stranding was present in the right parapharyngeal fat. No edema was noted in the right medial pterygoid muscle. A right jugulodigastric lymph node had a normal appearance. The patient was discharged home with a prescription for amoxicillin–clavulanate and was advised to schedule a follow-up visit at the otolaryngology clinic of the other hospital. Twenty-six days before the current admission, the patient was evaluated at the otolaryngology clinic of the other hospital. The right peritonsillar lesion was incised, and 3 ml of sanguineous fluid was drained. The next day, the patient returned to the otolaryngology clinic because of increased pain and swelling on the right side of the throat and bleeding from the incision site.



Initial CT Scans of the Neck.

Contrast-enhanced CT of the neck was performed on initial presentation to the other hospital. Axial (Panels A and B) and coronal (Panel C) images at the level of the oropharynx show a hypodense lesion (Panels A and C, asterisks) with no substantial rim enhancement centered in the right peritonsillar region of the oropharynx. The presence of the mass has resulted in mild effacement of the oropharynx. There is minimal, if any, fat stranding in the right parapharyngeal fat (Panel A, black arrow). The right medial pterygoid muscle (Panel A, white arrow) and right jugulodigastric lymph node (Panel B, red arrow) have a normal appearance.

On examination, the right peritonsillar area was more edematous than it had been the previous day, and ecchymosis, friable mucosa, and some necrotic granulation tissue were noted. The incision site was partially open with oozing of bloody fluid. A repeat drainage of fluid at this site was attempted, and a hematoma was evacuated with suction. Bleeding was treated with silver nitrate and oxidized regenerated cellulose; however, oozing at the site continued. The patient was taken to the operating room urgently.

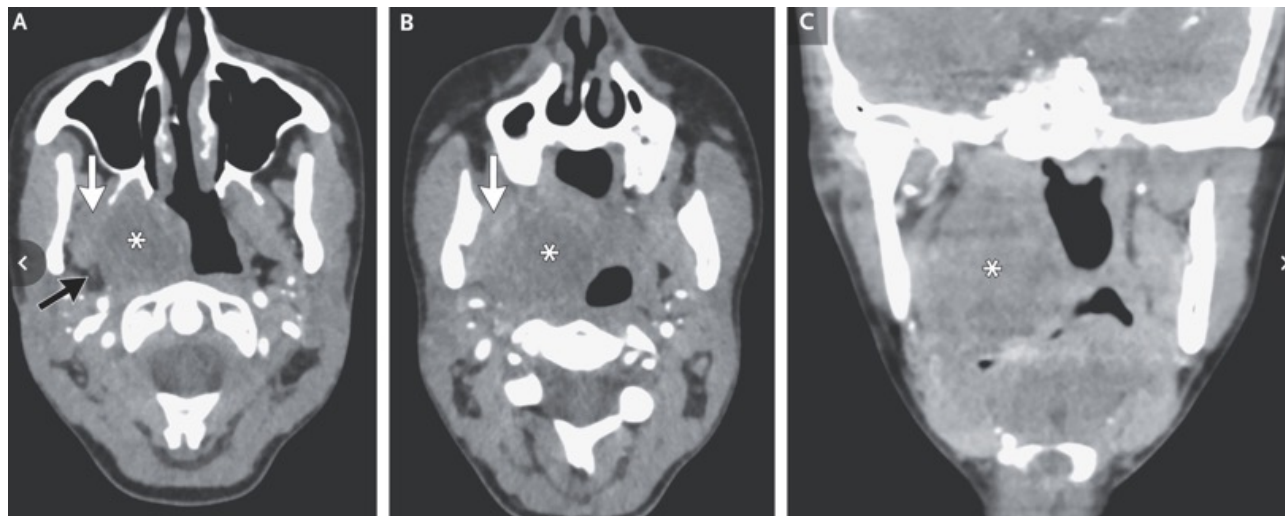
On examination while the patient was under anesthesia, there was oozing of bloody fluid from multiple sites in the right peritonsillar area. Oxymetazoline-soaked gauze and a human gelatin–thrombin matrix sealant were used to achieve hemostasis. The patient was admitted to the other hospital. Dexamethasone and ampicillin–sulbactam were administered, and an infusion of lactated Ringer’s solution was initiated. On the second hospital day, after confirmation that bleeding had stopped, she was discharged home with instructions to resume treatment with amoxicillin–clavulanate and to take acetaminophen and oxycodone as needed for pain.

During the next 2 weeks, the pain and swelling on the right side of the throat decreased. However, 8 days before the current admission, the patient noticed that her voice sounded “froggy.” She returned to the otolaryngology clinic of the other hospital, and treatment with clindamycin and methylprednisolone was started. During the subsequent 4 days, the patient noticed intermittent bleeding on the right side of the throat. She was referred to the otolaryngology clinic of a second hospital. Four days before the current admission, aspiration of the swollen area of the right peritonsillar region reportedly yielded dark blood.

On the morning of the current admission, the patient awoke with increased pain and swelling on the right side of the throat. Several hours later, she felt a “pop” and noticed bleeding on the right side of the throat. She presented to the otolaryngology clinic of the second hospital, where she received oral vitamin K and aminocaproic acid. She was advised to seek evaluation in the emergency department of this hospital.

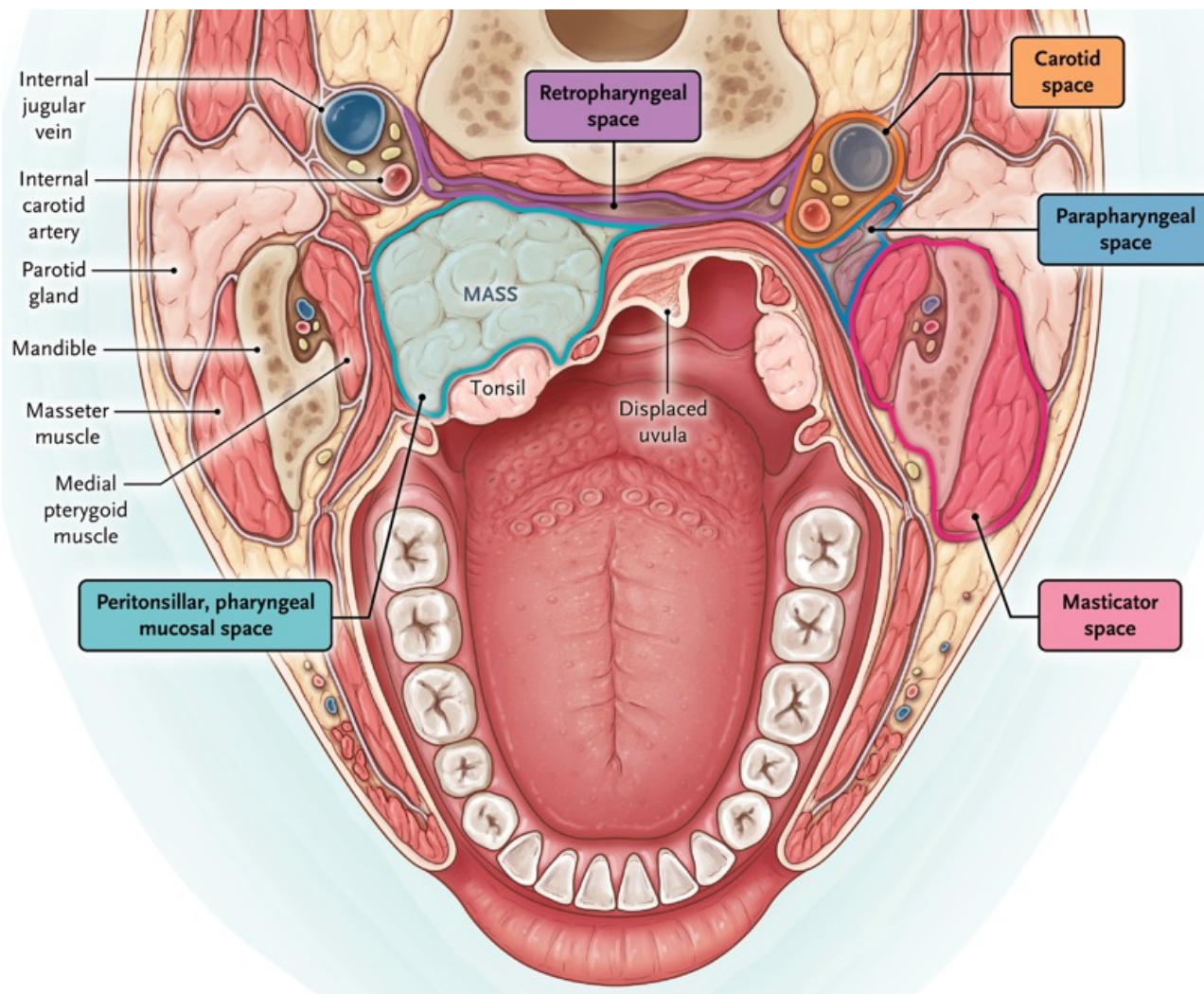
CT angiography of the neck, performed after the intravenous administration of contrast material, revealed that the size of the hypodense right peritonsillar lesion had increased to 3.4 cm by 3.6 cm by 4.6 cm, with mildly complex attenuation. The lesion involved the soft palate and extended into the submucosal nasopharynx. Minimal rim enhancement and mild fat stranding in the right parapharyngeal fat were unchanged from the previous imaging study. The lesion was inseparable from the right medial pterygoid muscle, which was not enlarged or edematous. No extravasation of contrast material was seen.

Treatment with ampicillin–sulbactam was started. Vitamin K and aminocaproic acid therapy were stopped. Intravenous hydromorphone, acetaminophen, and ondansetron were administered. The patient was admitted to the surgical intensive care unit.



CT Angiogram of the Neck Obtained 1 Month after Initial Presentation.

Contrast-enhanced CT angiography of the neck was performed 1 month after the patient's initial presentation to the first hospital. Axial (Panels A and B) and coronal (Panel C) images show enlargement of the right peritonsillar lesion (asterisks), which now extends above the soft palate and into the submucosal nasopharynx. Although the lesion is inseparable from the right medial pterygoid muscle, no enlargement or edema is present within the muscle (Panels A and B, white arrows). Minimal fat stranding is seen in the right parapharyngeal fat (Panel A, black arrow).



Deep Neck Spaces and Their Associated Tissues.

Shown is the location of the patient's mass (approximately 4 cm in diameter) in the right peritonsillar, pharyngeal mucosal space with medial displacement of the palatine tonsil. The mass does not invade the pterygoid muscles in the masticator space. The parapharyngeal fat is displaced posterolaterally, without fat stranding that would have suggested inflammation. The neurovascular structures within the carotid space are intact and displaced posteriorly. There is no extension into the retropharyngeal space.

Peritonsillar Abscess

This patient initially presented for a consultation with an otolaryngologist after a 3-week history of pain on the right side of the throat, dysphagia, peritonsillar edema, and identification of a 3.8-cm hypodense lesion within the peritonsillar space on CT.

Benign Neoplasm

At this point, a neoplastic process rises to the top of the differential diagnosis. A number of benign neoplasms (papillomas, fibromas, muscle and connective-tissue tumors, vascular tumors, and salivary-gland tumors) are related to the tissue types located in the peritonsillar and pharyngeal mucosal spaces of the oropharynx.

Malignant Neoplasm

Malignant neoplasms that warrant consideration in this patient are squamous-cell carcinoma, lymphoma, salivary-gland cancer, and sarcoma.

Squamous-Cell Carcinoma

Squamous-cell carcinoma is the most common cancer that involves the tonsils. Although squamous-cell carcinoma of the tonsils has historically been caused primarily by tobacco-related and alcohol-related carcinogenesis, it is now more commonly associated with human papillomavirus types 16 and 18.

Lymphoma

When a rapidly growing tonsillar mass is encountered in a young patient, it is important to consider lymphoma. Extranodal non-Hodgkin's lymphoma of the head and neck region usually develops within the lymphoid tissues of Waldeyer's ring; the palatine tonsils are the most common site of involvement.

Salivary-Gland Cancer

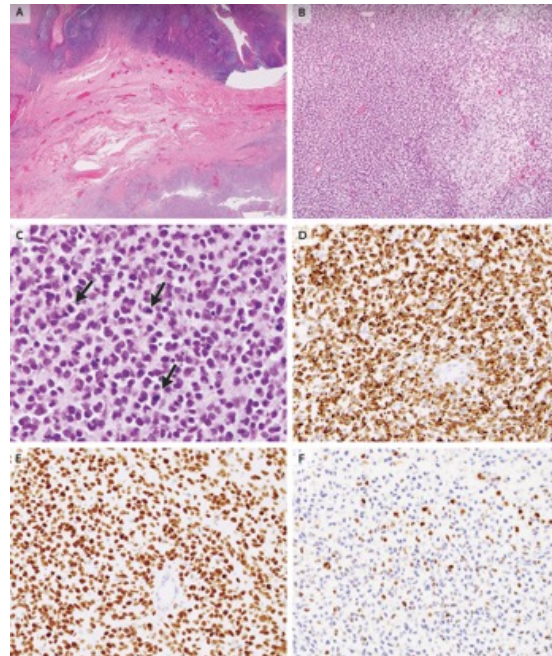
Minor salivary-gland cancers, which account for less than 3% of head and neck cancers, may develop within the soft tissues surrounding the tonsils and inside the soft palate.³ Low-grade tumors may lack the clinical and radiographic evidence of local invasion and lymphadenopathy, as in this patient, but would also have a slow rate of growth

Sarcoma

Sarcomas are rare tumors that may arise from the musculoskeletal and connective tissues of the neck. Nearly 200 different subtypes have been reported in adults. These tumors may appear as a painless mass without lymph-node involvement. When I evaluated this patient, I thought that the most likely diagnosis was a malignant neoplasm — possibly minor salivary-gland cancer, lymphoma, or sarcoma — but it is not possible to distinguish among these cancers without first obtaining tissue for pathological evaluation. Given this patient's presentation involving bleeding from a large oropharyngeal mass and concerns about airway complications, examination and biopsy while the patient was under anesthesia was recommended.

Diagnosis

Malignant neoplasm consistent with minor salivary-gland cancer, lymphoma, or sarcoma.



Biopsy Specimen of the Oropharyngeal Mass.

Hematoxylin and eosin staining of the oropharyngeal tissue specimen (Panel A) shows an infiltrative round-cell neoplasm deep in the tonsil tissue. At higher magnification, an alternating hypocellular and hypercellular pattern of growth is seen in a myxoid background (Panel B), and round-to-oval cells with a high nuclear-to-cytoplasmic ratio, scant amphophilic cytoplasm, and numerous mitoses are noted (Panel C, arrows). Immunohistochemical staining shows that the tumor cells are diffusely positive for desmin (Panel D) and myoD1 (Panel E) and multifocally positive for myogenin (Panel F).

A representative formalin-fixed, paraffin-embedded tissue specimen containing tumor cells was sent for molecular testing. Fluorescence in situ hybridization, performed with break-apart probes to the *FOXO1* locus, did not detect the presence of *FOXO1* rearrangements, which effectively ruled out a diagnosis of alveolar rhabdomyosarcoma. Next-generation sequencing revealed variants in the RAS pathway, including single-nucleotide variants in *HRAS* and *GNAS* and copy-number variants in *HRAS*. Somatic driver mutations involving the RAS pathway have been identified in genomic studies of embryonal rhabdomyosarcoma. Cytogenetic analysis of fresh tumor tissue obtained from this patient revealed a complex karyotype, including trisomy 8. Although not specific, trisomy 8 is a recurrent aberration observed in patients with rhabdomyosarcoma.

Management

Diagnostic tonsillectomy, chemotherapy, and radiotherapy.

Pathological Diagnosis

Embryonal rhabdomyosarcoma.

Patient Perspective

The Patient: My first symptom was a sore throat that never went away. As the swelling and list of unusual symptoms grew, my confidence that it was nothing shrank. It was confusing and exhausting.

Self-advocacy is often imagined as tenacity, but it was just how I was channeling my frustration. Frustration at my body for being so mysterious and stumping a competent medical community. Frustration at not having answers. Looking for a diagnosis felt like being underwater and seeing the reflection of the sun, trying to swim to the surface but realizing you're too far below and running out of air. I firmly believe that if patients speak up in these moments and physicians use stories like mine to inform how they approach the unusual, maybe one fewer person will experience what I did.

Final Diagnosis

Embryonal rhabdomyosarcoma of the pharynx.



Prevalence of sexual violence against children and age at first exposure: a global analysis by location, age, and sex (1990–2023)

Summary

Background Measuring sexual violence against children (SVAC) is vital to prevention and advocacy efforts, yet existing prevalence studies present estimates for few countries. Here we estimate the prevalence of SVAC for 204 countries by age and sex, from 1990 to 2023, and also report the age at which young survivors of lifetime sexual violence first experienced sexual violence.

Methods We reviewed publicly available repositories for data on the prevalence of SVAC. To harmonise heterogeneity in the identified input data, we adjusted for alternative case definitions of SVAC and differential disclosure by survey mode. We then used a spatiotemporal Gaussian process regression to estimate a full time series of exposure to SVAC for each age-sex-country combination. We accounted for uncertainty in the underlying data and modelling processes. We also analysed the age at which adolescent and young adult survivors of lifetime sexual violence first experienced this type of violence by sex, data source, and world region.

Findings We estimate that the global age-standardised prevalence of SVAC was 18·9% (95% uncertainty interval [UI] 16·0–25·2) for females and 14·8% (9·5–23·5) for males in 2023. At the super-region level, these estimates ranged from 12·2% (9·0–17·2) in southeast Asia, east Asia, and Oceania to 26·8% (21·9–32·7) in south Asia for females and from 12·3% (5·2–24·6) in central Europe, eastern Europe, and central Asia to 18·6% (9·7–32·3) in sub-Saharan Africa for males. At the country level, age-standardised estimates ranged from 6·9% (4·8–9·6) in Montenegro to 42·6% (34·4–52·1) in Solomon Islands among females and from 4·2% (1·7–9·2) in Mongolia to 28·3% (13·2–49·8) in Côte d'Ivoire among males. Globally, these estimates remained relatively stable since 1990, with slight variations at the country and regional levels. We also find that the first experience of sexual violence among adolescents and young people occurred before the age of 18 years for 67·3% of female and 71·9% of male survivors.

Interpretation The prevalence of SVAC is extremely high for both females and males across the globe. Given data sparsity and ongoing measurement challenges, findings probably underestimate the true pervasiveness of SVAC. An overwhelmingly high proportion of survivors first experienced sexual violence during childhood, revealing a narrow yet sensitive window that should be targeted in future prevention efforts. It is a moral imperative to protect children from violence and mitigate its compounding impacts on health across the lifecourse.

Funding The Gates Foundation.

Introduction

Sexual violence against children (SVAC) is a pervasive health and human rights issue that curtails the safety and wellbeing of children globally and accounts for a substantial portion of morbidity.^{1,2} Existing studies on the health effects of SVAC have made its long-term somatic (eg, asthma and STIs) and psychiatric (eg, major depression and anxiety) effects increasingly clear,^{3,4} and others have documented SVAC's association with stress-response behaviours such as alcohol and substance use.^{5,6} In addition to its direct impacts on health, violence against children limits individual development, hindering both educational attainment and economic achievement,^{7,8} ultimately leading to diminished wellbeing trajectories for survivors. These consequences extend beyond survivors too, as exposure to SVAC is associated with increased odds of future violence perpetration and criminal offending, thus perpetuating a cycle of violence within communities and across generations.^{9,10} To counter these adverse outcomes and their compounding effects, there have been increasing investments in global movements towards prevention and ending SVAC and other forms of violence against children, including the first-ever Global Ministerial Conference on Ending Violence Against Children in 2024.^{11–14}

Accurately monitoring SVAC is essential to the future success of such prevention efforts, national and international zero-target goals, and support programmes for survivors and their families. Better evidence on the prevalence, characteristics, and consequences of SVAC can guide primary and secondary prevention efforts from health care, educational, criminal justice, and social welfare systems. Prevalence estimates can also provide benchmarks for global initiatives like the Sustainable Development Goals (SDGs), which were established by the UN to reduce global inequalities and include targets like SDG 16.2.3 that measures the proportion of young people who have experienced SVAC.¹³

Methods

Overview

Here we summarise the main steps in the prevalence estimation process, and the appendix provides further details on data sources and modelling strategies (pp 5–13). All analyses were done in R. This study adheres to the GATHER¹⁹ recommendations (appendix pp 3–4).

Definitions and data sources

The case definition of SVAC used in this study is having ever experienced intercourse or other contact sexual violence (ie, fondling and other sexual touching) before the age of 18 years, in which the contact was unwanted (ie, physically forced or coerced). This case definition does not include online abuse or exploitation, as information on these forms of violence is usually measured separately.²⁰ It also closely aligns with SDG Indicator 16.2.3¹³ and the International Classification of Violence Against Children (ICVAC),²¹ a framework established by UNICEF that provides a set of internationally agreed upon operational concepts and definitions. In keeping with this system and the UN Convention on the Rights of the Child,^{12,21} we use the term violence to refer to any sexual violence against children, regardless of victim–perpetrator relationship. We consider alternative case definitions in our data seeking, extraction, processing, and modelling stages as described below.

We searched the Global Health Data Exchange, the WHO Global Database on the Prevalence of Violence against Women,²² and the United Nations Entity for Gender Equality and the Empowerment of Women (UN Women) Global Database on Violence against Women²³ for data reporting on exposure to SVAC based on our case definition or an acceptable alternative definition (appendix pp 6–7). Each database was selected for employing targeted and systematic search strategies to identify data on sexual violence against children, resulting in a comprehensive list of sources spanning multiple time periods, geographies, and populations. Briefly, the Global Health Data Exchange is a catalogue of health and demographic surveys, censuses, disease registries, surveillance systems, statistical yearbooks, and scientific publications that have been identified by systematic and targeted data seeking efforts by the Institute for Health Metrics and Evaluation and its network of collaborators. The WHO Global Database on Prevalence of Violence Against Women contains representative prevalence studies of sexual violence that were identified via a systematic review of six electronic databases²⁴ and supplemented by targeted, manual searches of grey literature. Lastly, UN Women's Global Database on Violence against Women contains relevant surveillance systems, reports, surveys, laws, and legislations submitted by UN member states. Further details on each database can be found in the appendix (pp 5–6).

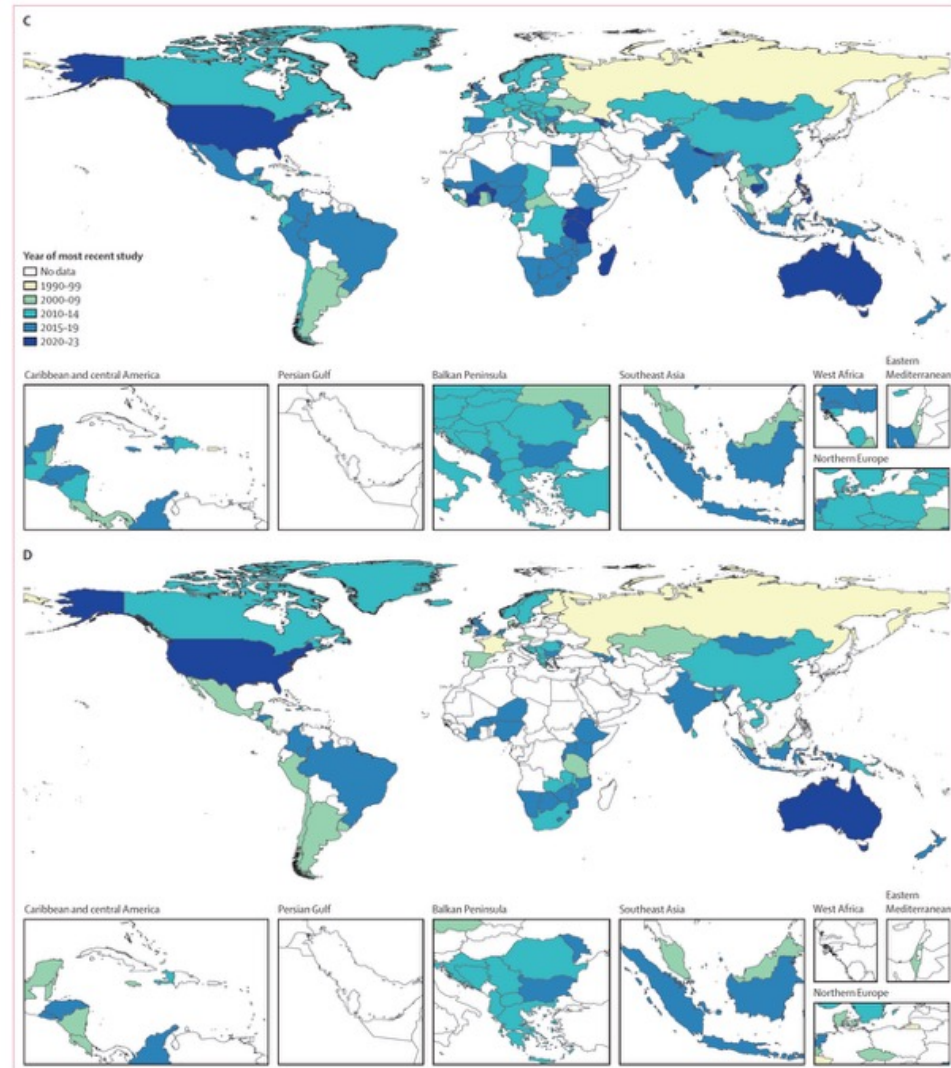


Figure 1: Number of sexual violence against children data sources for females (A) and males (B); most recent year of data for females (C) and males (D)
 These maps display the sources used in our estimation models for the prevalence of sexual violence against children. Maps A and B denote the total number of sources available in each country for females and males, respectively. Maps C and D display the most recent year of data available in each country for females and males, respectively.

| | Females, age-standardised (% [95% UI]) | Males, age-standardised (% [95% UI]) | Females aged 20–24 years (% [95% UI]) | Males aged 20–24 years (% [95% UI]) |
|---|---|---|--|--|
| (Continued from previous page) | | | | |
| Mozambique | 14.4 (6.5–27.2) | 14.8 (6.9–28.2) | 15.9 (9.3–25.8) | 14.7 (9.6–21.3) |
| Rwanda | 30.4 (23.9–40.2) | 18.7 (8.8–31.8) | 34.9 (22.5–49.6) | 12.8 (5.9–22.8) |
| Somalia | 20.8 (7.8–42.5) | 13.6 (5.5–27.6) | 20.9 (7.9–42.9) | 13.6 (5.5–27.7) |
| South Sudan | 20.8 (7.8–42.5) | 13.6 (5.5–27.6) | 20.9 (7.9–42.9) | 13.6 (5.5–27.7) |
| Uganda | 18.1 (8.3–33.0) | 20.0 (10.7–33.2) | 23.2 (11.8–38.4) | 22.5 (13.5–34.1) |
| Tanzania | 18.8 (12.0–29.9) | 20.6 (11.9–33.8) | 24.7 (10.9–45.6) | 20.3 (9.9–35.7) |
| Zambia | 26.6 (13.3–45.9) | 16.4 (8.0–30.1) | 27.2 (15.1–43.0) | 16.5 (9.3–25.7) |
| Southern sub-Saharan Africa | 25.1 (10.4–48.8) | 18.2 (7.5–36.1) | 23.4 (12.4–42.1) | 16.8 (7.4–32.7) |
| Botswana | 28.9 (14.3–46.8) | 27.1 (14.0–42.2) | 22.9 (11.2–38.4) | 17.0 (8.5–29.1) |
| Eswatini | 17.5 (9.9–28.4) | 9.9 (4.9–17.2) | 11.4 (6.9–17.6) | 7.1 (3.8–12.0) |
| Lesotho | 22.1 (9.4–42.6) | 12.0 (5.1–24.2) | 20.3 (11.8–32.4) | 10.5 (5.7–17.4) |
| Namibia | 21.4 (9.1–41.5) | 15.2 (6.9–29.2) | 19.0 (11.2–30.3) | 13.8 (8.5–21.5) |
| South Africa | 25.1 (8.5–52.3) | 20.1 (7.5–40.7) | 24.5 (8.0–51.2) | 19.4 (7.1–40.0) |
| Zimbabwe | 26.1 (16.1–41.8) | 7.9 (3.5–15.8) | 21.5 (11.7–34.6) | 7.6 (3.7–13.6) |
| Western sub-Saharan Africa | 21.8 (10.7–37.8) | 22.4 (11.6–38.4) | 23.0 (12.1–39.1) | 19.6 (9.3–35.1) |
| Benin | 16.5 (5.9–35.5) | 20.7 (9.0–39.2) | 15.8 (5.6–34.4) | 19.6 (8.5–37.8) |
| Burkina Faso | 21.7 (8.1–44.5) | 13.2 (5.4–27.0) | 21.5 (8.0–44.4) | 11.7 (4.7–24.3) |
| Cabo Verde | 19.2 (7.1–39.9) | 20.7 (9.0–39.2) | 19.2 (7.1–40.2) | 19.6 (8.5–37.8) |
| Cameroon | 10.4 (5.8–17.1) | 20.7 (9.0–39.2) | 12.9 (7.5–20.7) | 19.6 (8.5–37.8) |
| Chad | 19.2 (7.1–39.9) | 20.7 (9.0–39.2) | 19.2 (7.1–40.2) | 19.6 (8.5–37.8) |
| Côte d'Ivoire | 32.4 (13.9–58.2) | 28.3 (13.2–49.8) | 34.4 (15.0–60.7) | 28.8 (13.5–50.6) |
| The Gambia | 19.2 (7.1–39.9) | 20.7 (9.0–39.2) | 19.2 (7.1–40.2) | 19.6 (8.5–37.8) |
| Ghana | 19.2 (7.1–39.9) | 20.7 (9.0–39.2) | 19.2 (7.1–40.2) | 19.6 (8.5–37.8) |
| Guinea | 19.2 (7.1–39.9) | 20.7 (9.0–39.2) | 19.2 (7.1–40.2) | 19.6 (8.5–37.8) |
| Guinea-Bissau | 19.2 (7.1–39.9) | 20.7 (9.0–39.2) | 19.2 (7.1–40.2) | 19.6 (8.5–37.8) |
| Liberia | 19.2 (7.1–39.9) | 20.7 (9.0–39.2) | 19.2 (7.1–40.2) | 19.6 (8.5–37.8) |
| Mali | 19.2 (7.1–39.9) | 20.7 (9.0–39.2) | 19.2 (7.1–40.2) | 19.6 (8.5–37.8) |
| Mauritania | 19.2 (7.1–39.9) | 20.7 (9.0–39.2) | 19.2 (7.1–40.2) | 19.6 (8.5–37.8) |
| Niger | 19.9 (7.4–41.1) | 17.8 (7.5–34.7) | 19.7 (7.3–40.9) | 16.8 (7.1–33.3) |
| Nigeria | 23.9 (13.3–37.7) | 24.2 (13.5–38.2) | 25.6 (14.5–40.0) | 19.0 (9.9–31.5) |
| São Tomé and Príncipe | 15.2 (9.2–23.9) | 11.9 (6.6–19.6) | 18.6 (11.6–28.4) | 11.0 (6.3–18.1) |
| Senegal | 19.2 (7.1–39.9) | 20.7 (9.0–39.2) | 19.2 (7.1–40.2) | 19.6 (8.5–37.8) |
| Sierra Leone | 19.2 (7.1–39.9) | 20.7 (9.0–39.2) | 19.2 (7.1–40.2) | 19.6 (8.5–37.8) |
| Togo | 19.2 (7.1–39.9) | 20.7 (9.0–39.2) | 19.2 (7.1–40.2) | 19.6 (8.5–37.8) |
| UI=uncertainty interval. | | | | |
| Table 1: Age-standardised (20 years and older) and age-specific (20–24 years) prevalence of sexual violence against children among females and males globally and by country, region, and super-region, in 2023 | | | | |

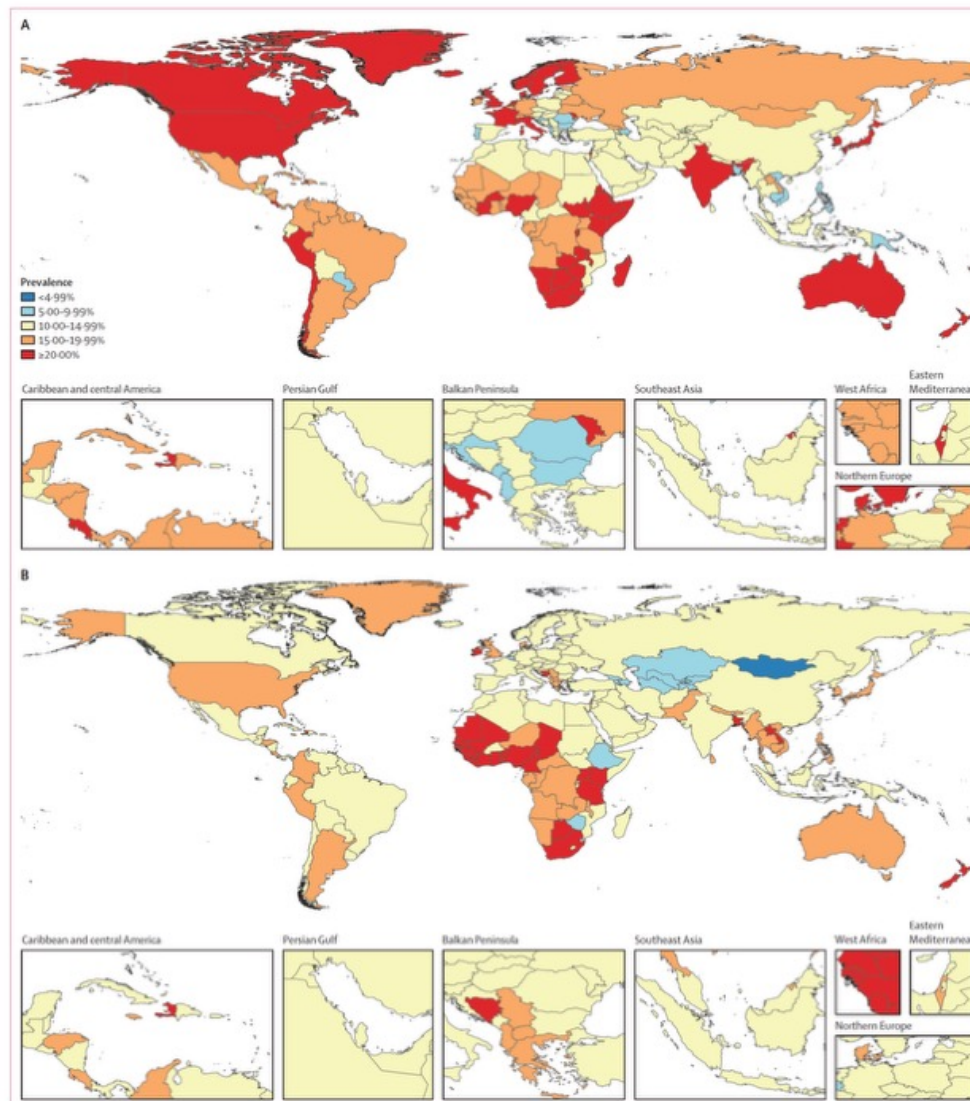


Figure 2: Age-standardised prevalence of sexual violence against children among females (A) and males (B) aged 20 years and older, in 2023

| | Percent of first sexual violence experiences which occurred before age: | | | N |
|--|---|----------|----------|--------|
| | 12 years | 16 years | 18 years | |
| Central Europe, eastern Europe, and central Asia | | | | |
| Female, VACS | 7.4 | 47.2 | 76.1 | 163 |
| Male, VACS | 1.1 | 33 | 65.9 | 88 |
| Latin America and Caribbean | | | | |
| Female | | | | |
| Aggregate | 15.8 | 50.5 | 72.9 | 2141 |
| VACS | 22.3 | 63.4 | 83.7 | 1092 |
| DHS | 9.0 | 37.2 | 61.6 | 1049 |
| Male, VACS | 17.0 | 57.7 | 79.4 | 690 |
| South Asia | | | | |
| Female, DHS | 1.8 | 27.5 | 57.8 | 109 |
| Male | NA | NA | NA | NA |
| Southeast Asia, east Asia, and Oceania | | | | |
| Female | | | | |
| Aggregate | 7.1 | 33.6 | 60.3 | 746 |
| VACS | 10.1 | 37.1 | 65.2 | 89 |
| DHS | 6.7 | 33.2 | 59.7 | 657 |
| Male, VACS | 50.7 | 70.7 | 84.0 | 75 |
| Sub-Saharan Africa | | | | |
| Female | | | | |
| Aggregate | 6.5 | 40.7 | 66.8 | 13 627 |
| VACS | 7.7 | 46.1 | 72.6 | 4697 |
| DHS | 5.90 | 37.9 | 63.7 | 8930 |
| Male, VACS | 12.6 | 44.3 | 69.4 | 2235 |
| All data | | | | |
| Female | | | | |
| Aggregate | 7.7 | 41.6 | 67.3 | 16 786 |
| VACS | 10.3 | 49.1 | 74.6 | 6041 |
| DHS | 6.2 | 37.4 | 63.2 | 10 745 |
| Male, VACS | 14.2 | 47.6 | 71.9 | 3088 |

The table displays the distribution percentiles of experiences of sexual violence that first occurred before ages 12, 16, and 18 years, among survey respondents aged 13–24 years who had ever experienced sexual violence in their lifetime. These results draw upon surveys with less than 50% missingness in the variable denoting the age at first experience. Female data are derived from the DHS (for individuals aged 15–24 years) and VACS (for individuals aged 13–24 years), while male data are exclusively from the VACS (for individuals aged 13–24 years). In locations with both female DHS and VACS data, results were pooled to create an aggregate percentile distribution. For females, no data were available for countries within the high-income or North Africa and the Middle East super-regions. For males, no data were available for countries within the high-income, North Africa and the Middle East, or south Asia super-regions. DHS=Demographic and Health Surveys. NA=not available. VACS=Violence Against Children and Youth Surveys.

Table 2: Distribution percentiles of the age at first experience of sexual violence by super-region, sex, and data source among respondents aged 13–24 years

Research in context

Evidence before this study

Available studies suggest that sexual violence against children (SVAC) is a widespread human rights and public health issue, yet current estimates remain limited by data sparsity and measurement challenges. Global systematic reviews to date have identified relatively few studies, the majority of which describe populations in high-income countries. Meta-analyses available from existing reviews suggest that 12–19% of girls and around 8% of boys have experienced SVAC; however, there exists a high degree of input data variability due to heterogeneous case definitions, survey instruments, and safety and privacy protocols. Several multicountry survey series, including Demographic and Health Surveys (DHS) and Violence Against Children and Youth Surveys (VACS), provide comparable estimates using standard survey instruments across many low-income and middle-income countries. UNICEF released a set of global and regional prevalence estimates for 2023 based, in part, on synthesis of many of these surveys. However, to date, there has not been a systematic effort to synthesise these primary survey data to produce estimates of SVAC by country, age, sex, and year. Even more, underlying SVAC studies and surveys are limited by differential disclosure, a form of self-report bias that has been documented extensively by WHO, among others. Thus, while the existing evidence shows a high burden of SVAC across a range of contexts, there remains a pressing need to synthesise all available data while accounting for between-study differences and differential reporting to create estimates of SVAC that are comparable over time, geography, and demographic characteristics.

Added value of this study

This study generates estimates of SVAC prevalence for all age groups and sexes across 204 locations for the years 1990–2023. We reviewed three global epidemiological databases managed by the Institute for Health Metrics and Evaluation, WHO, and the United Nations Entity for Gender Equality and the Empowerment of Women for population-based survey data reporting on exposure to SVAC. Our case definition of SVAC aligns with Sustainable Development Goal Indicator 16.2.3 and

the International Classification of Violence Against Children framework. This study provides one of the first sets of national, regional, and global estimates of SVAC prevalence that can be used to track progress towards zero target policy goals. Studies using alternate case definitions were adjusted using data-driven patterns and methods, allowing us to leverage the maximum amount of available data and enhance comparability between sources. Adjustments were also made to account for differential reporting across survey modes in violence surveys, addressing a well established challenge in the field. In addition, we drew upon two multicountry datasets (DHS and VACS) to characterise the age windows at which individuals aged 13–24 years first experience sexual violence, information which is crucial for the prevention of, and screening for, sexual violence against young people.

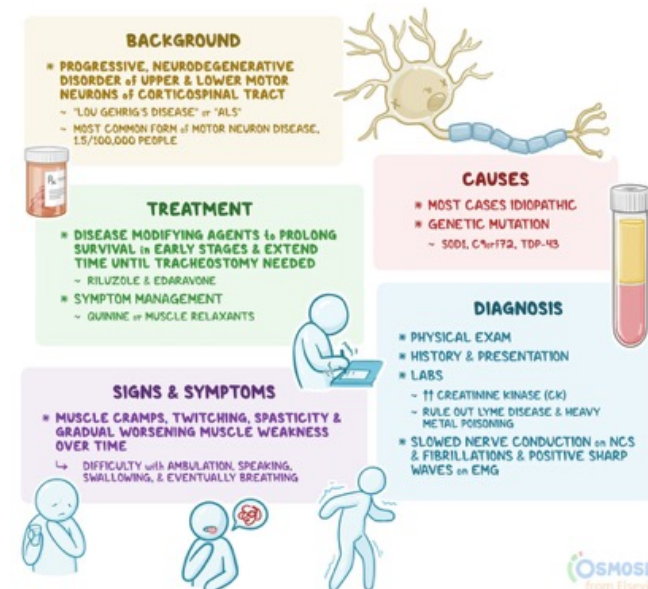
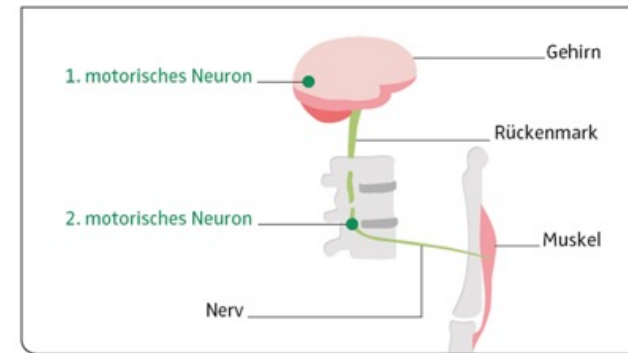
Implications of all the available evidence

After reviewing all available evidence, we find persistent data gaps, emphasising the need for expanded survey and surveillance programmes. The variability in the instruments used across countries also highlights the urgent need for best practices for the measurement of SVAC to be implemented across all national and multinational survey programmes. Despite the inherent data limitations, our synthesis of existing data shows that SVAC prevalence is high among males and females, even in recent generations, and that sexual violence usually first occurs early in life. SVAC has life-long consequences which span health, social, and educational spheres, and the protection of children from sexual violence requires multisectoral interventions and approaches which create safe environments, foster gender-equity, and increase access to support services. The location-specific and population-specific results we present are crucial to informing advocates and policy makers and law makers as they continue to address SVAC. Given the wide range in estimated prevalence across countries, more research is also needed to understand these variations and explore whether they reflect differences in effective child protection policies or are instead driven by barriers to disclosure, reporting, and care.

Die **Amyotrophe Lateralsklerose** ist eine sehr ernste Erkrankung des zentralen und peripheren Nervensystems. Sie ist seit mehr als 100 Jahren bekannt und kommt weltweit vor. Ihre Ursache ist mit Ausnahme der seltenen erblichen Formen bisher unbekannt.

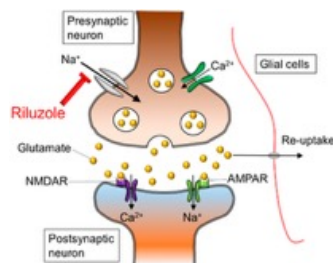
Die ALS betrifft nahezu ausschließlich das motorische Nervensystem. Die Empfindung für Berührung, Schmerz und Temperatur, das Sehen, Hören, Riechen und Schmecken, die Funktionen von Blase und Darm bleiben in den meisten Fällen normal. Leichtgradige, meist nur in speziellen Tests feststellbare Einschränkungen der geistigen Leistungsfähigkeit können auftreten, etwa 5 % der Patienten entwickeln das Bild einer frontotemporalen Demenz mit Auffälligkeiten im Bereich der Kognition und des Verhaltens.

Das motorische System, das unsere Muskeln kontrolliert und die Bewegungen steuert, erkrankt sowohl in seinen zentralen („oberes oder 1. Motorisches Neuron“ im Gehirn mit Pyramidenbahn bis ins Rückenmark) als auch in seinen peripheren Anteilen („unteres oder 2. motorisches Neuron“ in Hirnstamm und Rückenmark mit den motorischen Nervenfasern bis zum Muskel).



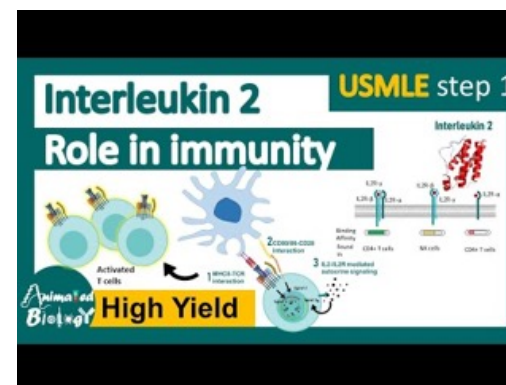
Riluzol (Handelsname Rilutek®) ist ein Arzneistoff, der zur Behandlung der amyotrophen Lateralsklerose (ALS) angewandt wird. Er verlängert bei dieser Krankheit die Überlebensdauer der Patienten. Basierend auf zwei Studien hat die Food and Drug Administration (FDA) Riluzol 1995 zur Behandlung der ALS zugelassen.

Es wird angenommen, dass der exzitatorische Neurotransmitter Glutamat eine wichtige Rolle in der Pathogenese der ALS spielt, insbesondere im Prozess der Apoptose der Nervenzellen. Der genaue Wirkmechanismus von Riluzol ist noch (2020) unbekannt. **Es wird jedoch vermutet, dass Riluzol als Glutamatantagonist agiert**, indem es durch Hemmung präsynaptischer spannungsgesteuerter Natriumkanäle den Calciumeinstrom und somit die Glutamatfreisetzung hemmt.



Interleukin-2 (IL-2) ist ein Zytokin, das eine wichtige Rolle im Immunsystem spielt. Es wird von aktivierten T-Zellen produziert und stimuliert das Wachstum und die Aktivität anderer T- und B-Lymphozyten. IL-2 wird auch in der Krebstherapie eingesetzt, z.B. bei fortgeschrittenem Nierenzellkrebs und Melanom.

Die wichtigste Aufgabe von Interleukin-2 besteht in der autokrinen Stimulation von T-Zellen. Diese sezernieren es selbst und stimulieren dadurch ihre eigene klonale Expansion. T-Zellen, die ein Antigen gebunden und erkannt haben, werden somit zur Zellvermehrung, zum Wachstum und zur Differenzierung angeregt.



Efficacy and safety of low-dose IL-2 as an add-on therapy to riluzole (MIROCALS): a phase 2b, double-blind, randomised, placebo-controlled trial

Summary

Background Amyotrophic lateral sclerosis (ALS) is a life-threatening disease characterised by progressive loss of motor neurons with few therapeutic options. The MIROCALS study tested the hypothesis that low-dose interleukin-2 (IL-2_{LD}) improves survival and function in ALS.

Methods In this randomised, double-blind, placebo-controlled trial, male and female riluzole-naïve participants, with either a possible, laboratory-supported probable, probable, or definite ALS diagnosis (revised El Escorial criteria), aged 18–76 years, with symptom duration of 24 months or fewer, and slow vital capacity of 70% or more, underwent a riluzole-only 12–18 week run-in period before randomisation in a 1:1 ratio to either 2 million international units (MIU) IL-2_{LD} or placebo by subcutaneous injection daily for 5 days every 28 days over 18 months. The primary endpoint was survival at 640 days (21 months). Secondary outcomes included safety, ALS Functional Rating Scale-Revised (ALSFRS-R) score, and biomarker measurements including regulatory T-cells (Tregs), cerebrospinal fluid (CSF)-phosphorylated-neurofilament heavy-chain (CSF-pNFH), and plasma and CSF-chemokine ligand 2 (CCL2). The primary endpoint analysis used unadjusted log-rank and Cox's model adjusted analyses using pre-defined prognostic covariates to control for the disease and treatment response heterogeneity. The study was 80% powered to detect a two-fold decrease in the risk of death by the log-rank test in the intention-to-treat (ITT) population, including all randomly allocated participants. MIROCALS is registered with ClinicalTrials.gov (NCT03039673) and is complete.

Findings From June 19, 2017, to Oct 16, 2019, 304 participants were screened, of whom 220 (72%) met all criteria for random allocation after the 12-to-18-week run-in period on riluzole. 136 (62%) of participants were male and 84 participants (38%) were female. 25 (11%) of the 220 randomly allocated participants were defined as having possible ALS under El Escorial criteria. At the cutoff date there was no loss to follow-up, and all 220 patients who were randomly allocated were documented as either deceased (90 [41%]) or alive (130 [59%]), so all participants were included in the ITT and safety populations. The primary endpoint unadjusted analysis showed a non-significant 19% decrease in risk of death with IL-2_{LD} (hazard ratio 0·81 [95% CI 0·54–1·22], $p=0\cdot33$), failing to demonstrate the expected two-fold decrease in risk of death. The analysis of the primary endpoint adjusted on prognostic covariates, all measured at time of random allocation, showed a significant decrease of the risk of death with IL-2_{LD} (0·32 [0·14–0·73], $p=0\cdot007$), with a significant treatment by CSF-pNFH interaction (1·0003 [1·0001–1·0005], $p=0\cdot001$). IL-2_{LD} was safe, and significantly increased Tregs and decreased plasma-CCL2 at all timepoints. Stratification on CSF-pNFH levels measured at random allocation showed that IL-2_{LD} was associated with a significant 48% decrease in risk of death (0·52 [0·30–0·89], $p=0\cdot016$) in the 70% of the population with low (750–3700 pg/mL) CSF-pNFH levels, while in the 21% with high levels (>3700 pg/mL), there was no significant difference (1·37 [0·68–2·75], $p=0\cdot38$).

Interpretation With this treatment schedule, IL-2_{LD} resulted in a non-significant reduction in mortality in the primary unadjusted analysis. However, the difference between the results of unadjusted and adjusted analyses of the primary endpoint emphasises the importance of controlling for disease heterogeneity in ALS randomised controlled trials. The decrease in risk of death achieved by IL-2_{LD} therapy in the trial population with low CSF-pNFH levels requires further investigation of the potential benefit of this therapy in ALS.

Funding European Commission H2020 Programme; French Health Ministry PHRC2014; and Motor Neurone Disease Association.

Introduction

Amyotrophic lateral sclerosis (ALS) is a rare disease of the voluntary motor system, associated with loss of motor neurons in the brain and spinal cord, leading to relentlessly progressive disability and death, with a median survival of 2–3 years from symptom onset.¹ While riluzole^{2,3} has a modest effect on survival, there is still a pressing need for more effective disease-modifying treatments. However, identification of more effective treatments for ALS has been hampered by poor understanding of relevant targets, the clinical and pathogenic heterogeneity of the ALS syndrome,^{4,5} and failure to assess drug target response.

Neuroinflammation was shown to be involved in a broad spectrum of ALS phenotypes, thus providing a promising therapeutic target.⁶ We developed a methodology to test the hypothesis that modifying the inflammatory components of ALS pathogenesis could improve survival and slow the functional deterioration in ALS.

CD4⁺FOXP3⁺ regulatory T-cells (Tregs) are a T-cell subset with wide immunoregulatory properties in which

numerical and functional impairments have been linked to ALS severity, progression and survival.^{7–10} Tregs require cytokine interleukin-2 (IL-2) for their generation, activation, and survival,¹¹ presenting a feasible and measurable therapeutic route to enhance immune tolerance and dampen neuroinflammation.

In a previous phase 2a trial of low-dose IL-2 (IL-2_{LD}), we showed that 1 million international units (MIU) or 2 MIU was safe, well tolerated, and led to a dose-dependent increase in Treg number and function in people with ALS.¹² Moreover, chemokine ligand 2 (CCL2, also known as monocyte chemoattractant protein-1 [MCP-1]), a marker of microglial activation shown to reflect disease severity,^{13,14} was significantly reduced in the plasma of treated participants.

Here we report the main outcomes of a phase 2b, randomised, double-blind, placebo-controlled, clinical trial with a primary objective of evaluating the clinical efficacy and safety of IL-2_{LD} over 18 months treatment. A key element in our trial design was the incorporation of prespecified biomarkers: Tregs for drug target engagement, cerebrospinal fluid (CSF)-CCL2 (CSF-CCL2)

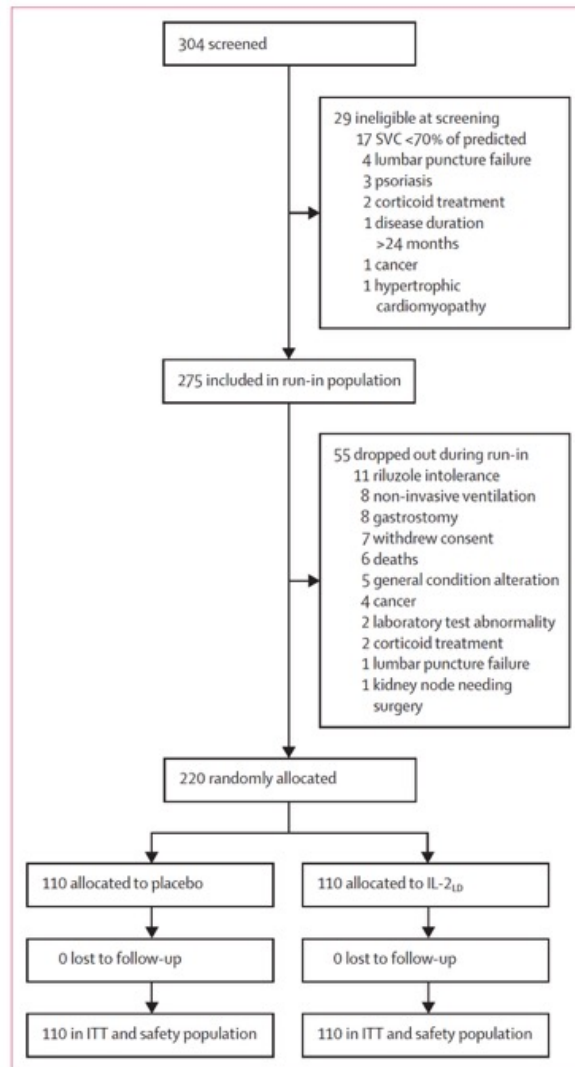


Figure 1: Trial profile

IL-2_{low}=low-dose interleukin-2. ITT=intention-to-treat. SVC=slow vital capacity.

| | Placebo (N=110) | IL2 _{low} (N=110) |
|---|------------------------|----------------------------|
| Patients per country | | |
| France | 69 (63%) | 68 (62%) |
| UK | 41 (37%) | 42 (38%) |
| Sex | | |
| Female | 43 (39%) | 41 (37%) |
| Male | 67 (61%) | 69 (63%) |
| ALS diagnosis* | | |
| Clinically definite | 30 (27%) | 22 (20%) |
| Clinically probable | 33 (30%) | 43 (39%) |
| Clinically probable—laboratory supported | 33 (30%) | 34 (31%) |
| Clinically possible | 14 (13%) | 11 (10%) |
| Site of symptom onset | | |
| Bulbar | 23 (21%) | 22 (20%) |
| Limb | 86 (78%) | 88 (80%) |
| Other† | 1 (1%) | 0 |
| Family history‡ | | |
| Yes | 13 (12%) | 14 (13%) |
| No | 91 (83%) | 89 (81%) |
| Unknown | 6 (5%) | 7 (6%) |
| Age, years | 60.4 (23.4 to 74.8) | 59.0 (35.9 to 76.1) |
| Disease duration since first symptom, months | 11.1 (2.4 to 23.9) | 10.7 (2.8 to 23.5) |
| Time since diagnosis at inclusion, months | 1.3 (0.0 to 12.0) | 1.6 (0.0 to 9.5) |
| Percentage of predicted SVC at inclusion | 93% (70 to 138) | 94% (71 to 138) |
| ALSFRS-R at random allocation, point score 0–48 | 39 (16 to 48) | 40 (25 to 47) |
| ALSFRS-R slope run-in, point score per month | -0.6 (-5.8 to 1.2) | -0.7 (-4.1 to 1.3) |
| Core biomarkers | | |
| Treg percentage of CD4 at random allocation | 5.1% (2.5 to 10.1) | 5.2% (2.2 to 15.1) |
| Treg percentage of CD4 run-in change | 0.56% (-2.1 to 3.1) | 0.84% (-12.2 to 4.78) |
| Absolute number of Treg per µL at random allocation | 36.4 (9.3 to 91.4) | 35.8 (2.9 to 76.2) |
| Absolute number of Treg per µL at run-in change | 2.7 (-17.1 to 46.2) | 3.0 (-133.8 to 32.5) |
| CSF-pNFH at random allocation, pg/mL | 2442 (140 to 10981) | 2306 (55.3 to 8515) |
| CSF-pNFH run-in change, pg/mL | 129 (-3785 to 3717) | 97 (-2412 to 1847) |
| Plasma-CCL2 at random allocation, pg/mL | 298 (189 to 486) | 295 (170 to 497) |
| Plasma-CCL2 run-in change, pg/mL | -3.8 (-229.8 to 200.1) | 7.8 (-283.7 to 123.7) |
| CSF-CCL2 at random allocation, pg/mL | 571 (322 to 1168) | 554 (276 to 1493) |
| CSF-CCL2 run-in change, pg/mL | 29.5 (-276.2 to 305.3) | 19.5 (-242.3 to 1145.7) |

Data are n (%) or median (range). ALS=amyotrophic lateral sclerosis. ALSFRS-R=ALS Functional Rating Scale-Revised. CCL2=chemokine ligand 2. CSF=cerebrospinal fluid. IL2_{low}=low-dose interleukin 2. ITT=intention-to-treat. pNFH=phosphorylated neurofilament heavy chain. SVC=slow vital capacity. Treg=regulatory T-cells. *El Escorial criteria. †Other site of onset=respiratory (randomly allocated to the limb stratum). ‡Family history as assessed in the clinic was not a criterion for exclusion.

Table 1: Demographic and clinical parameters at baseline in the ITT population

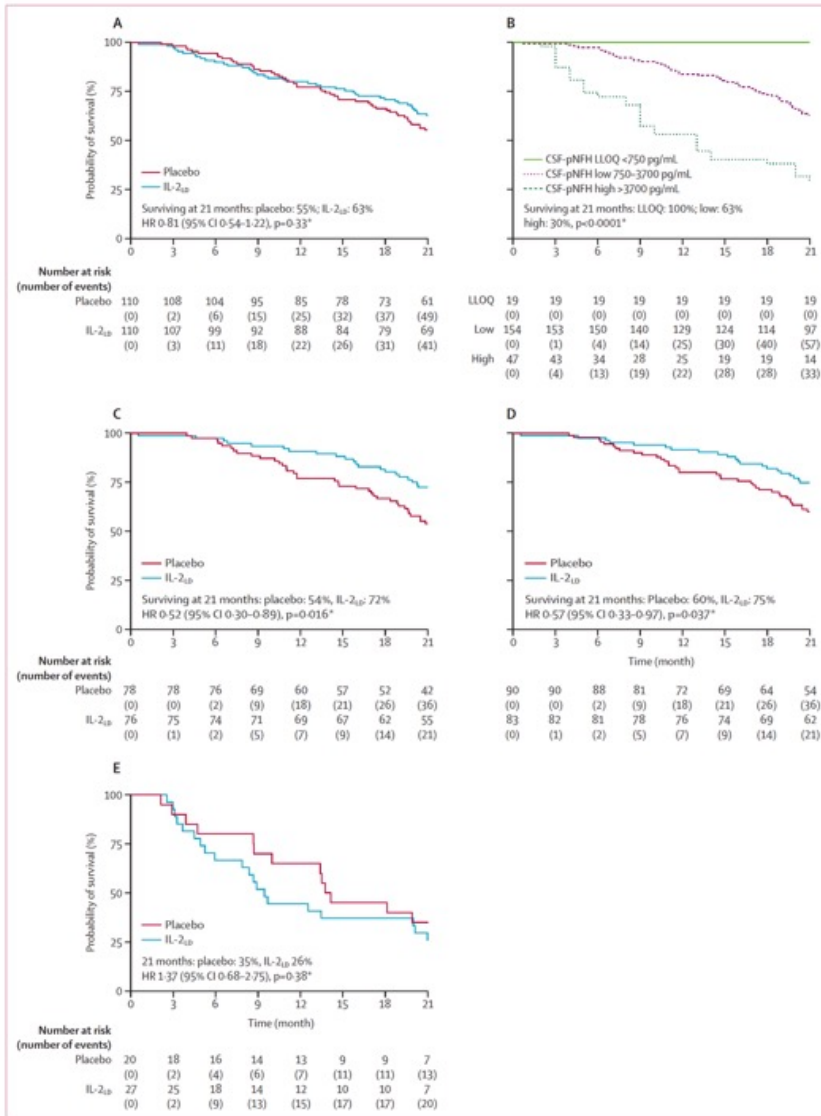


Figure 2: Primary outcome: survival

(A) Kaplan-Meier curves of all randomly allocated participants by treatment group. (B) Kaplan-Meier curves of all randomly allocated participants by CSF-pNFH strata. (C) Kaplan-Meier curves of participants by treatment group for the low CSF-pNFH stratum. (D) Kaplan-Meier curves of participants by treatment group, pooled LLOQ and low CSF-pNFH strata. (E) Kaplan-Meier curves of participants by treatment group, high CSF-pNFH stratum. The survival numbers are given in the appendix (p 24). CSF=cerebrospinal fluid. HR=hazard ratio. IL-2_{L0}=low-dose interleukin-2. LLOQ=lower limit of quantification. pNFH=phosphorylated neurofilament heavy chain. *p value from the log-rank test.

| | Hazard ratio (95% CI) | p value |
|---|-------------------------|---------|
| ALSFRS-R at random allocation, point score 0-48 | 0.86 (0.83-0.89) | <0.0001 |
| Age, years 18-75 | 1.029 (1.004-1.054) | 0.021 |
| CSF-pNFH at random allocation, pg/mL | 1.0002 (1.00004-1.0003) | 0.0091 |
| Number of Tregs per µL at random allocation | 0.982 (0.968-0.997) | 0.018 |
| Plasma-CCL2 at random allocation, pg/mL | 1.0033 (0.9996-1.0069) | 0.077 |
| IL-2 _{L0} treatment | 0.32 (0.14-0.73) | 0.0070 |
| Treatment by CSF-pNFH interaction | 1.0003 (1.0001-1.0005) | 0.0011 |

Hazard ratios were generated by a multivariate Cox's model analysis for each of the covariates in the model. A hazard ratio greater than 1.0 denotes an increase in risk of death for each unit increase of the parameter (eg, age, CSF-pNFH, and CCL2), and a hazard ratio under 1.0 denotes a decrease in risk of death for each unit increase of the parameter (eg, ALSFRS-R score and number of Tregs). ALSFRS-R=Revised Amyotrophic Lateral Sclerosis Functional Rating Scale. CCL2=chemokine ligand 2. CSF=cerebrospinal fluid. IL-2_{L0}=low-dose interleukin-2. pNFH=phosphorylated neurofilament heavy chain.

Table 2: Multivariate analysis of the primary outcome (survival) in the intention-to-treat population

| | Number of events, total (N _{total} /N _{at risk}) | Number of deaths in events, n (%) | Factors in Cox's model analysis | | | | | |
|-----------------------------|---|-----------------------------------|---------------------------------|---------|-------------------------|---------|---|---------|
| | | | Treatment HR (95% CI) | p value | CSF-pNFH HR (95% CI) | p value | Treatment by CSF-pNFH interaction HR (95% CI) | p value |
| Death only | 90 (49/41) | 90/90 (100%) | 0.27 (0.12-0.62) | 0.0017 | 1.0002 (1.0001-1.0003) | <0.0001 | 1.0004 (1.0002-1.0006) | <0.0001 |
| NIV, tracheostomy, or death | 133 (70/63) | 45/133 (34%) | 0.33 (0.17-0.64) | 0.0009 | 1.0001 (1.00004-1.0002) | 0.0066 | 1.0004 (1.0002-1.0006) | <0.0001 |
| Gastrostomy or death | 122 (65/57) | 55/122 (45%) | 0.39 (0.19-0.78) | 0.0089 | 1.0003 (1.0002-1.0004) | <0.0001 | 1.0003 (1.0001-1.0005) | 0.0009 |
| Any event | 250 (80/170) | 38/250 (15%) | 0.48 (0.25-0.90) | 0.021 | 1.0003 (1.0002-1.0004) | <0.0001 | 1.0002 (1.00007-1.0004) | 0.0056 |

CSF=cerebrospinal fluid. HR=hazard ratio. IL-2_{L0}=interleukin-2 low dose. NIV=non-invasive ventilation. pNFH=phosphorylated neurofilament heavy chain.

Table 3: Composite event outcomes: supportive analysis using Cox's model in the intention-to-treat population

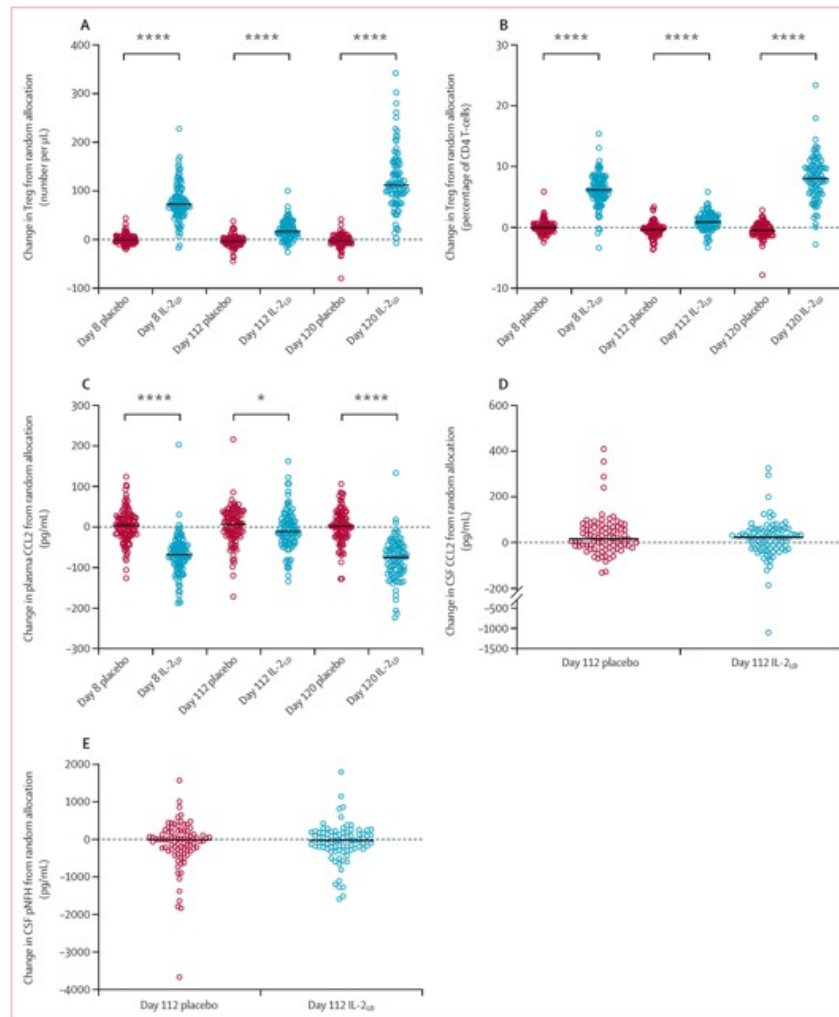


Figure 3: Effect of IL-2_L treatment on core biomarkers in blood and CSF

Tregs changes from random allocation in (A) number and (B) frequency at day 8 (maximum of first cycle), day 112 (trough level following four cycles), and day 120 (maximum of fifth cycle). CCL2 concentration changes from random allocation in (C) plasma, measured at day 8, day 112, and day 120 and (D) CSF, measured at day 112. (E) pNFH concentration changes in CSF from random allocation at day 112. All verum to placebo comparison tests were performed by the Mann-Whitney U test. Black lines indicate the median of the distribution of changes from random allocation. CCL2=chemokine ligand 2. CSF=cerebrospinal fluid. IL-2_L=low-dose interleukin-2. pNFH, phosphorylated neurofilament heavy chain. Tregs=regulatory T-cells. *indicates $p<0.05$. ****indicates $p<0.0001$.

Research in context

Evidence before this study

For the background in preparing the protocol (submitted to regulators on April 11, 2016) we searched MEDLINE, PubMed, ClinicalTrials.gov, EudraCT, Embase, the COCHRANE Central Register of Clinical trials, and WHO Clinical Trials Registry Platform from Jan 1, 1990, to April 1, 2016, using the keywords “ALS”, “amyotrophic lateral sclerosis”, “motor neuron disease”, “motor neurone disease”, “Lou Gehrig’s disease”, “randomised clinical trials”, “interleukin-2”, AND “interleukin2” without language restrictions. We also hand-searched reviews with these search terms between Jan 1, 1990, and April 1, 2016. All searches were updated to Aug 31, 2024, which revealed one phase 2a randomised, double-blind, placebo-controlled trial of interleukin-2 low dose (IL-2_{LD}) in amyotrophic lateral sclerosis (ALS). There were no other reports of randomised, double-blind, placebo-controlled trials of IL-2_{LD} in ALS, motor neurone disease, or Lou Gehrig’s disease. We identified three small, non-randomised, open-label trials of IL-2_{LD} in ALS—either alone or in combination with other agents—but no reliable conclusions could be drawn on the efficacy or safety of IL-2_{LD} in ALS due to the absence of adequate masking, lack of placebo controls, and inadequate power due to small numbers of participants.

Added value of this study

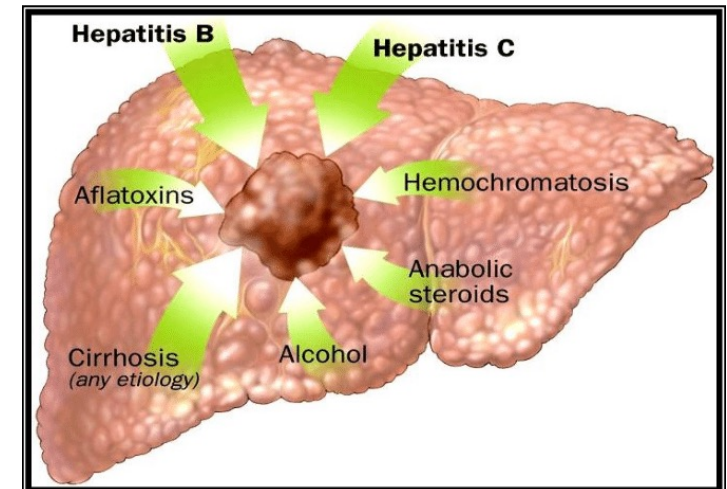
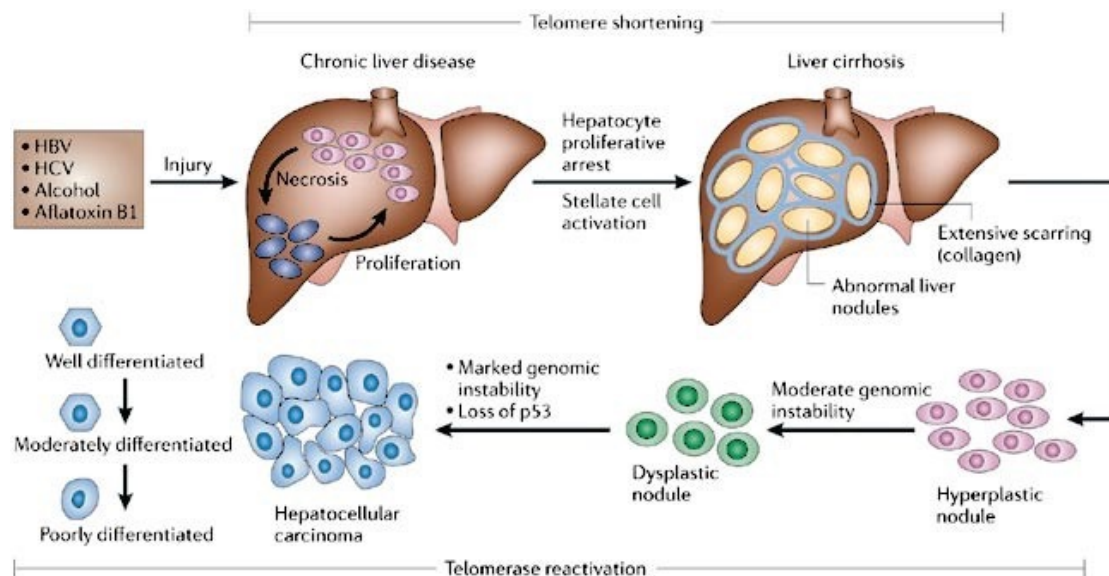
MIROCALS represents the first large, long-term, randomised, double-blind, placebo-controlled trial of treatment with subcutaneous IL-2_{LD} as add-on to riluzole in people with ALS, powered for efficacy. The primary endpoint measure was

survival, and there was no loss to follow-up at the cutoff of 21 months from random allocation. By design, we recruited an incident population more representative of the real-world ALS population than previous ALS trial samples. We also applied a strategy to control for disease heterogeneity—a major confounding factor in previous ALS trials—using systematic measures of a biomarker (cerebrospinal fluid [CSF] phosphorylated neurofilament heavy chain [CSF-pNFH]) to adjust for disease activity and rate of progression. IL-2_{LD} was safe and well tolerated, suggesting that it is suitable for larger trials assessing its therapeutic value in this vulnerable population.

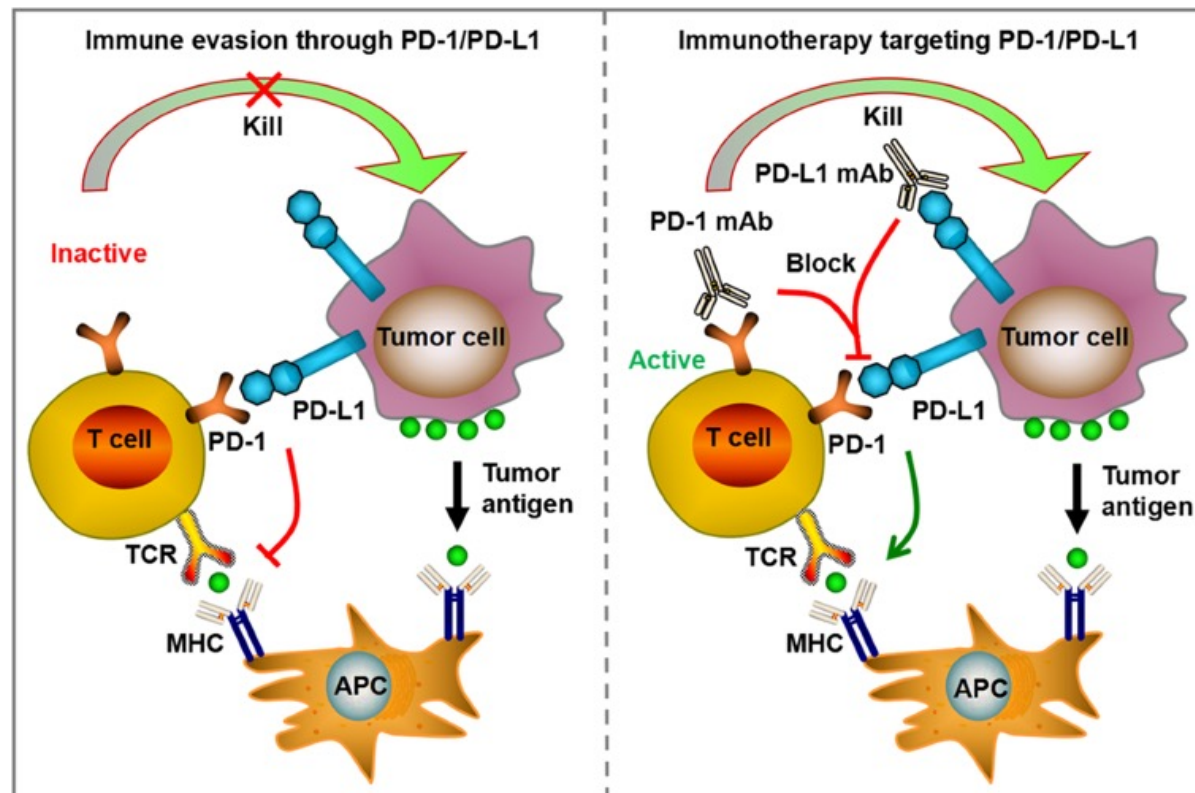
Implications of all the available evidence

At present, the only drug approved in the USA and Europe with a proven effect on survival is riluzole. Despite our primary outcome not reaching statistical significance, our findings indicate that IL-2_{LD} offers the possibility of a much-needed, safe, and well-tolerated agent conferring useful survival benefit in addition to riluzole across the ALS spectrum. Nonetheless, further trials are required to support our observations and to explore different treatment schedules. The integration of biomarkers of disease activity and target response into our trial design offers a new approach to control for disease heterogeneity, an important and poorly understood confounding factor in ALS trials. Our findings also indicate that targeting Tregs to boost immune tolerance is a worthwhile strategy for developing new therapies in ALS.

Carcinoma hepatocellulare; nicht zu verwechseln mit Lebermetastase, auch Leberkrebs genannt) ist eine Krebserkrankung, die sich direkt aus den Leberzellen entwickelt. Meist geht dem eine chronische Schädigung der Leberzellen voraus.



Checkpoint-Hemmer, oder Checkpoint-Inhibitoren, sind Medikamente, die die T-Zellen des Immunsystems aktivieren, um Krebszellen zu erkennen und zu zerstören, indem sie die sogenannten "Immun-Checkpoints" blockieren. Diese Checkpoints sind eigentlich hemmende Signale, die T-Zellen normalerweise nutzen, um zu verhindern, dass sie andere Zellen (einschließlich Krebszellen) angreifen. Durch die Blockade dieser Checkpoints können T-Zellen ihren "Halt" aufheben und die Krebszellen effektiver bekämpfen.



Nivolumab plus ipilimumab versus lenvatinib or sorafenib as first-line treatment for unresectable hepatocellular carcinoma (CheckMate 9DW): an open-label, randomised, phase 3 trial

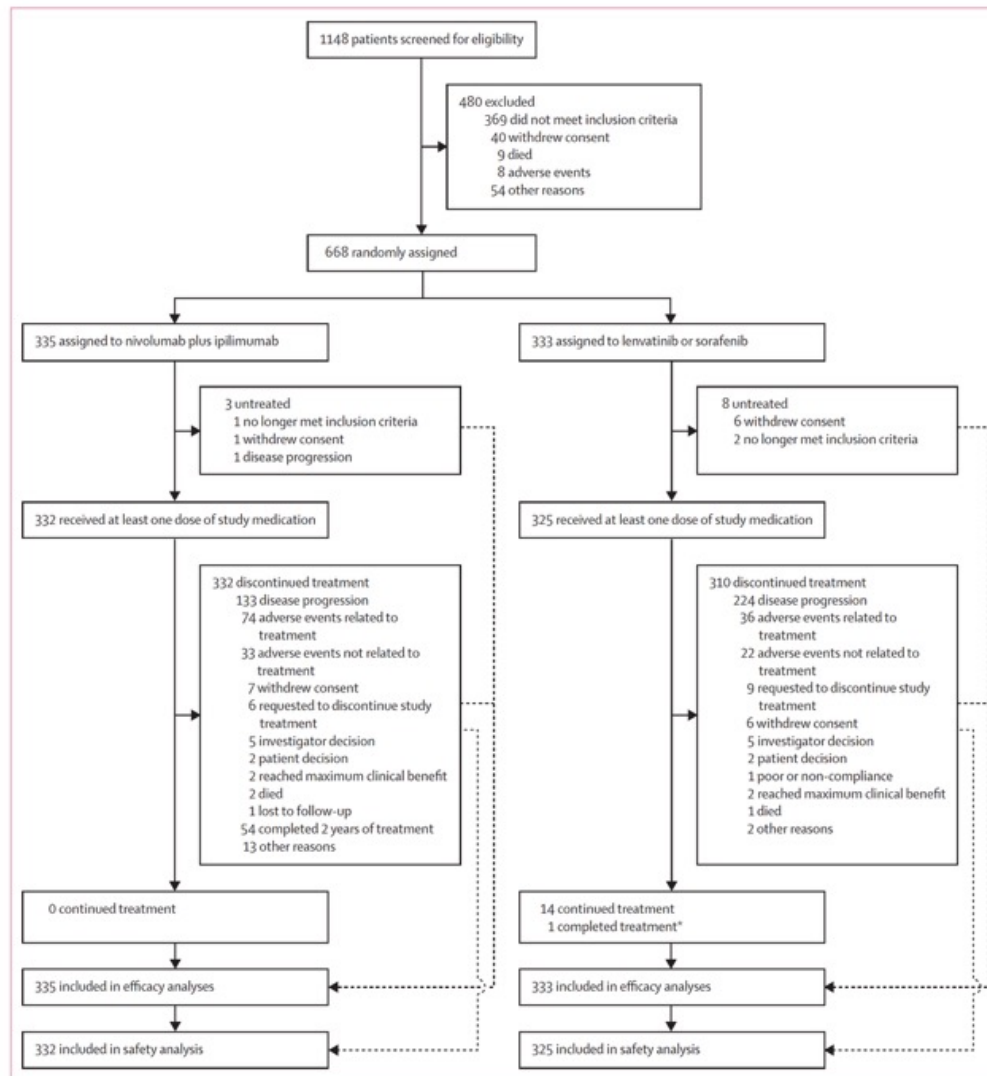
Summary

Background Patients with unresectable hepatocellular carcinoma have a poor prognosis, and treatments with long-term benefits are needed. We report results from the preplanned interim analysis of the CheckMate 9DW trial assessing nivolumab plus ipilimumab versus lenvatinib or sorafenib for unresectable hepatocellular carcinoma in the first-line setting.

Methods This open-label, randomised, phase 3 trial enrolled patients aged 18 years or older with unresectable hepatocellular carcinoma without previous systemic therapy at 163 hospitals and cancer centres across 25 countries in Asia, Australia, Europe, North America, and South America. Patients had at least one measurable untreated lesion per Response Evaluation Criteria in Solid Tumours (RECIST) version 1.1, a Child–Pugh score of 5 or 6, and an Eastern Cooperative Oncology Group performance status of 0 or 1. Patients were randomly assigned (1:1) via an interactive response technology system to receive nivolumab (1 mg/kg) plus ipilimumab (3 mg/kg) intravenously every 3 weeks for up to four doses, followed by nivolumab 480 mg every 4 weeks or investigator's choice of either oral lenvatinib (8 mg or 12 mg daily depending on bodyweight) or oral sorafenib (400 mg twice daily). Randomisation was stratified by aetiology; the presence of macrovascular invasion, extrahepatic spread, or both; and baseline alpha-fetoprotein concentration. The primary endpoint was overall survival, which was assessed in all randomly assigned patients; safety was an exploratory endpoint and was assessed in all randomly assigned patients who received at least one dose of study medication. This trial is registered with ClinicalTrials.gov, NCT04039607 (ongoing).

Findings Between Jan 6, 2020, and Nov 8, 2021, 668 patients were randomly assigned to nivolumab plus ipilimumab (n=335) or lenvatinib or sorafenib (n=333). Early crossing of the overall survival Kaplan–Meier curves reflected a higher number of deaths during the first 6 months after randomisation with nivolumab plus ipilimumab (hazard ratio 1·65 [95% CI 1·12–2·43]) but was followed by a sustained separation of the curves thereafter in favour of nivolumab plus ipilimumab (0·61 [0·48–0·77]). After a median follow-up of 35·2 months (IQR 31·1–39·9), overall survival was significantly improved with nivolumab plus ipilimumab versus lenvatinib or sorafenib (median 23·7 months [95% CI 18·8–29·4] vs 20·6 months [17·5–22·5]; hazard ratio 0·79 [0·65–0·96]; two-sided stratified log-rank $p=0·018$); respective overall survival rates were 49% (95% CI 44–55) versus 39% (34–45) at 24 months and 38% (32–43) versus 24% (19–30) at 36 months. Overall, 137 (41%) of 332 patients receiving nivolumab plus ipilimumab and 138 (42%) of 325 patients receiving lenvatinib or sorafenib had grade 3–4 treatment-related adverse events. 12 deaths were attributed to treatment with nivolumab plus ipilimumab and three were attributed to treatment with lenvatinib or sorafenib.

Interpretation Nivolumab plus ipilimumab showed a significant overall survival benefit versus lenvatinib or sorafenib and manageable safety in patients with previously untreated unresectable hepatocellular carcinoma. These results support nivolumab plus ipilimumab as a first-line treatment in this setting.



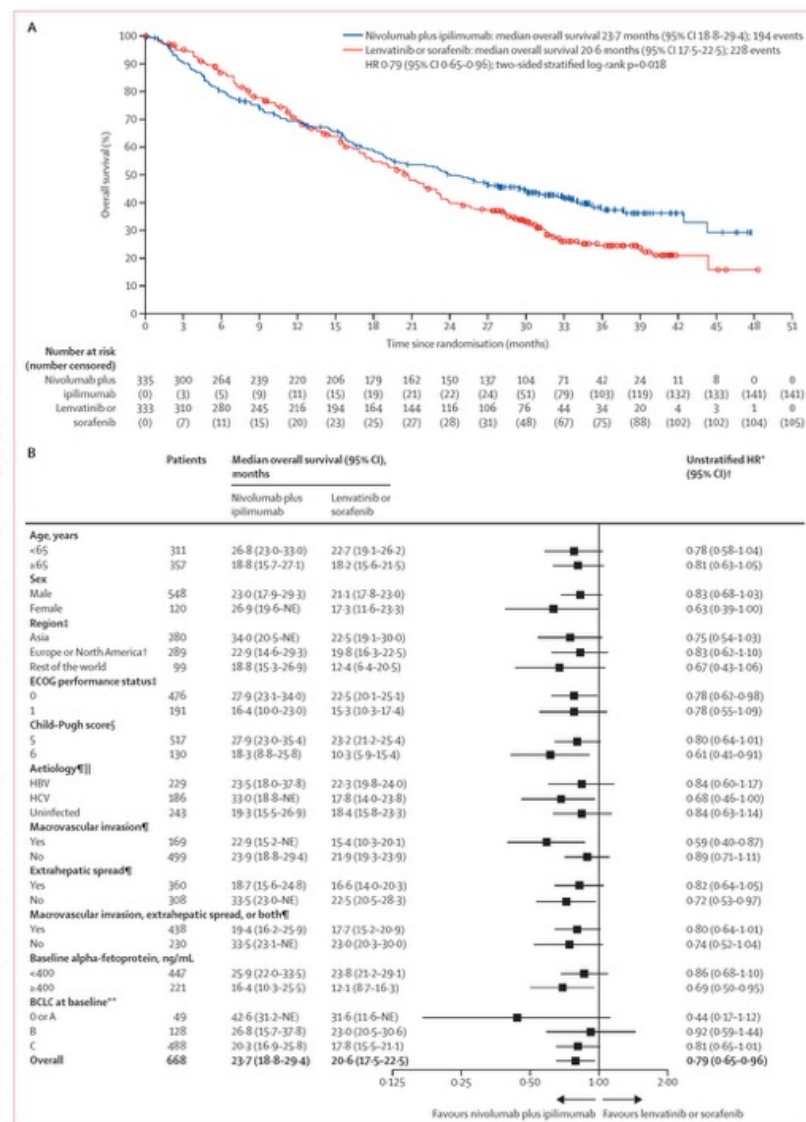
| | Nivolumab plus ipilimumab group (n=335) | Lenvatinib or sorafenib group (n=333) |
|---|---|---------------------------------------|
| Age, years | 65 (59–71) | 66 (59–73) |
| Sex | | |
| Male | 271 (81%) | 277 (83%) |
| Female | 64 (19%) | 56 (17%) |
| Race | | |
| White | 179 (53%) | 174 (52%) |
| Asian | 140 (42%) | 152 (46%) |
| Black | 11 (3%) | 4 (1%) |
| Other | 5 (1%) | 3 (1%) |
| Geographical region | | |
| Europe or North America | 144 (43%) | 145 (44%) |
| Asia | 133 (40%) | 147 (44%) |
| Rest of the world | 58 (17%) | 41 (12%) |
| Aetiology† | | |
| HBV | 114 (34%) | 115 (35%) |
| HCV | 90 (27%) | 96 (29%) |
| Uninfected | 124 (37%) | 119 (36%) |
| HBV and HCV‡ | 7 (2%) | 3 (1%) |
| ECOG performance status | | |
| 0 | 233 (70%) | 243 (73%) |
| 1 | 102 (30%) | 89 (27%) |
| Missing | 0 | 1 (<1%) |
| Child–Pugh score | | |
| 5 | 254 (76%) | 263 (79%) |
| 6 | 72 (21%) | 58 (17%) |
| ≥7 | 9 (3%) | 11 (3%) |
| Missing | 0 | 1 (<1%) |
| BCLC stage | | |
| 0 or A | 28 (8%) | 21 (6%) |
| B | 61 (18%) | 67 (20%) |
| C | 246 (73%) | 242 (73%) |
| Unknown | 0 | 3 (1%) |
| Macrovascular invasion, extrahepatic spread, or both† | 221 (66%) | 217 (65%) |
| Macrovascular invasion | 77 (23%) | 92 (28%) |
| Extrahepatic spread | 188 (56%) | 172 (52%) |
| Alpha-fetoprotein concentration, ng/mL | | |
| <400 | 227 (68%) | 220 (66%) |
| ≥400 | 108 (32%) | 113 (34%) |
| Previous local non-systemic therapy | 142 (42%) | 158 (47%) |

Data are median (IQR) or n (%). Percentages might not sum to 100 because of rounding. BCLC=Barcelona Clinic Liver Cancer; ECOG=Eastern Cooperative Oncology Group; HBV=hepatitis B virus; HCV=hepatitis C virus. *Randomisation was stratified according to aetiology (HBV vs HCV vs uninfected); macrovascular invasion, extrahepatic spread, or both (present vs absent); and alpha-fetoprotein concentration (<400 ng/mL vs ≥400 ng/mL). †Per case report form. ‡These patients did not have active co-infection with HBV and HCV.

Table 1: Baseline demographics and disease characteristics in all randomly assigned patients*

Figure 2: Kaplan-Meier estimates of overall survival among all randomly assigned patients and subgroup analysis of overall survival

(A) Overall survival in all randomly assigned patients. Vertical lines and circles indicate censored data.
(B) Subgroup analysis of overall survival. HR=hazard ratio. NE=not estimable. *The HR was not computed for subset categories with ten or fewer patients per treatment group. †15 patients in the nivolumab plus ipilimumab group and five in the lenvatinib or sorafenib group were from North America. ‡Not reported for one patient in the lenvatinib or sorafenib group. §Nine patients in the nivolumab plus ipilimumab group and 11 in the lenvatinib or sorafenib group had a score of 7 or higher, and the score was not reported for one patient in the lenvatinib or sorafenib group. ¶Per case report form. ||Seven patients in the nivolumab plus ipilimumab group and three in the lenvatinib or sorafenib group were reported as having both HBV and HCV; these patients did not have active co-infection. **BCLC was unknown for three patients in the lenvatinib or sorafenib group.



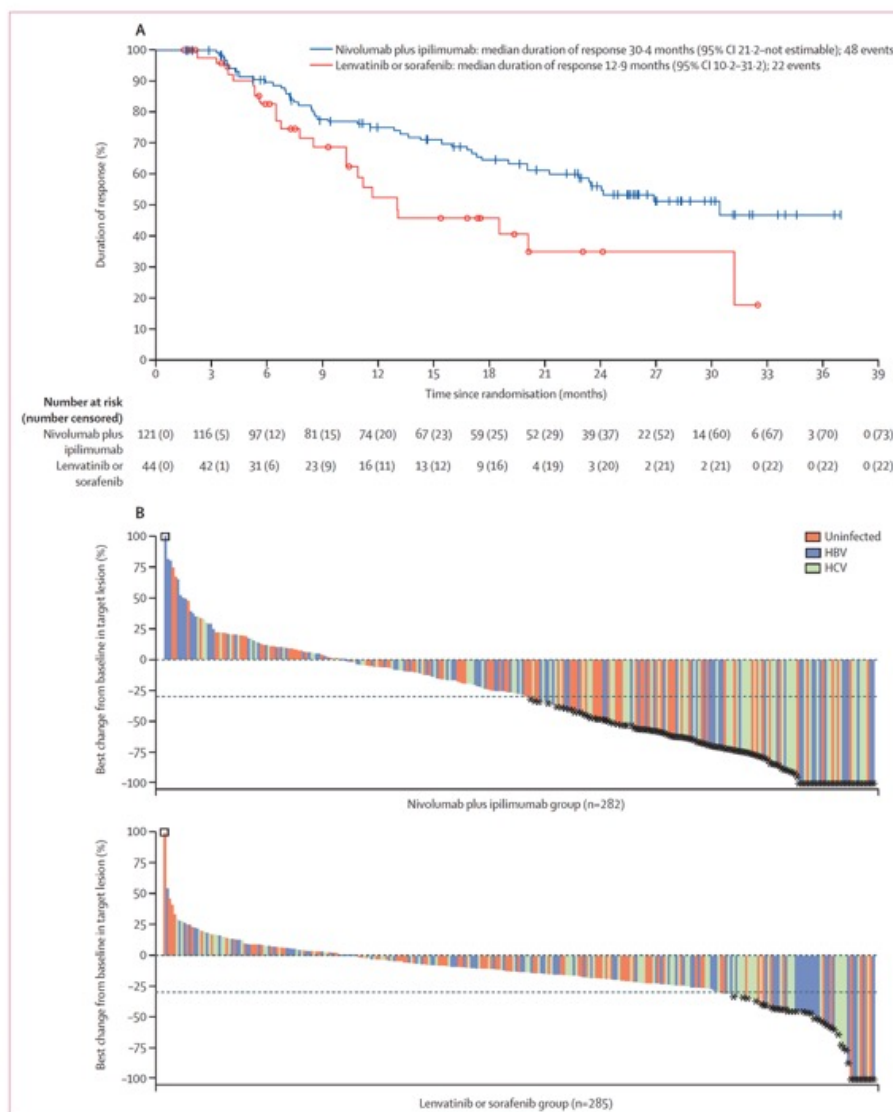
| | Nivolumab plus ipilimumab group (n=335) | Lenvatinib or sorafenib group (n=333) |
|---|---|---------------------------------------|
| Objective response rate* (%; 95% CI) | 121 (36%; 31-42) | 44 (13%; 10-17) |
| Best overall response† | | |
| Complete response | 23 (7%) | 6 (2%) |
| Partial response | 98 (29%) | 38 (11%) |
| Stable disease‡ | 108 (32%) | 205 (62%) |
| Progressive disease | 67 (20%) | 47 (14%) |
| Could not be evaluated§ | 39 (12%) | 37 (11%) |
| Median duration of response (95% CI), months¶ | 30.4 (21.2-NE) | 12.9 (10.2-31.2) |
| Patients with duration of response (%; 95% CI)¶ | | |
| ≥24 months | 55% (44-64) | 35% (17-53) |
| ≥36 months | 47% (34-59) | NA |
| Median time to response (IQR), months | 2.2 (2.1-3.8) | 3.7 (2.1-5.6) |

NA=not applicable. NE=not estimable. *Patients who had confirmed complete response or partial response per Response Evaluation Criteria in Solid Tumours (version 1.1). The objective response rate 95% CI is based on the Clopper and Pearson method. The two-sided p value was less than 0.0001 and was calculated with a stratified Cochran-Mantel-Haenszel test. †Percentages might not sum to 100 because of rounding. ‡Includes patients with non-complete response or non-progressive disease (six [2%] in the nivolumab plus ipilimumab group and seven [2%] in the lenvatinib or sorafenib group). §Includes one patient from the lenvatinib or sorafenib group who did not have a baseline lesion per blinded independent central review and thus did not have their response evaluated. ¶Assessed in patients with a confirmed partial or complete response. Based on Kaplan-Meier estimates of duration of response. ||Assessed in patients with a confirmed partial or complete response.

Table 2: Response outcomes, as assessed by blinded independent central review

Figure 3: Kaplan-Meier estimates of duration of response and change from baseline in all response-evaluable patients by aetiology

(A) Kaplan-Meier estimates are based on all patients with a confirmed objective response per blinded independent central review using Response Evaluation Criteria in Solid Tumours version 1.1. Vertical lines and circles indicate censored data. (B) Waterfall plots represent best change from baseline in response evaluable patients by aetiology, defined as patients with a best overall response of complete response, partial response, stable disease, non-complete response or non-progressive disease, or progressive disease. Best change is maximum change in sum of diameters of target lesions (a negative value means true reduction, and a positive value means increase only observed over time) up to radiographic progression or start of subsequent systemic therapy date. Horizontal dashed lines indicate a 30% reduction consistent with response per Response Evaluation Criteria in Solid Tumours version 1.1. Asterisks represent confirmed responders. Square symbols represent percentage change truncated to 100%. Patients with HBV-HCV co-infection based on the case report form were categorised to HCV. HBV=hepatitis B virus. HCV=hepatitis C virus.



| | Nivolumab plus ipilimumab group (n=332) | | Lenvatinib or sorafenib group (n=325) | |
|---|---|------------|---------------------------------------|------------|
| | Grade 1-2 | Grade 3-4† | Grade 1-2 | Grade 3-4† |
| Any treatment-related adverse event | 141 (42%) | 137 (41%) | 159 (49%) | 138 (42%) |
| Treatment-related serious adverse event | 11 (3%) | 83 (25%) | 5 (2%) | 42 (13%) |
| Treatment-related adverse event leading to discontinuation‡ | 15 (5%) | 44 (13%) | 13 (4%) | 21 (6%) |
| Treatment-related adverse events§ | | | | |
| Pruritus | 88 (27%) | 5 (2%) | 10 (3%) | 0 |
| Rash | 58 (17%) | 6 (2%) | 26 (8%) | 3 (<1%) |
| ALT increased | 47 (14%) | 16 (5%) | 16 (5%) | 3 (<1%) |
| AST increased | 45 (14%) | 20 (6%) | 25 (8%) | 2 (<1%) |
| Diarrhoea | 43 (13%) | 4 (1%) | 104 (32%) | 10 (3%) |
| Hypothyroidism | 40 (12%) | 0 | 79 (24%) | 0 |
| Asthenia | 33 (10%) | 1 (<1%) | 46 (14%) | 5 (2%) |
| Hyperthyroidism | 32 (10%) | 2 (<1%) | 5 (2%) | 0 |
| Decreased appetite | 22 (7%) | 1 (<1%) | 65 (20%) | 5 (2%) |
| Lipase increased | 20 (6%) | 17 (5%) | 14 (4%) | 4 (1%) |
| Fatigue | 27 (8%) | 0 | 44 (14%) | 6 (2%) |
| Nausea | 19 (6%) | 0 | 29 (9%) | 2 (<1%) |
| Blood bilirubin increased | 13 (4%) | 1 (<1%) | 18 (6%) | 5 (2%) |
| Weight decreased | 7 (2%) | 0 | 32 (10%) | 5 (2%) |
| Colitis | 6 (2%) | 8 (2%) | 0 | 0 |
| PPE syndrome | 6 (2%) | 0 | 88 (27%) | 11 (3%) |
| Hypertension | 5 (2%) | 0 | 96 (30%) | 38 (12%) |
| Platelet count decreased | 4 (1%) | 0 | 17 (5%) | 5 (2%) |
| Hypertransaminasaemia | 2 (<1%) | 4 (1%) | 1 (<1%) | 1 (<1%) |
| Neutropenia | 2 (<1%) | 2 (<1%) | 4 (1%) | 5 (2%) |
| Immune-mediated hepatitis | 1 (<1%) | 7 (2%) | 0 | 0 |
| Autoimmune hepatitis | 1 (<1%) | 5 (2%) | 0 | 0 |
| Thrombocytopenia | 1 (<1%) | 1 (<1%) | 24 (7%) | 4 (1%) |
| Dysphonia | 1 (<1%) | 0 | 48 (15%) | 0 |
| Hepatic failure | 0 | 4 (1%) | 0 | 1 (<1%) |
| Proteinuria | 0 | 0 | 48 (15%) | 17 (5%) |

Data are n (%). ALT=alanine aminotransferase. AST=aspartate aminotransferase. PPE=palmar-plantar erythrodysaesthesia. *Includes patients who received at least one dose of the study treatment. All events were reported between the first dose and 30 days after the last dose of study therapy. †No grade 5 treatment-related adverse events occurred in either treatment group. Note that only events that led to death within 24 h of onset were documented as grade 5; events leading to death more than 24 h after onset are reported at the worst grade before death. ‡This category refers to adverse events leading to discontinuation of any drug in the regimen. §Individual treatment-related adverse events that occurred at grade 1 or 2 in at least 10% of patients in either treatment group or at grade 3 or 4 in at least 1% of patients in either treatment group.

Table 3: Treatment-related adverse events in all treated patients*

Research in context

Evidence before this study

We searched PubMed for randomised controlled trials published between Oct 24, 2019, and Oct 21, 2024, using the terms “unresectable hepatocellular carcinoma” OR “advanced hepatocellular carcinoma” AND “phase 3” OR “phase III” in the title or abstract. No language restriction was applied. Among the identified randomised phase 3 studies of unresectable or advanced hepatocellular carcinoma in the first-line setting, the investigated systemic treatments included immunotherapy alone (nivolumab in CheckMate 459 and tislelizumab in RATIONALE-301), immunotherapy combined with anti-angiogenic therapy (atezolizumab plus bevacizumab in IMbrave150 and camrelizumab plus rivoceranib in CARES-310), immunotherapy combined with targeted agents (atezolizumab plus cabozantinib in COSMIC-312 and pembrolizumab plus lenvatinib in LEAP-002), and dual immunotherapy regimens (durvalumab plus tremelimumab in HIMALAYA). The comparator group in all phase 3 studies was sorafenib, with the exception of one that had lenvatinib as the comparator (LEAP-002). Additionally, IMbrave152/SKYSCRAPER-14 (NCT05904886) is currently recruiting patients to assess the efficacy of the atezolizumab, bevacizumab, and tiragolumab combination versus atezolizumab plus bevacizumab plus placebo. TRIPLET HCC (NCT05665348) is also currently recruiting patients to assess the effectiveness of adding ipilimumab to the combination atezolizumab plus bevacizumab versus atezolizumab plus bevacizumab alone. Although some of these treatments have shown improved efficacy compared with single-agent tyrosine kinase inhibitors (sorafenib or lenvatinib), responsiveness to treatment, long-term benefit, and safety and tolerability are suboptimal, and therefore additional treatment options are needed. In the phase 2 CheckMate 040 trial, nivolumab plus ipilimumab showed long-term efficacy and manageable safety in patients with advanced hepatocellular carcinoma previously treated with sorafenib,

providing the rationale to investigate this treatment in the first-line setting.

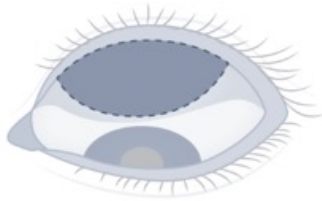
Added value of this study

The CheckMate 9DW trial met the primary endpoint of overall survival for nivolumab plus ipilimumab versus lenvatinib or sorafenib in the first-line setting for patients with unresectable hepatocellular carcinoma. To our knowledge, the median overall survival of 23.7 months in the nivolumab plus ipilimumab group, along with overall survival rates of 49% at 24 months and 38% at 36 months, are the longest and highest reported for the approved systemic treatments in this setting. Additionally, CheckMate 9DW is the first trial to show improved overall survival with an immunotherapy-based regimen versus both lenvatinib and sorafenib individually. Nivolumab plus ipilimumab also showed a higher objective response rate by blinded independent central review versus lenvatinib or sorafenib (36% vs 13%) and durable responses (median duration of response 30.4 months vs 12.9 months). Additionally, many patients receiving nivolumab plus ipilimumab remained in response after discontinuing treatment, with 47% of responders having an ongoing response at 36 months. The regimen had a manageable safety profile, and no new safety concerns were identified. These results are consistent with previous findings for this treatment in the second-line setting.

Implications of all the available evidence

In CheckMate 9DW, nivolumab plus ipilimumab showed a significant survival benefit over lenvatinib or sorafenib as first-line treatment in patients with unresectable hepatocellular carcinoma. The safety profile was manageable and consistent with that previously reported for the regimen in second-line hepatocellular carcinoma and for other indications, with no new safety concerns. These results support nivolumab plus ipilimumab as a first-line treatment option for patients with unresectable hepatocellular carcinoma.

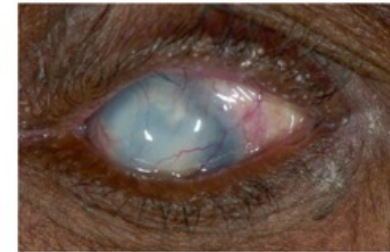
Area to be examined for follicles



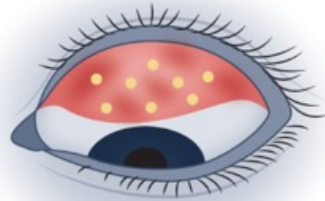
Trachomatous trichiasis



Corneal opacity



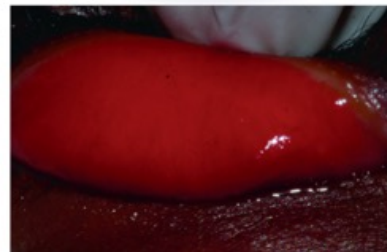
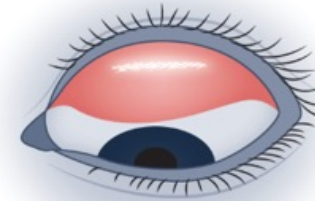
Trachomatous inflammation
—follicular



Trachomatous inflammation
—intense



Trachomatous scarring



Trachoma

Trachoma, the leading infectious cause of blindness worldwide, is one of several neglected tropical diseases targeted by WHO for elimination by 2030. The disease starts in childhood with repeated episodes of conjunctival *Chlamydia trachomatis* infection. This infection is associated with recurrent conjunctivitis (active trachoma), which, if left untreated, leads to cicatricial trachoma characterised by scarring of the conjunctiva, and potentially in-turned eyelashes (trachomatous trichiasis) in later life. Trachoma mainly affects the poorest and most rural communities; these populations typically have limited access to water and hygiene facilities. Blinding complications are most common in women who, in many cultures, act as caregivers from a young age for infected children. To eliminate trachoma as a public health problem, programmes implement a package of interventions known as SAFE; namely, surgery to treat trachomatous trichiasis, antibiotic mass drug administration to treat infection, facial cleanliness, and environmental improvement to limit transmission. The SAFE strategy has brought considerable success in the last two decades. As of December, 2024, 21 countries have eliminated the disease, and several others are on track to eliminate it soon. However, persistent and recrudescent active trachoma in some populations might challenge the success of the 2030 global elimination target. In such settings, novel, or more intensive, approaches must be promptly developed, tested, and scaled up to accelerate elimination.

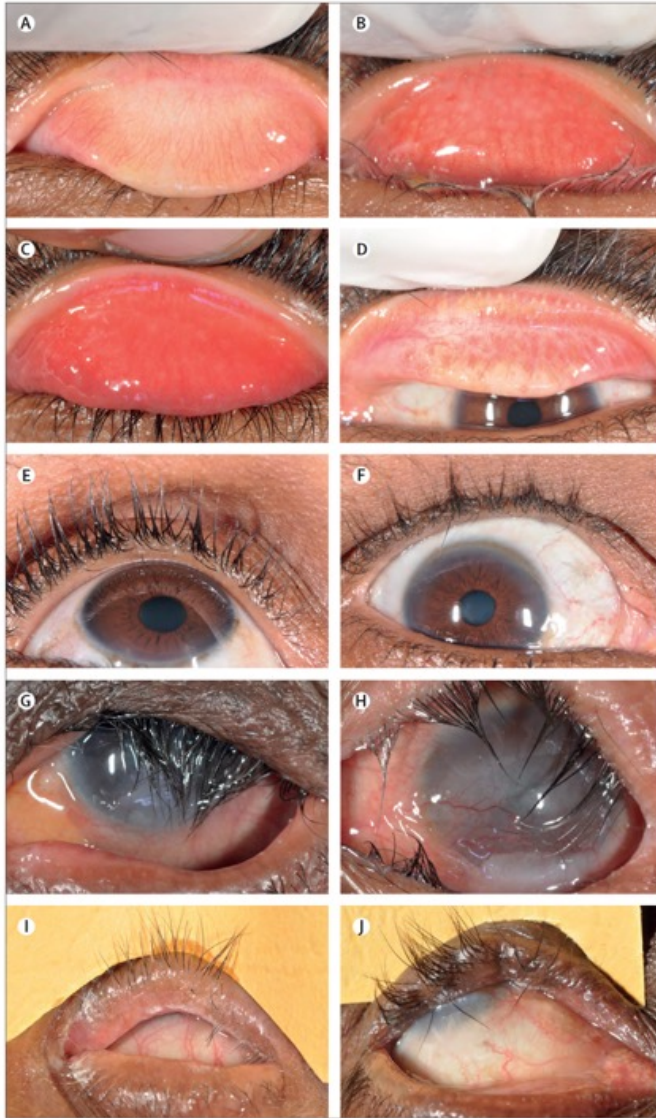


Figure 1: Clinical features of trachoma and the WHO simplified grading system (as amended in 2020)¹³

(A) A healthy upper tarsal conjunctiva. (B–H) The clinical features of trachoma along with the WHO simplified grading system. (B) Trachomatous inflammation—follicular, as defined by the presence of five or more follicles, each at least 0.5 mm in diameter, in the central part of the upper tarsal conjunctiva (equivalent to zone 2 plus zone 3 in the WHO Follicles-Papillae-Cicatricae system and simplified system). (C) Trachomatous inflammation—intense, as defined by pronounced inflammatory thickening of the upper tarsal conjunctiva that obscures more than half of the deep normal vessels. (D) Trachomatous scarring, as defined by the presence of easily visible scarring in the upper tarsal conjunctiva. (E–H) At least one eyelash from the upper eyelid touches the eyeball, or evidence of recent epilation of in-turned eyelashes from the upper eyelid (trachomatous trichiasis without entropion [E], without corneal opacity [F], with entropion [G], with corneal opacity [H]). (H) Easily visible corneal opacity that is so dense that at least part of the pupil margin is blurred when viewed through the opacity. (I, J) Postoperative trachomatous trichiasis.

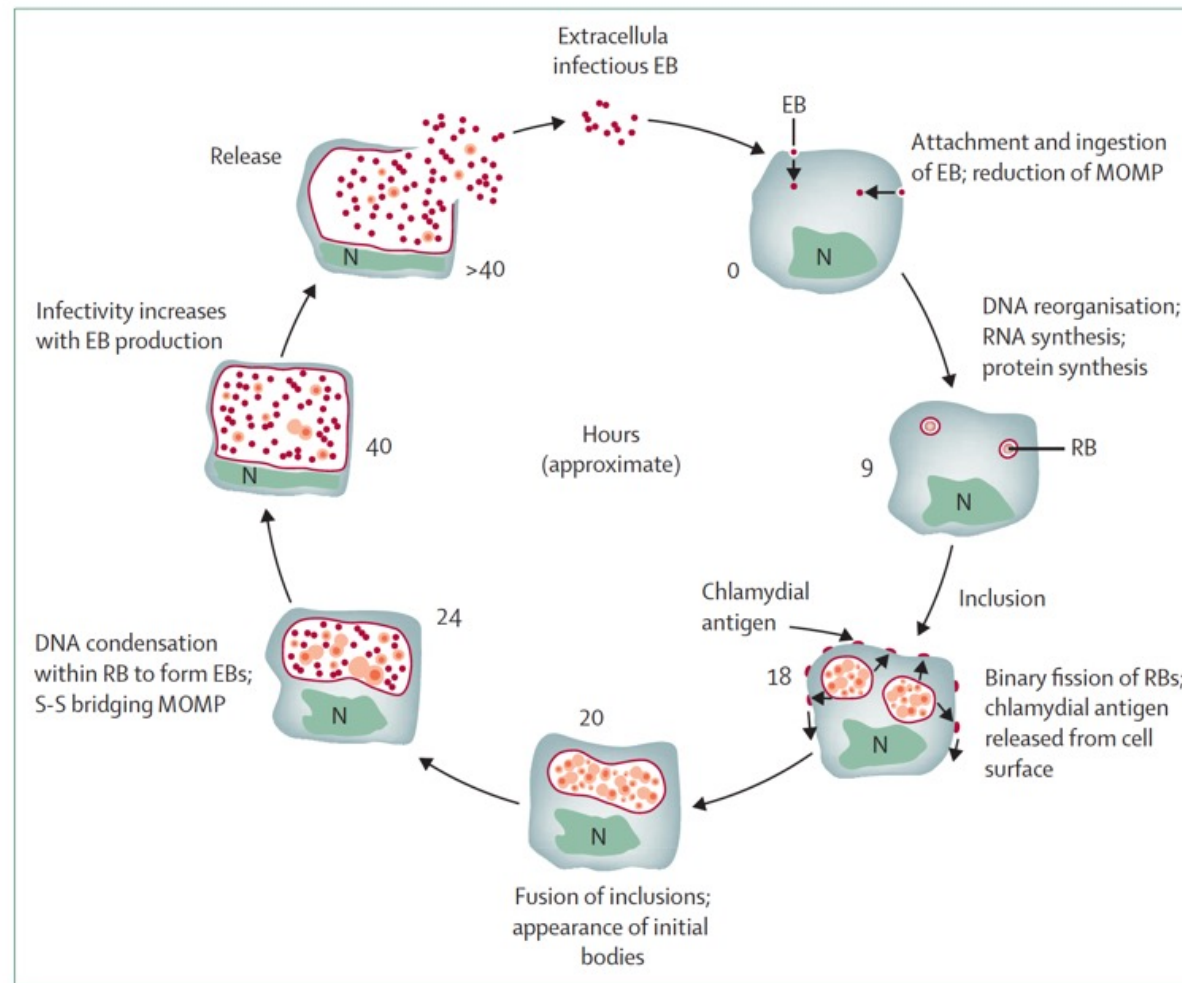


Figure 2: Life cycle of *Chlamydia trachomatis*

Adapted from Mabey and colleagues.³⁵ EB=elementary body. MOMP=major outer membrane protein. N=nucleus. RB=reticulate body. S-S=disulfide bonds.

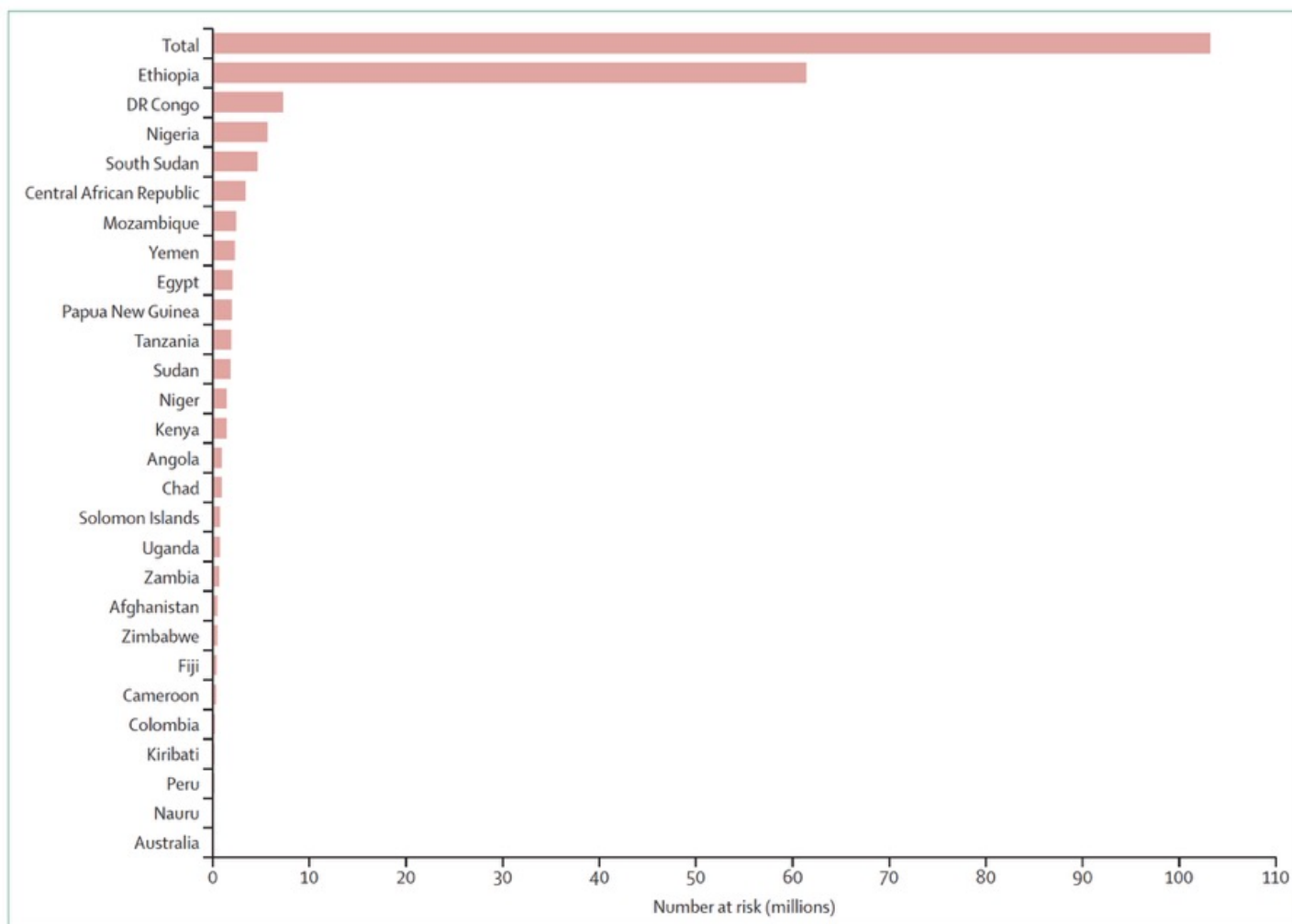


Figure 3: Estimates of the population at risk for trachoma by country
Data from WHO.³⁰

| Description | |
|--|--|
| Upper tarsal follicles | |
| F 0 | No follicles |
| F 1 | Follicles present, but no more than five in zone 2 and zone 3 together (figure 4) |
| F 2 | More than five follicles in zone 2 and zone 3 together, but less than five in zone 3 |
| F 3 | Five or more follicles in each of the three zones |
| Upper tarsal papillary hypertrophy and diffuse inflammation | |
| P 0 | Absent: normal appearance |
| P 1 | Minimal: individual vascular tufts (papillae) prominent, but deep subconjunctival vessels on the tarsus not obscured |
| P 2 | Moderate: more prominent papillae, and normal vessels appear hazy, even when seen by the naked eye |
| P 3 | Pronounced: conjunctiva thickened and opaque, normal vessels on the tarsus are hidden over more than half of the surface |
| Conjunctival scarring | |
| C 0 | No scarring on the conjunctiva |
| C 1 | Mild: fine scattered scars on the upper tarsal conjunctiva, or scars on other parts of the conjunctiva |
| C 2 | Moderate: more severe scarring, but without shortening or distortion of the upper tarsus |
| C 3 | Severe: scarring with distortion of the upper tarsus |
| Trichiasis or entropion, or both | |
| T/E 0 | No trichiasis or entropion |
| T/E 1 | Lashes deviated towards the eye, but not touching the globe |
| T/E 2 | Lashes touching the globe but not rubbing the cornea |
| T/E 3 | Lashes constantly rubbing the cornea |
| Corneal scarring | |
| CC 0 | Absent |
| CC 1 | Minimal scarring or opacity, but not involving the visual axis, and with clear central cornea |
| CC 2 | Moderate scarring or opacity involving the visual axis, with the papillary margin visible through the opacity |
| CC 3 | Severe central scarring or opacity with the papillary margin not visible through the opacity |

C=conjunctival scarring. CC=corneal scarring. F=upper tarsal follicle. P=upper tarsal papillary hypertrophy and diffuse inflammation. T/E=trichiasis or entropion.

Table: WHO Follicles-Papillae-Cicatricae grading system^{45,46}

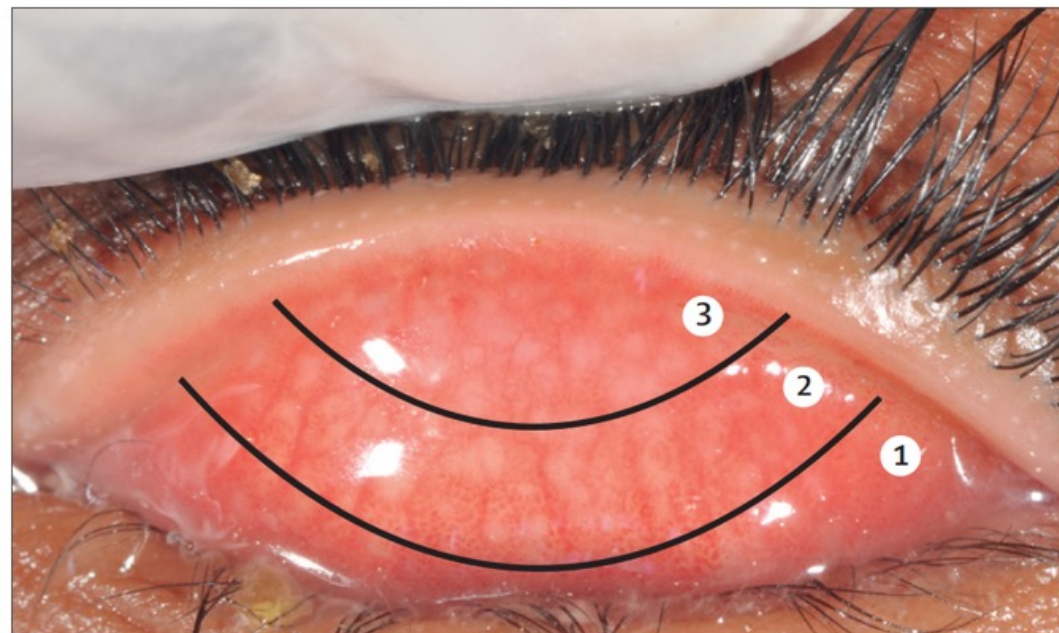


Figure 4: An everted upper eyelid, showing the gradable sections in the Follicles-Papillae-Cicatricae system and simplified grading system
The numbered zones refer to those in the Follicles-Papillae-Cicatricae grading system. Zone 3 and zone 2 are examined for trachomatous inflammation—follicular when using the simplified system.⁴⁷

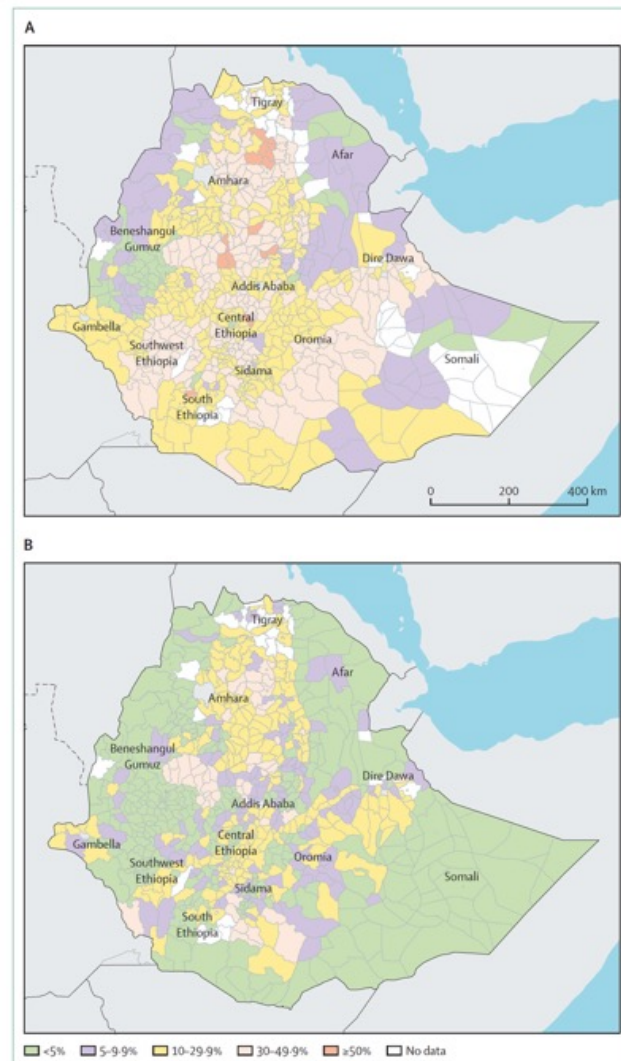


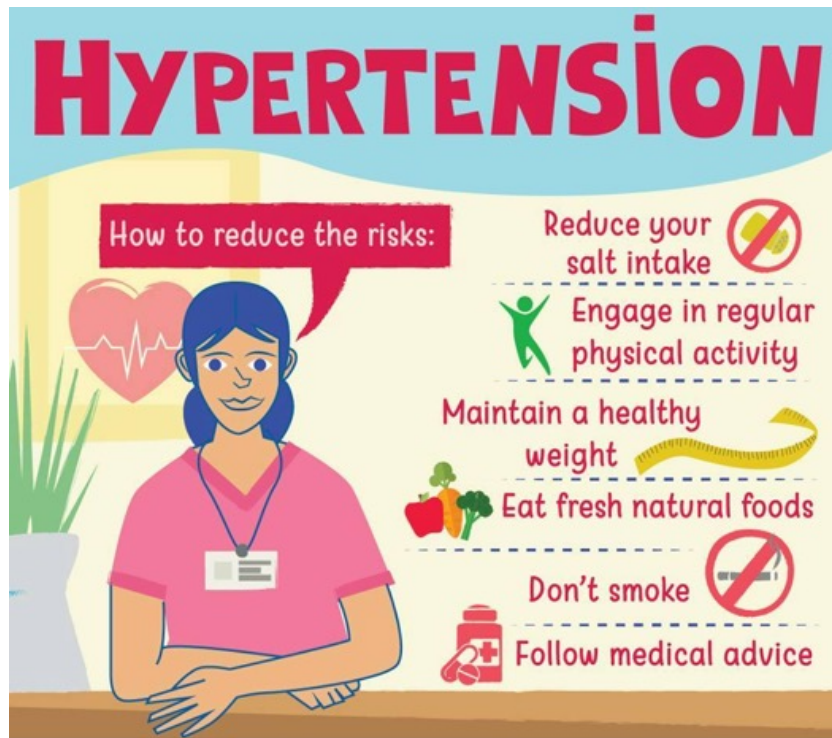
Figure 5: Ethiopia trachoma elimination progress
Trachomatous inflammation—follicular status in 2015 (A) and 2025 (B). Adapted from the Trachoma Atlas February 2025.

Conclusions

The SAFE strategy has proven effective in eliminating trachoma as a public health problem in several settings. Many countries are expected to eliminate trachoma as a public health problem by 2030. However, some countries with hyperendemic trachoma might struggle to achieve elimination by 2030 due to persistent and recrudescent active trachoma and insecurity. Although there is uncertainty as to why trachoma persists or recrudesces, in hyperendemic areas, once a year community-wide antibiotic MDA schedules appear insufficient to reliably achieve sustained elimination. In such settings, understanding the context-specific reasons for persistent and recrudescent trachoma should be a key area of research to develop tailored interventions.

Surgery for trichiasis, Antibiotics (azithromycin), Facial cleanliness, and Environmental improvements

Die Versorgung bei Bluthochdruck (Hypertonie) umfasst in der Regel eine Kombination aus Lebensstiländerungen, wie einer gesunden Ernährung, regelmäßiger Bewegung und Gewichtskontrolle, sowie, wenn erforderlich, Medikamenten.



Improved hypertension care requires measurement and management in health facilities, not mass screening

Improved hypertension control can save millions of lives, but mass hypertension screening, a commonly used approach, is a barrier to progress. Although politically appealing, mass screening diverts resources from improving services in primary health care. Hypertension treatment requires ongoing, long-term care. Mass screening is inefficient: many people with hypertension are not screened or not screened accurately; most people referred do not follow up; many who do follow up are found not to have hypertension; and among those who have hypertension, few initiate and adhere to treatment. Universal measurement of blood pressure among all adults attending health facilities is much more effective and facilitates treatment and ongoing care. Universal facility-based screening can improve diagnosis and control substantially, including among underserved populations. Implementing this approach requires that facilities have validated blood pressure monitors, routinely screen at least all patients aged 30 years and older, and increase the number and proportion of patients being treated for hypertension whose blood pressure is at target (eg, <140/90 mm Hg). The only way to control hypertension is to strengthen facility-based detection and treatment. To prevent heart attacks, strokes, death, and other complications of untreated and inadequately treated hypertension, countries should track and steadily increase the outcome that matters: the number of patients on treatment whose blood pressure is controlled.

nature

How we taste sweetness: long-sought structure of human receptor mapped at last

3D structure of the tongue's sweet-sensing protein could guide future food designs.





The structure of human sweetness

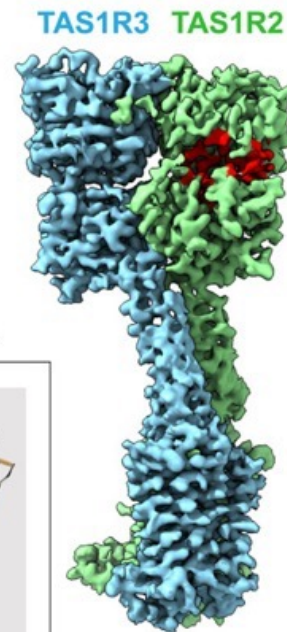
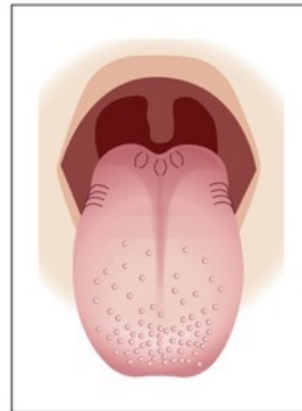
Highlights

- Two GPCR subunits assemble to recognize sweet ligands
- The TAS1R2 subunit binds the ligands and couples to the G protein
- A common binding pocket recognizes sucralose and aspartame
- 3D variability analysis shows coordinated structural changes between the subunits

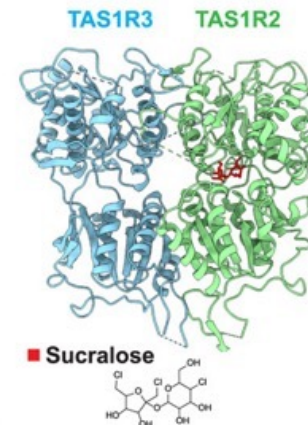
Summary

In humans, the detection and ultimately the perception of sweetness begin in the oral cavity, where taste receptor cells (TRCs) dedicated to sweet-sensing interact with sugars, artificial sweeteners, and other sweet-tasting chemicals. Human sweet TRCs express on their cell surface a sweet receptor that initiates the cascade of signaling events responsible for our strong attraction to sweet stimuli. Here, we describe the cryo-electron microscopy (cryo-EM) structure of the human sweet receptor bound to two of the most widely used artificial sweeteners—sucralose and aspartame. Our results reveal the structural basis for sweet detection, provide insights into how a single receptor mediates all our responses to such a wide range of sweet-tasting compounds, and open up unique possibilities for designing a generation of taste modulators informed by the structure of the human receptor.

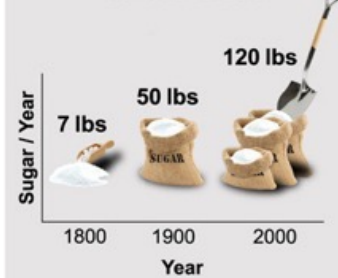
Human Sweet Taste Receptor



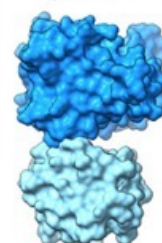
Sucralose Binding to the Human Sweet Receptor



Sugar Consumption in the USA

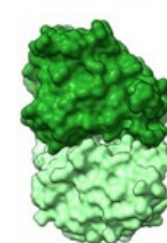


Open VFT



TAS1R3

Close VFT



TAS1R2

Discussion

The taste of sweet permeates every aspect of human experience, from the taste of a mother's milk to the current impact of sugar in packaged products and drinks in human health. Notably, a single receptor (TAS1R2+3) expressed in sweet taste receptor cells (TRCs) in the tongue and oral cavity mediates the taste of sweet in humans and other mammals.

The receptor, composed of two GPCR subunits, one unique (TAS1R2) and one shared with the umami receptor (TAS1R3), has the essential role of detecting and driving appetitive and consummatory responses to the most basic sources of metabolic energy (e.g., glucose, sucrose, lactose, and other sugars). Consequently, its primary structure is conserved among mammals, including in humans. Not surprisingly, there is significant polymorphism in the receptor in the human population, perhaps accounting for some of the variability in our “sweet-tooth” (i.e., the unique differences in sensitivity to sweet stimuli between subjects). While studies attempting to link polymorphic variants to differences in human sweet sensitivity are still very limited, a number of promising studies may provide additional insights.

We discovered and de-orphaned the TAS1R2+3 mammalian sweet taste receptor over 20 years ago and validated its essential role in sweet detection and sweet-evoked responses using a combination of genetics, cell-based assays, and physiological and behavioral studies. Non-caloric artificial sweeteners entered consumer products over 60 years ago. Artificial sweeteners can be 100× (e.g., saccharin, aspartame, and sucralose) to over 10,000× (e.g., neotame) more potent than sucrose.

Genetics of Korea's extreme divers could unlock chronic disease treatments



60 ft = 20 m, = 3 BAR; = 2300 mm Hg pressure

The secret to tackling one of the United States' most deadly chronic diseases may reside thousands of miles away in the chilly waters separating the Korean Peninsula and Japan, where generations of Jeju Island women have been diving to gather food from depths of up to 60 feet using only the bodies that genes and conditioning have given them.

They are known as the Haenyeo, or “sea women,” and when younger, many of them dove throughout pregnancy and resumed their gathering of seaweed, abalone and other food only a few days after giving birth. The practice is dying out, and most of those diving in the 50-degree waters today are in their 60s, 70s and 80s.

Now, an international team of researchers has found evidence of natural selection at work: a genetic variation found in Jeju Islanders that helps to keep their blood pressure from rising as much when diving, according to a paper published in the journal [Cell Reports](#).

Researchers measured physiological characteristics, such as blood pressure and heart rate, then sequenced the DNA of participants to look for genetic differences.

In a simulated dive, ordinary Jeju Islanders' heartbeats slowed by about 20 beats per minute, researchers found, about the same amount as women on the South Korean mainland. In the same circumstances, the Haenyeo, who have been diving their whole lives, slow their heartbeats by up to twice that number.

In simulated dives, participants held their breath and submerged their faces in a basin of cold water, which triggers the same response in the body as diving. The simulation allowed the researchers to carry out the study without having untrained, and possibly non-swimming, older women try to dive in the open ocean.



Der Tauchreflex (auch "diving reflex" genannt) ist eine physiologische Reaktion, die bei lungenatmenden Tieren (einschließlich Menschen) beim Eintauchen in Wasser auftritt. Er hilft, die Sauerstoffversorgung während des Tauchens zu optimieren und kann auch helfen, Stress und Angst zu reduzieren.

Bradykardie: Die Herzfrequenz sinkt, um den Sauerstoffverbrauch zu reduzieren.

Apnoe: Die Atmung wird gehemmt.

Vasokonstriktion: Die Blutgefäße in den Extremitäten verengen sich, um das Blut zu den lebenswichtigen Organen zu leiten

Genetic and training adaptations in the Haenyeo divers of Jeju, Korea

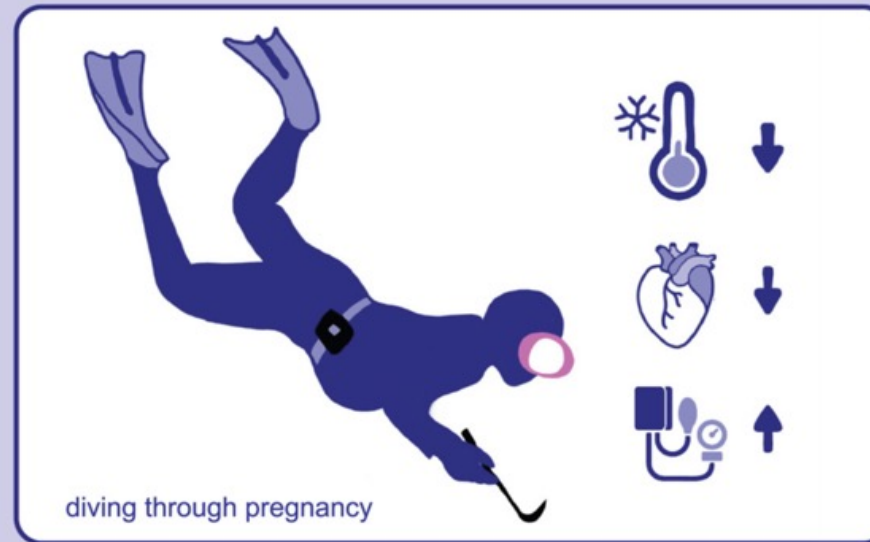
Highlights

- Evidence of selection that may increase the safety of diving during pregnancy
- Regular diving increases the magnitude of bradycardia in response to dive stimulus
- The Haenyeo may represent the second known population evolved for diving

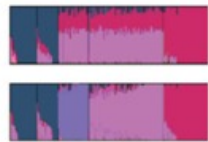
Summary

Natural selection and relative isolation have shaped the genetics and physiology of unique human populations from Greenland to Tibet. Another such population is the Haenyeo, the all-female Korean divers renowned for their remarkable diving abilities in frigid waters. Apnea diving induces considerable physiological strain, particularly in females diving throughout pregnancy. In this study, we explore the hypothesis that breath-hold diving has shaped physiological and genetic traits in the Haenyeo. **We identified pronounced bradycardia during diving, a likely training effect.** We paired natural selection and genetic association analyses to investigate adaptive genetic variation that may mitigate the effects of diving on pregnancy through an associated reduction of diastolic blood pressure. **Finally, we identified positively selected variation in a gene previously associated with cold water tolerance, which may contribute to reduced hypothermia susceptibility.** These findings highlight the importance of traditional diving populations for understanding genetic and physiological adaptation.

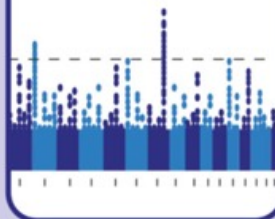
Haenyeo: all-female Korean breath-hold divers



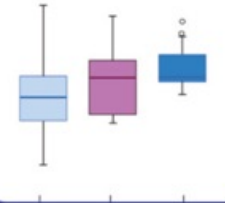
population structure



selection scan



adaptive phenotypes



- A variant in the sarcoglycan zeta gene is linked to cold tolerance, helping the Haenyeo withstand the cold waters.